2019

Cliff-Top Dunes in the Lower Chippewa River Valley of West-Central Wisconsin

Jason Millett
Minnesota State University, Mankato

Cliff-Top Dunes in the Lower Chippewa River Valley of West-Central Wisconsin

By

Jason Millett

A Thesis Submitted in Partial Fulfillment of the

Requirements for the Degree of

Master of Science

In

Geography

Minnesota State University, Mankato

Mankato, Minnesota

March, 2019

March 29th, 2019

Cliff-Top Dunes in the Lower Chippewa River Valley of West-Central Wisconsin

Jason Millett

This thesis has been examined and approved by the following members of the student's committee.

_____
Dr. Phil Larson
(Chairperson)

_____
Dr. Ron Schirmer

_____
Dr. Doug Faulkner

_____
Dr. Garry Running

Acknowledgements

I would like to thank the families of Mary Dooley and James Goff for providing the grants that funded my research. I would also like to thank the land owners who allowed me to conduct research on their property. I finally wish to thank my advisor and committee members for their guidance.

Abstract

The purpose of this Master's thesis is to investigate recently identified cliff-top sand dunes located within the Lower Chippewa River Valley (LCRV), Wisconsin, USA. Research within the LCRV notes the existence of a variety of aeolian deposits, but a comprehensive explanation of their complete spatial distribution, genesis, age, and paleoenvironmental significance does not exist. In particular, stabilized cliff-top dunes with a parabolic form remain poorly understood. This problem is exacerbated by a lack of clarity in the literature regarding the genesis of dunes in a cliff-top position. Therefore, this thesis begins by reviewing the literature concerning sand dunes in cliff-top position in order to clearly define and describe the cliff-top parabolic dune form within the various physical geographies it has been observed. A diagnostic classification scheme and formation models for cliff-top dune types are presented and based upon the landscape assemblage and geomorphic systems in which they are found. The classification scheme and formation models are then applied to cliff-top dunes along the LCRV to understand their origin, geomorphic, and paleoenvironmental significance in this actively evolving landscape. These cliff-top dunes exist in positions immediately adjacent to and above the highest fluvial terrace scarps in the LCRV. Other parabolic dunes are removed from cliff-top position and cover glacial outwash plains flanking the Chippewa River. However, the cliff-top dunes exhibit different morphologies, orientations, and ages compared to other aeolian deposits recently identified. Therefore, the results of this investigation indicate cliff-top dunes in the LCRV have a genesis involving complex fluvial-aeolian processes that occurred throughout the Holocene.

Table of Contents

List of Figures

List of Tables

Chapter 1

1.1 Introduction

The Lower Chippewa River valley (LCRV) of west-central Wisconsin, USA is a relict aeolian landscape that exhibits stabilized aeolian deposits. Parabolic and cliff-top dunes are investigated in order to determine the geomorphic processes and paleoenvironmental conditions related to aeolian deposition within the LCRV. Therefore, Chapter 1 is used to produce a basic understanding of parabolic and cliff-top dune morphology and formation processes. It then describes the study area of the LCRV and presents the research questions that are the focus of this thesis. In Chapter 2 a synthesis of cliff-top dune literature is provided and used to describe and define the cliff-top dune landform and the processes that lead to its formation. This comprehensive synthesis is then applied to newly discovered (Larson et al., 2008; Schaetzl et al., 2017), but poorly understood, cliff-top aeolian sand dunes at two sites within the LCRV. Chapter 3 then expands on the findings in Chapter 2 by applying an array of geospatial and geochronological methods to understand the spatial distribution, age, and potential geomorphic and paleoenvironmental significance of cliff-top dunes throughout the entire LCRV.

1.2 Aeolian Landscapes

Several terms are defined within this section to provide a fundamental understanding of aeolian dynamics. Aeolian landscapes are comprised of aeolian landforms, which cover at least 25% of the Earth's surface. Aeolian processes that shape these landforms and landscapes involve the erosion, transport, and deposition of material

by wind (Nickling and Neuman, 2009). These aeolian processes occur in both arid and non-arid environments (Nickling and Neuman, 2009). Arid environments exhibit a moisture deficit which has been defined as the ratio between precipitation and potential evapotranspiration (PE) (Parsons and Abrahams, 2009). Precipitation to evapotranspiration values less than .5 correspond to arid environments and values greater than .5 represent humid climates (Parsons and Abrahams, 2009). However, aeolian processes are not solely controlled by aridity. They depend upon other variables including wind regime, vegetative cover, surface roughness, soil moisture, and grain size of the transported material (Nickling and Neuman, 2009; Parsons and Abrahams, 2009). Aeolian landscapes can include relict and active landform genesis by erosion or deposition by wind. They exhibit diagnostic morphological features such as yardangs, deflation hollows, and sand dunes. Sand dunes are generally more common in arid environments where vegetative cover and soil moisture is reduced, thus making surface deposits available to aeolian processes. Nonetheless, sand dunes can be located semi-arid and even humid locations environments due to local-scale modifications to wind flow, vegetative cover, and soil moisture.

1.3 Parabolic Dunes

Parabolic sand dunes are a distinct depositional aeolian landform observed in arid, semi-arid, and humid environments (Sauchyn, 1993; Goudie, 2011). Parabolic dunes can occur as individual landforms or be grouped or merged into complexes (Sauchyn, 1993). The density of parabolic dunes in a landscape is linked to sediment supply (Sauchyn, 1993). Thus, individual and morphologically well-defined parabolic dunes occur where

there is low sediment supply and a high density of overlapping parabolic dunes occur where there is higher sediment supply (Sauchyn, 1993).

Parabolic dunes have been widely studied (Hack, 1941; Wolfe and David, 1997; Lancaster, 2009; Yan and Baas, 2015). Researchers have described variable morphologies and competing classification schemes for these landforms (Hack, 1941; Pye and Tsoar, 2009; Yan and Baas, 2015). However, parabolic dunes have morphologic commonalities, which include a U or crescent-shape, dune crest, stoss slope, slipface, and trailing and vegetated arms (i.e.,, horns, wings) (Fig. 1) (Hack, 1941; Wolfe and David, 1997; Pye and Tsoar, 2009; Yan and Baas, 2015). The stabilized trailing arms are connected by the lobate dune crest and stabilize the dune (Fig. 1) (Goudie, 2011; Yan and Baas, 2015).

Parabolic dunes' morphological form is determined by the aeolian processes that act on them. Crests of parabolic dunes are transported at faster rates than the trailing arms resulting in the distinct windward facing U-shape (Hack, 1941; Pye and Tsoar, 2009). The stoss slope (i.e., windward side) and slipface of parabolic dunes are locations of sand erosion and deposition, respectively (Fig. 1) (McKee, 1979; Pye and Tsoar, 2009; Yan and Baas, 2015) On the stoss slope air flow is vertically compressed and increases in velocity, thereby allowing the mobilization and transport of sand grains up the stoss slope. Upon reaching the crest, winds diverge, reducing their capacity for transport resulting in the deposition of sand grains at the crest (Fig. 1) (Yan and Baas, 2015). Under consistent conditions the accretion of sand grains atop the crest will continue until the angle of repose is exceeded on the lee side, resulting in their tumbling or avalanching down along a slip face (McKee, 1979; Lancaster, 2009; Goudie, 2011; Yan and Baas, 2015). The angle of the slipface slope is typically restricted only by the angle of repose,

and there exceeds that of the stoss slope (Yan and Baas, 2015). This process produces dipping strata (i.e., crossbedding) within the dune (Fig. 1) (McKee, 1979). Crossbedding within a parabolic dune can be used to infer past wind directions during dune formation (McKee, 1979) and can be imaged with non-invasive geophysical methods such as ground penetrating radar (Schaetzl et al., 2017).

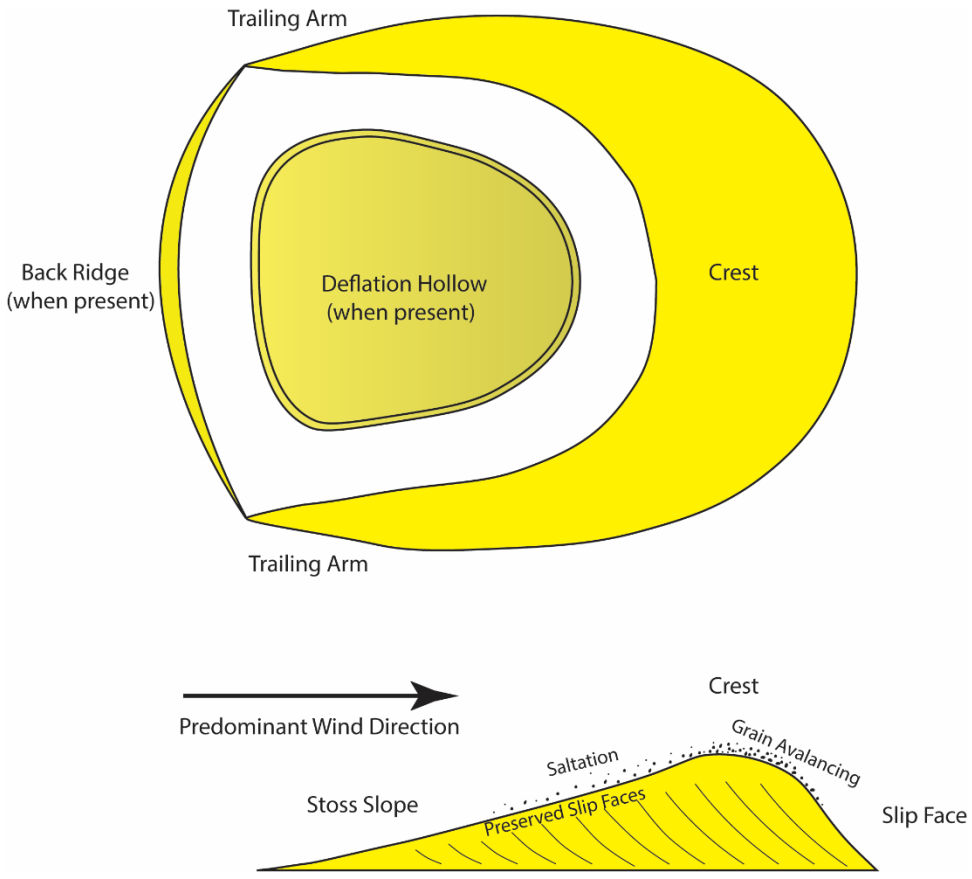

Fig. 1. An overhead and profile view of a parabolic dune.

A deflation hollow (i.e., blowout) from which wind erosion of sand grains takes place, is located upwind of the crest of some parabolic dunes (Wolfe and David, 1997; Goudie, 2011). Pye and Tsoar (2009) suggest the majority of parabolic dunes are formed from deflation hollows where upwind deflation and immediate downwind accumulation

of sand are linked. Conversely, Hack (1941, p.243) describes two avenues of genesis for parabolic dunes termed “parabolic dunes of deflation” and “parabolic dunes of accumulation”. The former are deflation hollows coupled with parabolic dunes and the latter can form independent of upwind deflation and thus are strictly depositional features. Additionally, Yan and Baas (2015) and Yan and Baas (2017) describe the means by which mobile barchanoid and transverse dunes can transform into parabolic dunes when their flanks become sufficiently vegetated. When this occurs, upwind deflation is not necessary for parabolic dune formation.

Parabolic dune morphology is affected by surrounding environmental conditions including wind regime, sand supply, soil moisture, and vegetative cover (Hack, 1941; Wolfe and David, 1997; Lancaster, 2009; Pye and Tsoar, 2009; Yan and Baas, 2015). Parabolic dunes with elongated trailing arms, are the result of unidirectional wind regimes. Wider parabolic dune crests and overlapping dune arms form under variable wind regimes (Yan and Baas, 2015). Parabolic dunes with a back ridge (Fig. 1), produced by aeolian accumulation upwind of the main body, are produced by a higher sand supply compared to those with a simple U-shape (Wolfe and David, 1997). Vegetation density and type profoundly affect the incidence and morphology of parabolic dunes (Hack, 1941; Goudie, 2011; Yan and Baas, 2015). Parabolic dunes with digitate forms and higher relief are associated with tree cover (Yan and Baas, 2015). Parabolic dunes associated with grasses are characterized by gentle relief (Yan and Baas, 2015). At the same time, high moisture content of the sand within the dunes requires greater wind velocities for sand transport which can limit or inhibit parabolic dune mobility (Wolfe and David, 1997; Yan and Baas, 2015).

Parabolic Dune Morphology	**Controlling Variable**
Elongated trailing arms	Unidirectional wind regime
Wide crests; overlapping trailing arms	Bimodal or variable wind regime
Parabolic dunes with a back ridge	High sand supply
Digitate form; greater relief	Forest cover
Gentle relief	Grass cover

Table 1. Parabolic dune morphologies corresponding to the variable that affect them.

Vegetative cover is also a primary control on parabolic dune morphology and stabilization (Sauchyn, 1993; Tsoar, 2001). Sand transport on parabolic dunes is halted when vegetative cover of the ground exceeds approximately 20%(Yan and Baas, 2015). When vegetative cover decreases, parabolic dunes can be reactivated and can even exhibit barchan dune morphologies (Yan and Baas, 2015). Aeolian landscapes characterized by parabolic sand dunes are unique because they occur in the transition between sand transport and stabilization and thus are sensitive to minor environmental changes such as variations in climate, vegetative cover, and sand supply (Hack, 1941; Yan and Baas, 2015). Therefore, parabolic dunes are useful to geomorphologists for interpreting present aeolian landscapes and reconstructing paleoenvironmental conditions.

1.4 Cliff-top Dunes

Despite an extensive body of research on parabolic dunes across the world (Yan and Baas, 2015), a relative paucity of research has focused on the distribution, variable

genesis, and broader paleoenvironmental significance of cliff-top dunes that are frequently described as having a parabolic morphology (Tate, 1879; Cowles, 1899; White, 1960; Bullard and Nash, 2000; Rawling, Fredlund and Mahan, 2003). These dunes will hereafter be referred to as cliff-top dunes. Textbook classifications of cliff-top dunes that exhibit parabolic morphologies are negligible to non-existent (Livingstone and Warren, 1996; Tsoar, 2001; Pye and Tsoar, 2009). Nonetheless, when cliff-top dunes are preserved, they exhibit morphology consistent with parabolic morphology described above (Snyder, 1986; Bégin, Michaud and Filion, 1995; Englebright et al., 2000; Schaetzl et al., 2017).

Pye and Tsoar (2009) classify cliff-top and parabolic dunes into different categories based upon the primary mechanisms by which they are formed. In their classification, cliff-top dunes are associated with topographic obstacles to the flow of wind. In contrast, parabolic dune formation is controlled by vegetative cover (Fig. 2). Although the agents for incipient formation of cliff-top and parabolic dunes are different, the formation mechanisms they invoke are remarkably similar for both types of dunes.

1

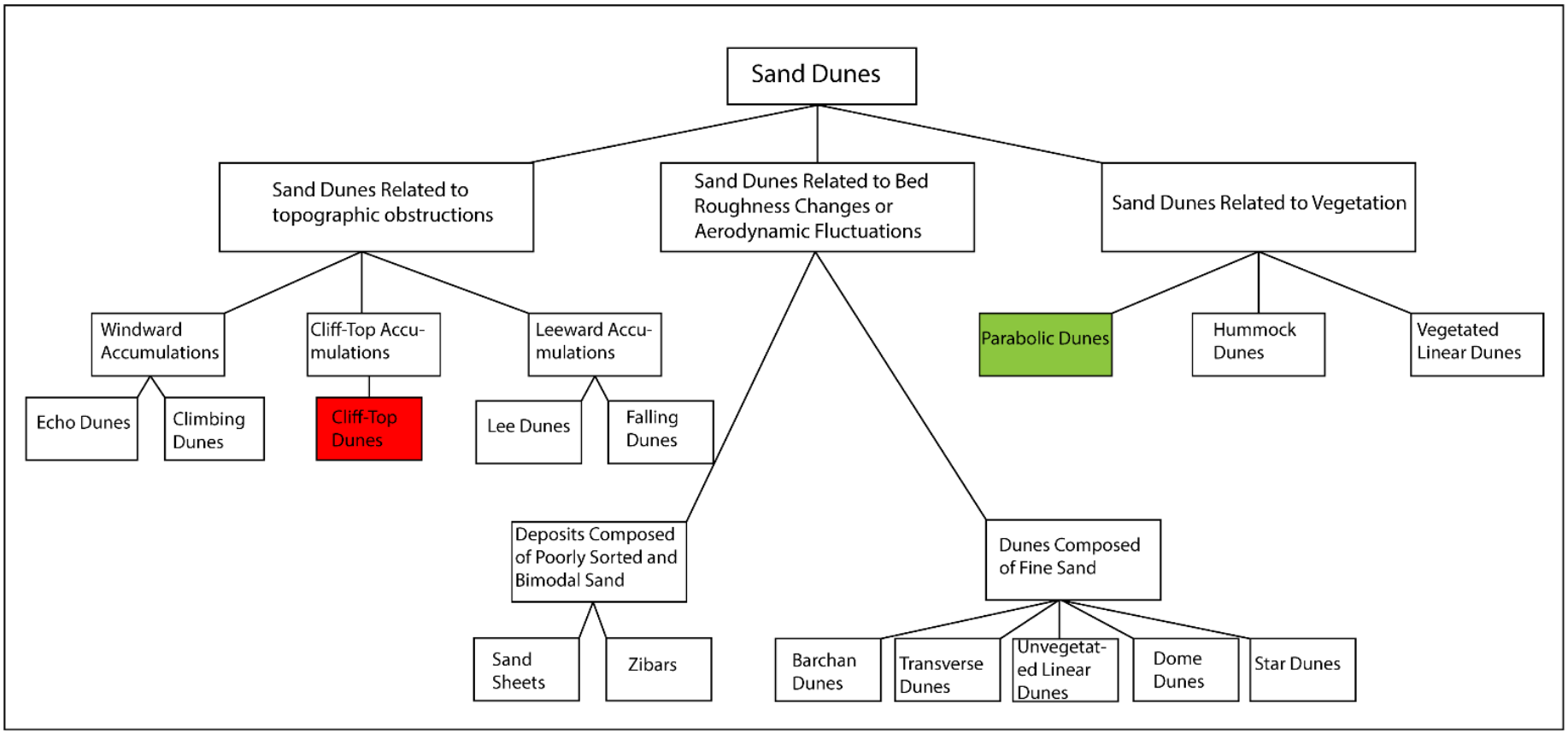

Fig. 2. An example of cliff-top and parabolic dune classifications that are based upon topographic and vegetative controls adopted from Pye and Tsoar (2009).

Cliff-top dunes are perched upwind of escarpments. The escarpments are produced by a variety of geomorphic erosional processes (e.g., fluvial undercutting and wave action). Cliff-top dune formation is primarily controlled by how escarpments modify local wind flow dynamics (Fig. 3). However, other local factors (e.g., vegetation and geomorphic processes) are at play and explain ambiguities in cliff-top morphology as well as the environments in which they are found (Hack, 1941; White, 1960; Snyder, 1986; Bégin, Michaud and Filion, 1995). Therefore, each cliff-top dune should be investigated holistically by integrating local and broader landscape scale processes. Cliff-top dunes are documented in disparate locations that include the Great Lakes Region (Cowles, 1899; Dow, 1937; Arbogast et al., 2017), Denmark (Saye, Pye and Clemmensen, 2006), Ireland (Carter and Wilson, 1993), Portugal (Jackson and Nevin, 1992), Italy (Sansò et al., 2016), Taiwan (Ho et al., 2017), New York State, USA (Englebright et al., 2000), South Dakota, USA (White, 1960), northwestern Canada

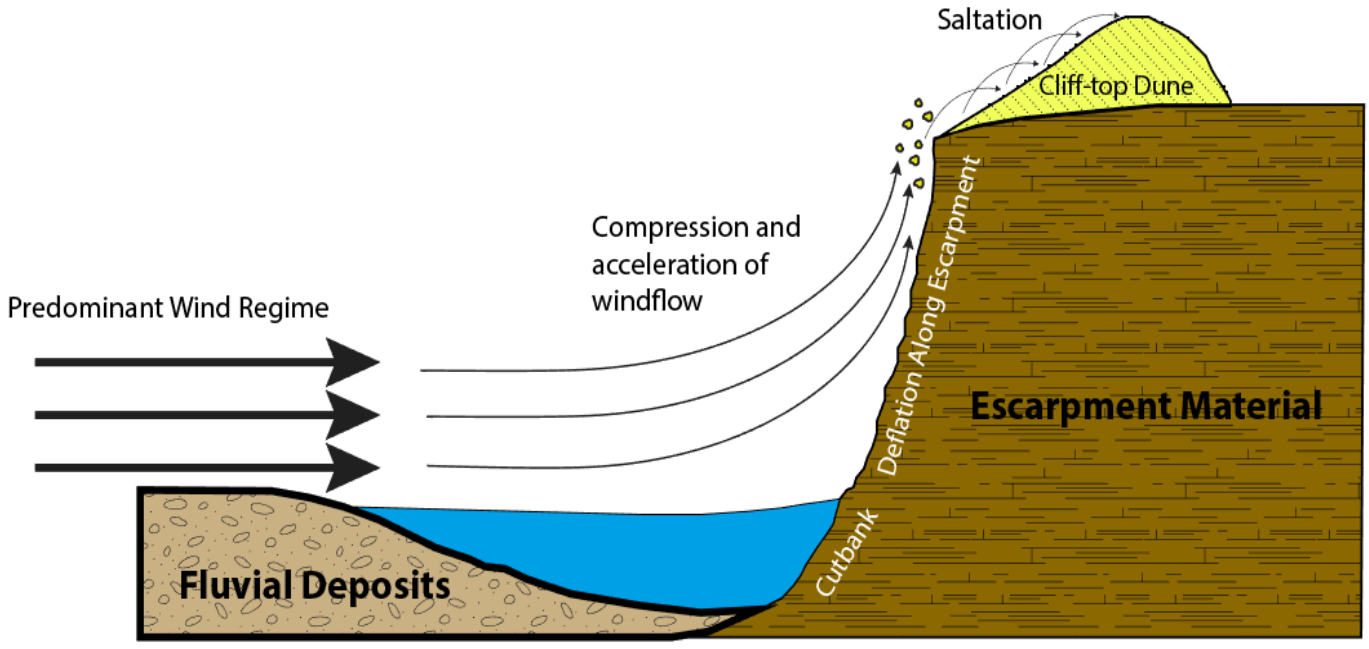

Fig. 3. An example of wind regime modifications and cliff-top dune formation in a fluvial environment. Adapted from Larson et al. (2008).

(Bégin, Michaud and Filion, 1995), and Oceania (Tate, 1879; Jennings, 1967; Pain, 1976) (Fig. 4). In this thesis, the distribution of cliff-top dunes are organized into two broad environmental regions: (1) those in coastal settings and (2) those in terrestrial settings. Given the prior literature, cliff-top dunes can classified as coastal normal, hybrid coastal, terrestrial normal, and terrestrial fluvial types. Coastal normal cliff-top dunes are related to geomorphic processes and sediment supply specific to coastlines. Coastal hybrid cliff-top dunes are formed by a combination of inland and coastline geomorphic processes and sources of sediment. Terrestrial cliff-top dunes are located in continental interiors and are related to the intricate interaction between climate and geomorphic processes. A complete review of cliff-top dune literature is included in Chapter 2.

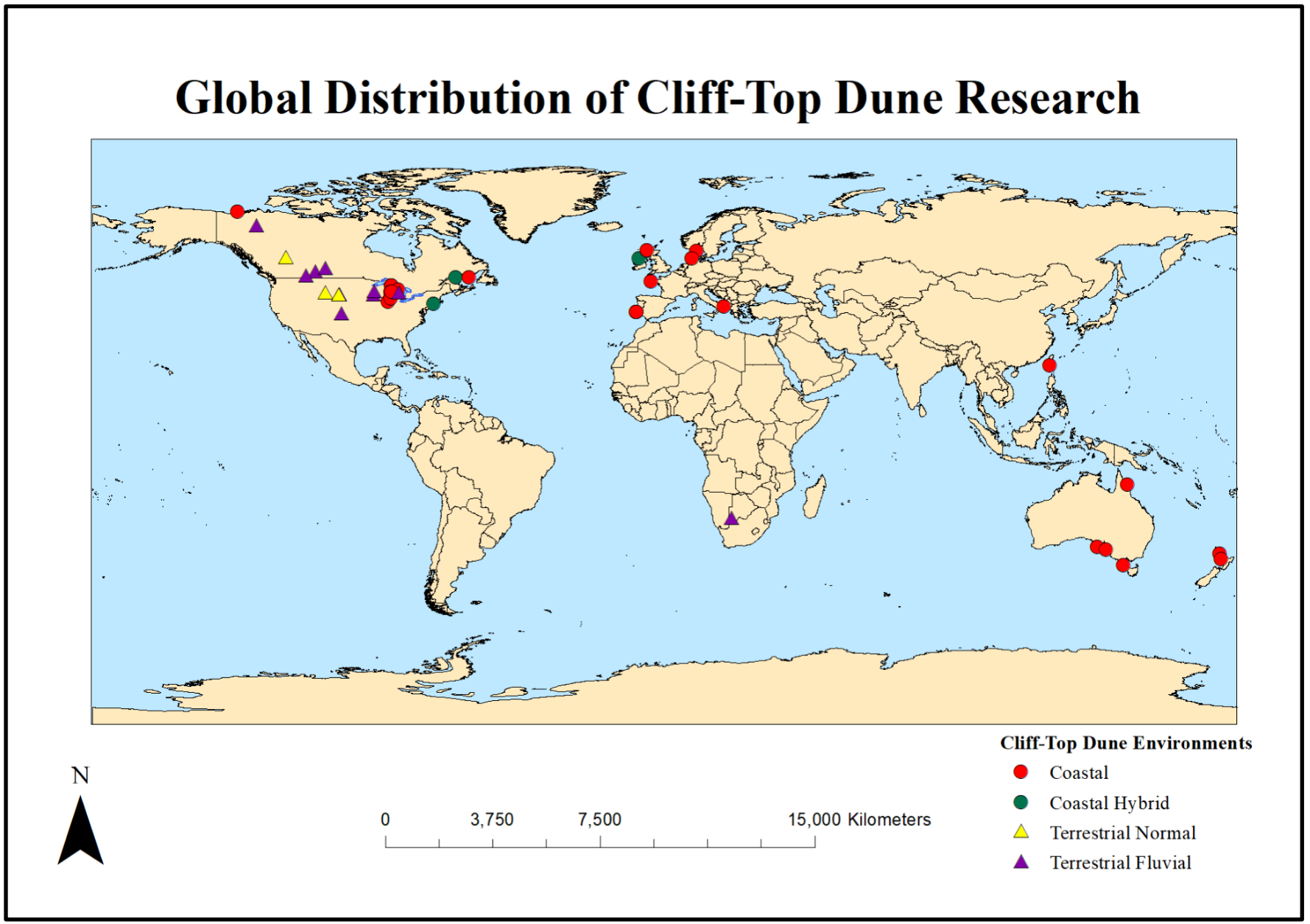

Fig. 4. A global distribution of cliff-top dune research available to the author. The circles represent coastal cliff-top dunes and the triangles represent terrestrial cliff-top dunes. A further of subset cliff-top dune types within each environmental setting is provided in Chapter 2.

Fig. 5. The Lower Chippewa River Valley study area. The counties that sourround the lower Chippewa River were used as hard boundaries to define the study area.

1.5 Study Area

The study area is located within west-central Wisconsin along the lower Chippewa River Valley (LCRV), which is encompassed by Chippewa, Dunn, Pierce, Pepin and Buffalo Counties (Fig. 5). The LCRV is located within a Dfb climate as denoted by the Köppen climate classification (Rohli and Vega, 2013). As such, the LCRV resides within a humid mid-latitude climate consisting of cold winters and warm summers with precipitation falling year round. The mean annual maximum daily temperature from 1981 to 2010 is 12.78 degrees Celsius (°C) (Young, 2019). The mean annual minimum daily temperature is 1.28°C (Young, 2019). The LCRV receives approximately 787 millimeters of annual precipitation (Young, 2019). Precipitation in the LCRV occurs throughout the year with an average of 119 days per year with measurable precipitation values (Young, 2019). The predominant wind regimes for the LCRV are from westerly and southerly directions (Fig. 6)((Iowa Environmental Mesonet, 2019). The average recorded wind

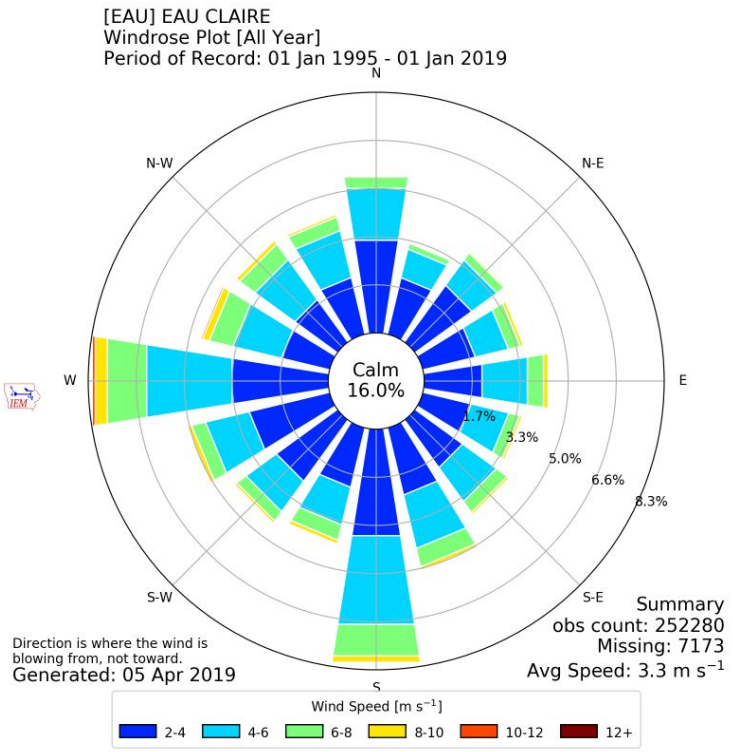

Fig. 6. Wind data collected from the Eau Claire airport from January 1995 to January 2019 (Iowa Environmental Mesonet, 2019).

velocity at the Eau Claire, Wisconsin airport from 1995 to 2019 was 3.3 meter per second (ms^{-1}). Yet winds regularly exceed this average velocity reaching values up to 12 ms^{-1}(Iowa Environmental Mesonet, 2019; Young, 2019). The minimum threshold velocity for aeolian transport is dependent upon factors including grain size, surface roughness, material shape, and degree of material sorting. Under optimal conditions with grain sizes around 80 micrometers (μm) the minimum threshold velocity for aeolian transport is around 5 ms^{-1} (David, 1977; Sloss, Hesp and Shepherd, 2012). Consequently, the LCRV's climate supplies sufficient wind velocities to entrain and transport sandy material (Nickling and Neuman, 2009). However, aeolian activity in the region is currently limited, perhaps by the present distribution and quantity of annual precipitation that allows for high soil moisture content and dense vegetative cover.

1.5.1 Geomorphic Setting of the Chippewa River Valley

As a major tributary to the upper Mississippi River, the Chippewa River drains approximately 25,000km^2 of western Wisconsin (Faulkner et al., 2016). During the late Wisconsinan glaciation (30ka to 10ka), the Chippewa River was an aggrading glacial meltwater stream as indicated by the glacio-fluvial fill underlying the highest standing terrace, the Wissota Terrace (Andrews, 1965; Faulkner et al., 2016). The upper reach of the Chippewa River was glaciated during the last glacial maximum of the Wisconsinan (Fig. 6), and thus the boundary between the upper and lower Chippewa River is demarcated by the terminal moraine from the late Wisconsinan Glaciation known as the Chippewa Moraine (Syverson and Colgan, 2011). The bedrock underlying the lower Chippewa River consists of Cambrian sandstones, which near the Mississippi River, are

capped by a more resistant dolomite (Andrews, 1965; Faulkner et al., 2016). As a result, the LCRV drains a weathered landscape consisting of incised valleys adjacent to steep bedrock outcrops (Faulkner et al., 2016; Schaetzl et al., 2017). The Chippewa River is bedrock constrained at its lowest reach thereby preventing significant lateral incision. In contrast, the middle and upper reaches of the lower Chippewa River are less laterally constrained and exhibit meandering and anastomosing patterns (Andrews, 1965; Faulkner et al., 2016).

The LCRV contains a suite of fill-cut terraces inset into the Wissota fill terrace. These terraces are the product of ongoing, transient incision of the landscape by the Chippewa River (Andrews, 1965; Faulkner et al., 2016). The terraces record a time-transgressive, complex response to an abrupt local base level lowering caused by Mississippi River incision. As a result of this ongoing landscape evolution, there are numerous locations of erosion into LCRV terrace escarpments. Many such exposures of terrace fill are found bounding the meandering and anastomosing reach of the Chippewa River upstream of Durand, Wisconsin and downstream of Eau Claire, Wisconsin (Andrews, 1965; Faulkner et al., 2016). Suites of terraces exist in abundance in the reach, but are not as well preserved in the lowest third of the LCRV downstream of Durand (Faulkner et al., 2016).

1.5.2 LCRV Paleoenvironmental Conditions

There have been few investigation into the paleoenvironmental record of the LCRV from the late Pleistocene through the Holocene (Schaetzl et al., 2017). Consequently, previous conditions in the LCRV are interpreted from records in nearby locations. The LCRV was glaciated during pre-Wisconsinan and perhaps pre-Illinoian advances. Yet the exact chronology of glaciation within the study area is unknown (Syverson and Colgan, 2004; Schaetzl et al., 2017). During the Wisconsinan Glaciation the LCRV was marginal to the maximum glacial extent (Fig. 7) and thus likely experienced periglacial conditions characteristic of a tundra environment with sparse vegetative cover, permafrost, and accelerated aeolian activity as noted in other locations

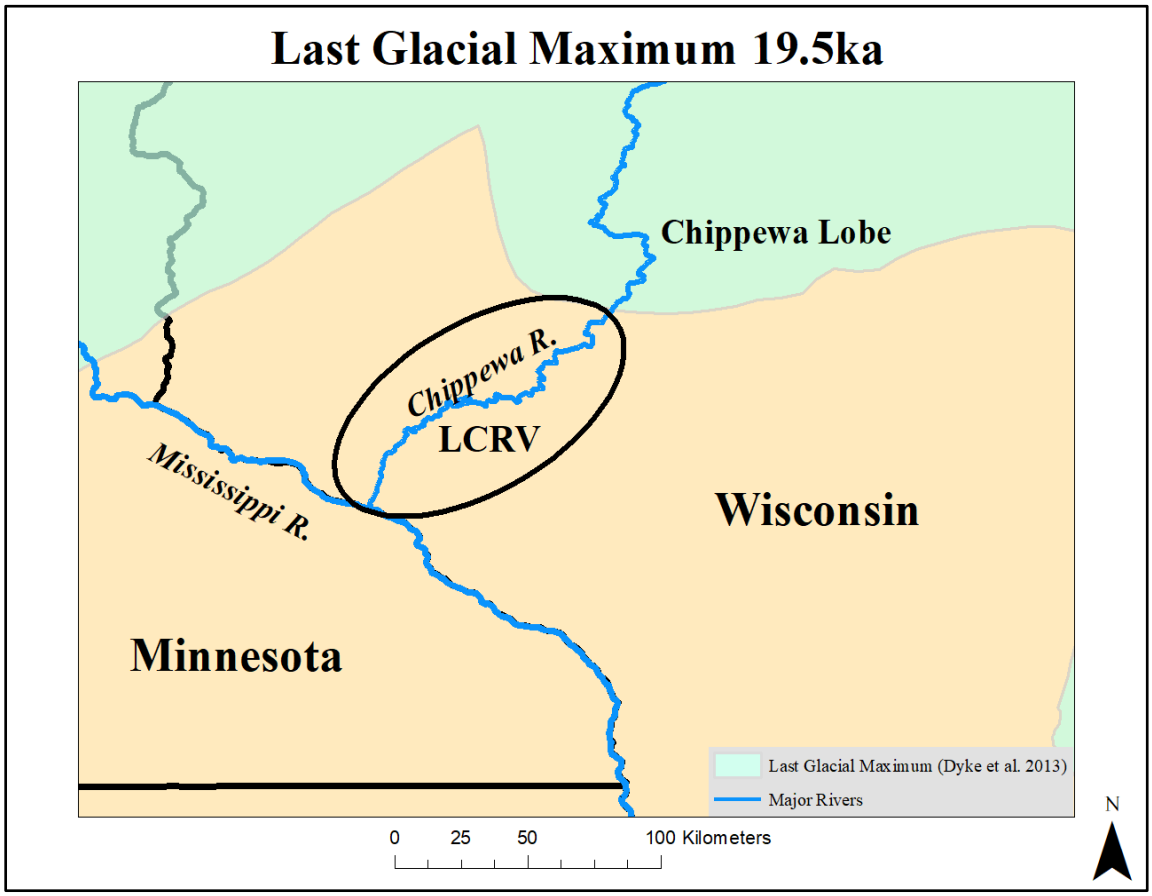

Fig. 7. The proximity of the Chippewa lobe to the LCRV during the last glacial maximum.

near the LCRV (Zanner, 1999; Mason, 2015). Ice-wedge casts, loess, and sandy aeolian deposits in northeast Iowa, southeast Minnesota, and western Wisconsin are evidence of this former periglacial environment (Mason et al., 1999; Zanner, 1999; Clayton, Attig and Mickelson, 2001; Mason, 2015; Schaetzl et al., 2017).

Sandy aeolian deposition during the late Pleistocene is interpreted within the LCRV and surrounding regions. These aeolian deposits consist of sand ramps (Hanson et al., 2015; Schaetzl et al., 2017), linear-shaped aeolian deposits (i.e., sand stringers)(Zanner, 1999; Schaetzl et al., 2017), and parabolic dunes (Zanner, 1999; Rawling et al., 2008; Miao et al., 2010; Mason, 2015; Schaetzl et al., 2017). Nonetheless, the exact chronology of sandy aeolian deposition within the LCRV and surrounding regions is poorly constrained (Mason, 2015).

Holocene paleoenvironmental conditions within the LCRV are also poorly understood. Therefore, proxy records from surrounding regions are used in this thesis to constrain Holocene climatic changes within the LCRV. These proxy records consist of lake cores (Dean, 1997), pollen records (Jacques, Cumming and Smol, 2008), radiocarbon dates (Booth et al., 2006), and speleothems (Denniston et al., 1999).

1.5 Conclusion and Research Questions

In this Master's thesis cliff-top dunes are 1) comprehensively defined based on a synthesis of prior literature and 2) are the focus of investigation to contribute to the understanding of aeolian deposition with the LCRV. The comprehensive review of research on cliff-top dunes and the mechanisms that have been ascribed to their formation

us discussed in Chapter 2. With this, a diagnostic classification scheme of cliff-top dunes is established to allocate these deposits to a set of unique environments based upon the findings of previous and research conducted by this thesis. Chapter 3 expands on this synthesis by investigating poorly understood cliff-top dunes in the LCRV to determine their spatial distribution, age, origin, and paleoenvironmental significance in this landscape. Therefore, this thesis will address the following questions:

1. What are cliff-top dunes how can a review of cliff-top dune research be a holistic and edifying document that guides future investigations to recognize the complexity of these features and affiliated landscape processes?
2. How did cliff-top and parabolic dunes in the LCRV form and what their spatial distribution and depositional chronology?
3. How do cliff-top and parabolic dunes fit into what is already known about the paleoenvironmental conditions during aeolian deposition and the landscape evolution of the LCRV?

Chapter 2

2.1 Introduction

Cliff-top dunes are prominent landforms in aeolian landscapes that record past geomorphic processes and climatic conditions. Additionally, archaeological artifacts have regularly been documented buried or adjacent to cliff-top dunes, which if not a causal relationship, provide a resource for investigation of previous peoples (White, 1960; Beaudoin, Wright and Ronaghan, 1996).

Cliff-top dunes are found in a variety of environments, formed by different geomorphic processes, supplied by varying sources of sediment, and composed of sediment with an assortment of sizes. Consequently, there are a wide range of terms and formation models for cliff-top dunes. To promote clarity, cliff-top dunes are defined as: aeolian deposits in cliff-top position that possesses a discernable morphology and are produced by a combination of geomorphic processes interacting with a topographically-altered wind regime. Each of the defining characteristics for cliff-top dunes will be examined within this chapter.

2.1.1 Disjointed Cliff-Top Dune Research

Despite their value as a geomorphic feature, the documentation and research on cliff-top dunes lacks synthesis. Jackson and Nevin (1992, pp. 81) stated that cliff-top dunes are a “rare and little researched category” which conflicts with Rawling, Fredlund and Mahan (2003, pp. 81), who suggested processes forming cliff-top dunes are “well

documented." To further highlight the discontinuity in cliff-top dune research, Jackson and Nevin (1992) were referring to cliff-top dunes in coastal settings in contrast to terrestrial cliff-top dunes described by (Rawling, Fredlund and Mahan, 2003). When present, textbook definitions of cliff-top dunes are incomplete as they are not inclusive of all landscape locations and processes that produce them (Livingstone and Warren, 1996; Tsoar, 2001; Pye and Tsoar, 2009). Rawling, Fredlund and Mahan (2003) provided a brief review of cliff-top dune research that was limited to terrestrial processes of the White River Badlands of South Dakota. Loope and Arbogast (2000) and Arbogast et al. (2017) summarized cliff-top dune research along the Great Lakes, which hosts the most extensive investigations of cliff-top dunes (Fig. 4) (Cowles, 1899; Olson, 1958a; Olson, 1958b; Olson, 1958c; Snyder, 1986). Yet, coastal cliff-top dune research is not integrated with terrestrial cliff-top dunes.

In an attempt to categorize "valley marginal dunes", Bullard and Nash (2000, pp. 370) described inherent flaws with sand dune classification methodologies, whereby differences in criteria and terminology promote confusing and redundant classification schemes. Sand dunes formed by the same processes can therefore be classified with different names (Bullard and Nash, 2000). Cliff-top dunes are subject to variable methods of classification, and indeed the valley marginal dunes described by Bullard and Nash (2000) are consistent with cliff-top dune processes. Thus cliff dunes (Sharp, 1949), cliff-top dunes (Jennings, 1967), bluff-top dunes (Arbogast et al., 2017), perched dunes (Dow, 1937), and valley marginal dunes (Bullard and Nash, 2000) describe landforms in the same landscape position. Moreover, these dunes with variable names share a common genesis that involves localized topographic modifications to the wind regime.

2.1.2 Objectives

Cliff-top dunes are a unique, valuable, and poorly understood geomorphic feature. Therefore, a comprehensive literature review of cliff-top dunes is provided and is used to describe commonalties in cliff-top dune formation processes and locations. From these common cliff-top dune research themes, a new classification scheme is constructed. Cliff-top dunes are classified based upon the environments in which they are found and characterized by the geomorphic processes that form them. Models adapted from literature are produced and describe cliff-top formation using the geomorphic processes within each environment. Finally, cliff-top dunes along the LCRV are used as a case study which applies the new classification scheme and models and contributes to the understanding cliff-top dune formation.

2.2 Topoclimatology and Cliff-Top Dunes

Although cliff-top dunes are found in variety of climates and landscapes, they share a single commonality. The escarpment they are situated upon modifies air flow, thereby allowing cliff-top dunes to form (Livingstone and Warren, 1996; Tsoar, 2001; Pye and Tsoar, 2009). Cliff-top dunes therefore are formed by localized wind conditions which may deviate from the regional wind regime (Bullard and Nash, 2000). In accordance, Pye and Tsoar (2009) categorized cliff-top dunes alongside climbing, lee, and falling dunes in their relation to topographical influences (Fig. 2).

Cliff-top dune formation invariably depends upon predominant wind directions that are perpendicular to the escarpment (Olson, 1958a; David, 1972; Bégin, Michaud

and Filion, 1995; Arbogast et al., 2017). As wind strikes the escarpment it is compressed, and in response accelerates to maintain energy transfer (Fig.8) (Olson, 1958a). The increased wind velocities thus have competence to entrain and transport exposed material along the escarpment (Bégin, Michaud and Filion, 1995; Larson et al., 2008; Schaetzl et al., 2017).

Several investigations have modeled an escarpment's effects on wind flow(Landsberg and Riley, 1943; Bowden and Lindley, 1977). Bowden and Lindley (1977) used wind tunnel measurements to determine the extent to which the air flow striking escarpments of varying slope angle is amplified. Bowden and Lindley (1977) described minor variability in modifications to flow with slope angles ranging from 90 to 45 degrees, with the largest increases in flow velocity occurring near the crest of the slope. Once past the crest of the slope, wind flow turbulence along the surface increased with a concomitant decrease in flow velocity (Bowden and Lindley, 1977). Isard (1987) found that wind velocities along a knoll increased at the crest by 4-10% compared to lower slopes and 21-32% comparedto theleeward slope.. Olson (1958a) and Landsberg and Riley (1943) recorded a similarly increased wind velocity near the crest of a sand dune. In contrast, Bullard and Nash (2000) suggested steep hills or escarpments obstruct wind and decrease its velocity, thereby depositing climbing dunes. Tsoar (1983) modeled wind flow along slopes ranging from 45 to 90 degree inclinations and similarly indicated decreased wind flow velocities occur near the base of escarpments. This is the result of winds deflecting downwards and away from an escarpment and creating vortices known as reverse-flow eddies (Tsoar, 1983). Reverse-flow eddies are critical to accumulation of echo and climbing dunes, which accumulate at the base of an escarpment. Cliff-top dunes

are formed by wind flow streamlines that are deflected upwards over an escarpment (Fig. 8). As a result, cliff-top dunes are related to echo and climbing dunes by escarpment modifications to wind flow, but are distinguished by different wind flow dynamics at different locations along an escarpment.

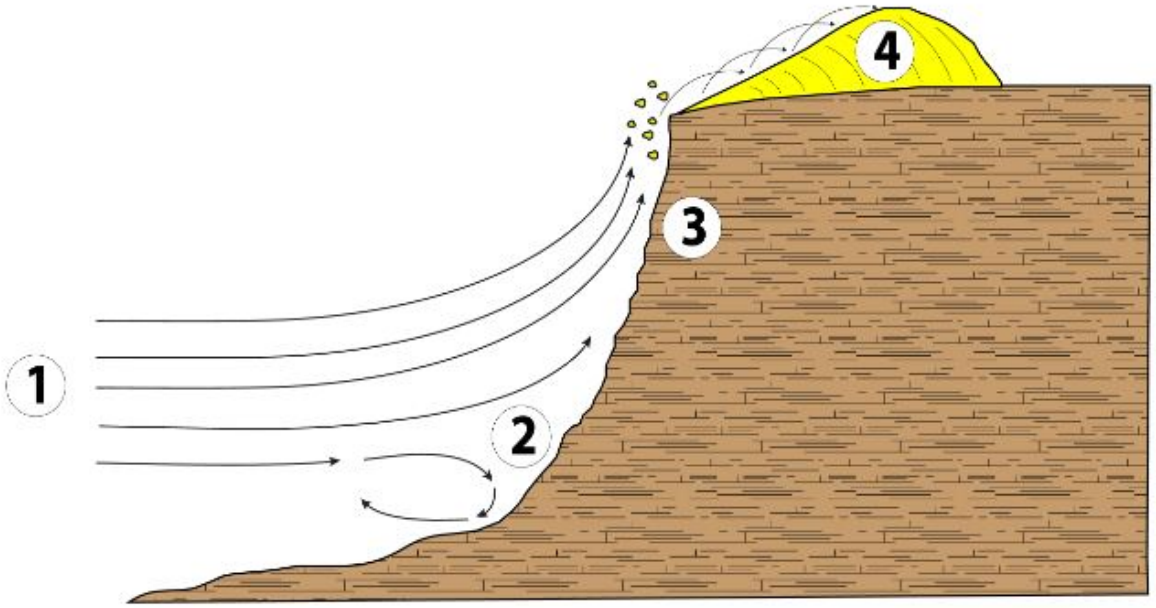

Fig. 8. Escarpment modification to wind flow enables cliff-top dune formation. 1: Wind regime perpendicular to the escarpment, 2: Wind streamline separate (i.e point of stagnation) into up-escarpment and down escarpment directions, 3: Compression and acceleration of wind flow and causes deflation of sediment near the escarpment's crest, 4:Cliff-top dune deposition.

Thornthwaite (1961, pp. 217) recognized the variable nature of climate at localized scales and created the term topoclimatology, which incorporates "the physical properties of the earth's surface that share in the development of climates". Topoclimatology describes how varying slopes and aspects of the earth's surface changes a climate's wind dynamics, heat and moisture exchanges, and soil and vegetation types at scales determined by the size of geomorphic features (Thornthwaite, 1961). Thus, escarpment wind flow modifications that produce cliff-top dunes are example of a

topoclimate. Cliff-top dunes are thus a geomorphic response to topography altering climates at small scales.

Wind flow measurements on slopes of varying angles reveal that wind velocities are accelerated and maximized near the windward crest of a topographic obstruction (Landsberg and Riley, 1943; Bowden and Lindley, 1977; Isard, 1987). Correspondingly, wind flow competency in transporting sedimentary material is maximized at an escarpment's crest, which is commonly ascribed as the primary source for cliff-top dune deposits (Anderton and Loope, 1995; Loope and Arbogast, 2000; Saye, Pye and Clemmensen, 2006; Mason, 2015). Unfortunately, previous research that suggests most cliff-top dune material derives from the escarpment (Saye, Pye and Clemmensen, 2006; Mason, 2015), does not specify the location along the escarpment from where it is derived. Cliff-top dunes are located on escarpments where accelerated wind velocities have decreased sufficiently to inhibit transport of aeolian material (Olson, 1958a). Moreover, the location of cliff-top dunes represents an environmental threshold. Cliff-top dunes are downwind of accelerated wind velocities and an exposed source of sediment and upwind of wind velocities unable to transport them (Fig. 8). Topoclimatology allows cliff-top dune formation to be understood in a broader field of research that describes climatic alteration by topography at geomorphic scales.

2.3 Diagnostic Classification Methodology

In order to provide a better-informed, holistic understanding of cliff-top dunes, a new classification is established here. Cliff-top dunes are found in a diversity of locations that possess variable climates (Fig. 4). Nonetheless, there are diagnostic landscapes

assemblages which are characterized by wind regimes, escarpments, and erosion processes that are consistently ascribed to cliff-top dune formation (e.g. White, 1960; Jennings, 1967; Saye, Pye and Clemmensen, 2006). As a result, a diagnostic classification methodology for cliff-top dunes is developed based upon the landscape assemblage that determines their formation (Fig. 9). This classification scheme is divided into two generalized environments consisting of: (1) a coastal setting, and (2) a terrestrial setting. Within each of these two environments there are two subset landscape assemblages. The first landscape assemblage within the coastal setting is termed *coastal normal* which is related to shoreline transgressions, geomorphic processes, and sources of sand that are unique to coastal settings. The second landscape assemblage within the coastal setting is termed *coastal hybrid*, which incorporates geomorphic processes and sources of sand inclusive of coastal and terrestrial settings. The first landscape assemblage within terrestrial settings is termed *terrestrial normal*, which is restricted to dryland escarpment geomorphic processes and non-littoral sources of sand. The second landscape assemblage within terrestrial settings is termed *terrestrial fluvial*, which involves escarpment destabilization by fluvial processes and non-littoral sources of sand. A literature review of cliff-top dune research in both environmental settings involving all four landscape assemblages is provided. A holistic model for the development of each cliff-top dune type is then produced. These models are based upon commonalities in geomorphic processes and sources of sand within cliff-top dune research.

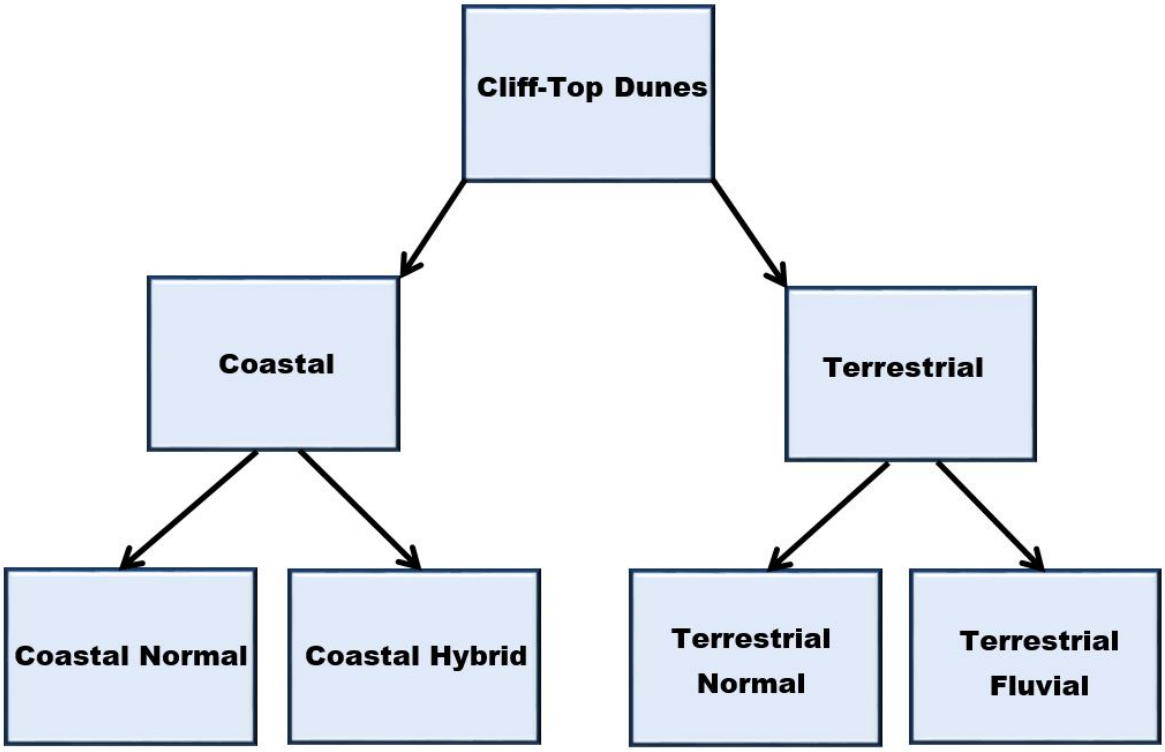

Fig. 9. A new classification method for cliff-top dunes.

2.4 Coastal Cliff-Top Dunes

Cliff-top dunes in coastal settings were the first cliff-top dune type to be scientifically documented and have since been researched more thoroughly than terrestrial cliff-top dunes (Table 2, Appendix A). Consequently, there are multiple hypotheses that model the formation of coastal cliff-top dunes (Howchin, 1923; Jennings, 1967; Saye, Pye and Clemmensen, 2006) These coastal cliff-top building models involve static shoreline levels (Saye, Pye and Clemmensen, 2006) shoreline transgressions (Olson, 1958c; Jennings, 1967; Ho et al., 2017) and inland geomorphic processes (Howchin, 1923; Jennings, 1967; Wilson, 1989; Hétu, 1992; Englebright et al., 2000). Thus, there is not a single formation process for coastal cliff-top dunes, as the variable models for their formation are specific to conditions limited to the respective research

study areas. To establish a better understanding of the multiple processes involved in coastal cliff-top dune formation, a brief review of coastal cliff-top dune formation research is provided. Coastal-cliff top dunes are then classified and a holistic model for their development is produced. This model is based upon commonalities in geomorphic processes and sources of sand within coastal cliff-top dune research.

2.4.1 Coastal Cliff-Top Dune Research

During the late 19th Century research of coastal cliff-top dunes first began along the coastlines of southern Australia (Tate, 1879) and the Great Lakes Region (Cowles, 1899). These two regions have subsequently become the two primary sources for coastal cliff-top dune research (e.g. Howchin, 1909; Gates, 1950; Olson, 1958; Olson, 1958a; Olson, 1958b; Olson, 1958c; Jennings, 1967; Snyder, 1986; Short, 1988; Anderton and Loope, 1995; Arbogast and Loope, 1999). The clustering of cliff-top dune research in these two locations can in part be attributed to them having a relatively high density of cliff-top dunes (Fig. 4). Cliff-top dunes in southern Australia for example, cover over 370 square kilometers (Short, 1988).

During a geological survey of the Great Australian Bight, Tate (1879, pp. 99) documented the existence of loose sand deposits "crowned" atop the Bunda sea cliffs. He described these deposits as "dome-like" and formed from sand blowing up 61m high sea cliffs Tate (1879, pp. 99). At the end of the 19th century, sand dunes were also described as being "perched" on high bluffs along the coast of Lake Michigan in northern Michigan (Cowles, 1899). Cowles (1899) ascribed the genesis of these cliff-top dunes to wind energy dissipating upon reaching the escarpment's crest (Cowles, 1899). During the early 20th Century, aeolian features along islands immediately off the southern coast of

Australia were documented as wind-blown “indurated sand hills” hardened by a travertine crust and located in cliff-top positions (Howchin, 1909, pp. 211). Howchin (1909) found that cliff-top dunes in coastal position along Australia’s Bight formed by aeolian transport of inland sources of sand.

Research by Jerry Olson described wind flow (Olson, 1958a), vegetative cover (Olson, 1958b), and shoreline transgressions (Olson, 1958c) that affected dune formation, including those in cliff-top positions, along Lake Michigan. Olson (1958a) description of ecological-landscape interactions expanded upon the previous work in the region (Cowles, 1899). Olson’s work was influential in its own right, but especially so when considering his model describing cliff-top formation in relation to lake levels. His model produced a new “paradigm” for aeolian processes in coastal environments (Loope and Arbogast, 2000, pp. 215).

In the model developed by Olson (1958c), sand dunes marginal to the shoreline (i.e., foredunes) develop during low lake levels and migrate inland where they accumulate in upland beaches. During high lake levels, the dunes that accumulated on the upland beaches are truncated and placed in cliff-top position (Olson, 1958c). In contrast, subsequent research along Lake Michigan and Lake Superior indicated that cliff-top dunes form during high shorelines when waves undercut and mobilized sedimentary material on lakeside escarpments (Snyder, 1986; Marsh and Marsh, 1987; Marsh, 1990; Anderton and Loope, 1995; Loope and Arbogast, 2000). The sedimentary material is then deflated and transported to cliff-top locations when winds have sufficient velocities and are perpendicular to the escarpment (Snyder, 1986; Marsh and Marsh, 1987; Marsh, 1990; Anderton and Loope, 1995; Loope and Arbogast, 2000). Loope and Arbogast

(2000, pp. 420) suggested that the two non-conforming processes of cliff-top dune formation along Lake Michigan "is probably due to differences in each factors [sic] as littoral sand supply, winds, and waves". Additionally, Arbogast, Hansen and Van Oort (2002) found that along southeastern Lake Michigan these two contrasting cliff-top formation processes of a high shoreline/escarpment undercutting and a low shoreline/littoral supply, could be active on the same cliff-top dunes at different time periods.

Outside of the Great Lakes region, there is even greater complexity in coastal cliff-top dune formation. Jennings (1967) developed a model that depicts four scenarios for cliff-top dune formation in southern Australia. Jennings's model involves varying coastline transgressions and sand supply for cliff-top dune formation (Fig. 10) (Jennings,

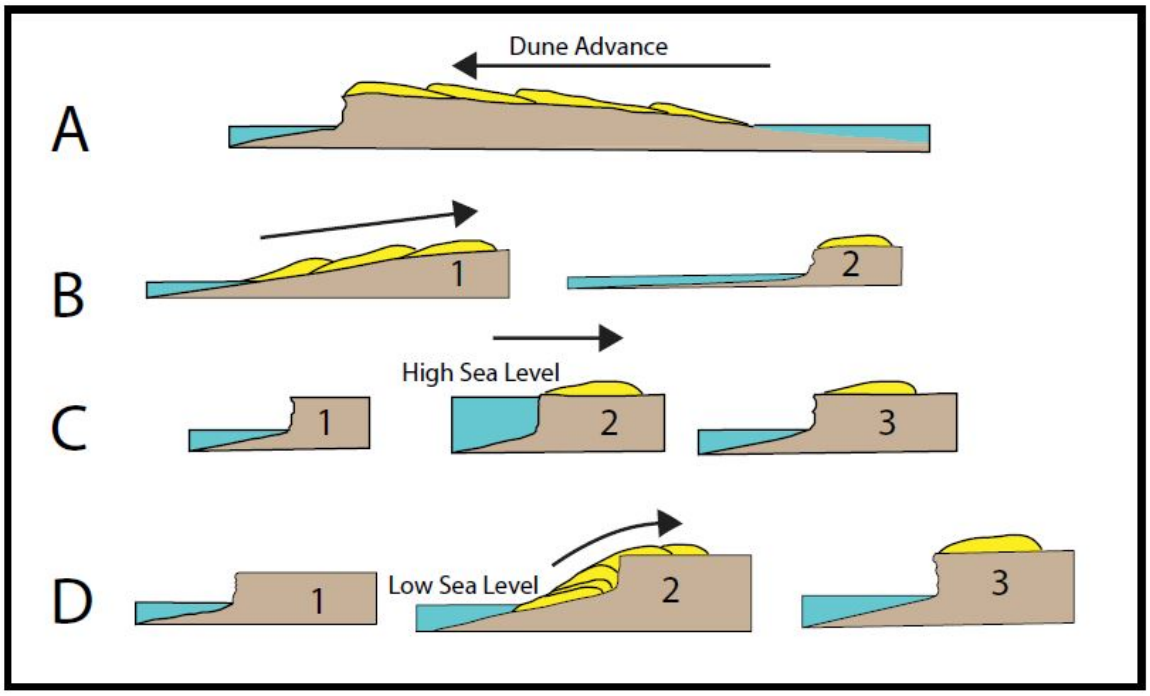

Fig. 10. Four means of cliff-top dune formation in a coastal setting adopted from Jennings (1967).

1967). In the first scenario of Jennings's model (Fig. 10, A), dunes in cliff-top position are supplied by inland sources of sand such as a dry embayment (Jennings, 1967). The second scenario (Fig. 10, B) involves beach marginal dunes supplied by littoral material which advance up a gentle bedrock incline (Jennings, 1967). Subsequent shoreline regression separates the dunes from their sand supply which are then left in cliff-top position (Jennings, 1967). In the third scenario (Fig. 10, C), high shore line levels allow dunes to develop along a pre-existing, inundated, escarpment (Jennings, 1967). When shore line levels drop, the escarpment is exposed and the dune is left in cliff-top position (Jennings, 1967). The 4th scenario (Fig. 10, D) involves a pre-existing escarpment produced by shoreline recession (Jennings, 1967). The lowered shoreline also exposes littoral sediment which is transported inland by wind and accumulates into dunes that climb and overtop the exposed escarpment (Jennings, 1967). When the shoreline rises, the climbing dune is truncated so that only the cliff-top deposits are preserved (Jennings, 1967). The shoreline then recedes again, exposing the escarpment and leaving behind cliff-top dunes.

Subsequent research on coastal cliff-top dunes (Pain, 1976; Short, 1988; Haslett, 2000; Saye, Pye and Clemmensen, 2006; Costas et al., 2010; Ho et al., 2017) utilized and expanded upon the model produced by Jennings (1967) in other regions. Haslett (2000, pp. 86) researched cliff-top dunes in Brittany, France and developed a model for their formation "that comprises elements of two models originally suggested by Jennings (1967)". Ho et al. (2017) investigated a cliff-top dune in Taiwan and found that its formation was consistent with the 4th scenario in the model by (Jennings, 1967), except the final shoreline lowering was supplanted by inland tectonic uplift. Saye, Pye and

Clemmensen (2006) suggested that coastal cliff-top dune formation in Denmark can be independent of shoreline transgressions. They created a model for cliff-top dune formation involving four scenarios under constant shoreline levels (Saye, Pye and Clemmensen, 2006).

2.4.1.1 Coastal Normal Model

Models for coastal normal cliff-top dune development are site-specific, as they vary according to geomorphic processes at localized scales. Nonetheless, there is a set of diagnostic geomorphic characteristics (e.g., wave undercutting; shoreline transgressions; strong offshore winds) for cliff-top dunes in coastal settings (Table 2, Appendix A). A generalized model is developed from these diagnostic geomorphic characteristics (Fig. 11). This model is inclusive of all pathways for cliff-top dune formation related to coastal geomorphic processes as described in the literature. The model is structured into two sets of two different time series. The first two time series (Fig. 11 A, C) describes the various locations and processes that supply sand to cliff-top dunes. The second two second time series (Fig. 11 B, D) describes the multiple coastal geomorphic processes that place dunes in cliff-top position.

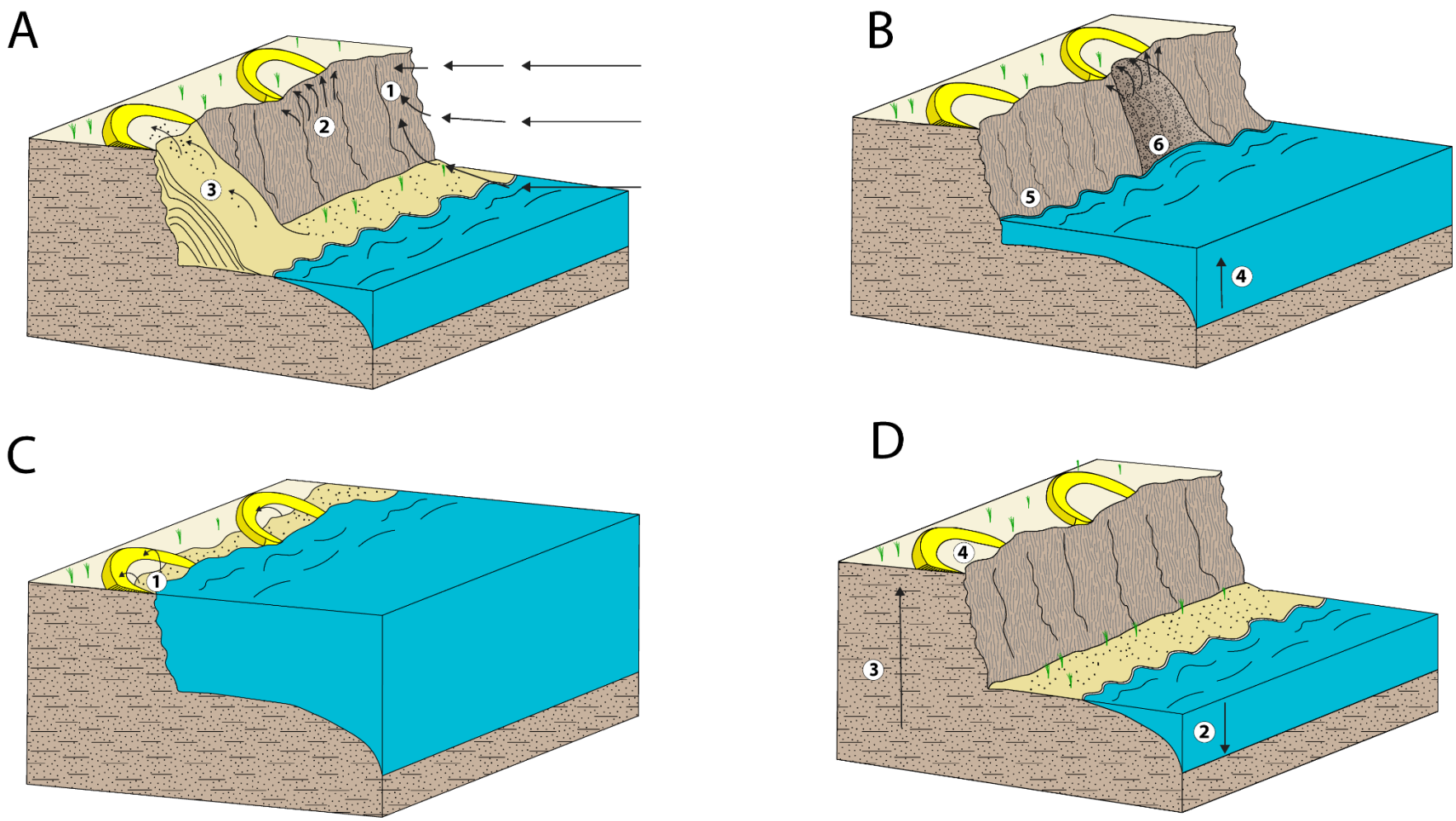

1

Fig. 11. An adatpted model for coastal normal cliff-top dune formation. A1: Escarpment compression of airflow and strong offshore winds, A2: Cliff-top dune produced by deflation of escarpment material, A3: Sand dune supplied by sand ramp built from littoral material. B4: Rise in shoreline, B5: Sand ramp eroded, cliff-top dune remnant, B6: Higher shoreline undermines escarpment and exposes unconsolidated material to deflation resulting in cliff-top dune formation.C1: High shoreline inundates escarpment and dunes are beach marginal dunes are built. D2: Lowered shoreline puts beach marginal dunes in cliff-top position or D3: Tectonic uplift puts beach marginal dunes in cliff-top position.

2.4.1.2 Coastal Hybrid Model

Cliff-top dunes in coastal settings can also form from a combination of inland and coastal sources of sand and geomorphic processes. Howchin (1923) described cliff-top dune features along the southern shore of Australia, which evidently were not supplied by the rocky littoral material at the base of the escarpment. He observed that sand blew off the cliff-top dunes and down the escarpment and concluded that the sandy material originated from inland fluvial systems (Howchin, 1923). Howchin (1923) in part, inspired Jennings (1967, pp. 48) to state:

> "Convergence of landforms owing their character to different origins and history is a principle well demonstrated…Nevertheless, even though we must not expect all cliff-top dunes to originate in the same manner, this principle of convergence must not dissuade us from attempting to assess the different mechanisms which have been proffered for their explanation and their probable frequencies. There can be little doubt that some cliff-top dunes arrived in their position by the 'back-door' as it were, that is from some source not apparent at first sight…"

Jennings (1967) thus, created the cliff-top dune formation model scenario A as described above (Fig. 10). Evidently without knowledge of Howchin's (1923) and Jennings' (1967) work, Englebright et al. (2000) described the formation of cliff-top dunes in Long Island, New York by using coastal and terrestrial landscape processes. Englebright et al. (2000) described the cliff-top dunes as parabolic dunes that have since been truncated by escarpment erosion along the Long Island north shore. Moreover, Englebright et al. (2000) suggested that despite being truncated, these cliff-top dunes were not produced by geomorphic processes along the shoreline. Instead, these dunes climbed the inland-facing slope of Harbor Hill Moraine opposite the 30m high sea-cliffs (Englebright et al., 2000). The sand composing the cliff-top dunes was deflated from the Long Island Sound which is presently inundated by seawater. Yet during the terminal Pleistocene lower sea levels and an enhanced wind regime exposed the Long Island Sound to aeolian deflation.

During these late Pleistocene conditions, the parabolic dunes climbed and summited the Harbor Hill Moraine and then stabilized following glacial retreat and climate amelioration (Englebright et al., 2000). The genesis of these cliff-top dunes was therefore a perplexing combination of coastal (sea-level transgression) and terrestrial (continental glacial, inland sand supply) processes (Englebright et al., 2000).

Additionally, aeolian cliff-top deposition of coarse sand to gravel-sized material in coastal environments has been recorded in high latitude locations such as Ireland, Canada, and Alaska (Wilson, 1989; Hétu, 1992). These aeolian deposits often lack a sand dune morphology, as they are partially composed of material coarser than sand (Wilson, 1989; Hétu, 1992). Deposition of coarse aeolian sediments in coastal environments is related to exceptionally strong wind regimes due to the fetch effect, which is the increase in sediment transport capacity with distance downwind of a change in surface-type (i.e., leading edge) (Oke, 1987). Coastal winds are then accelerated by the topoclimatic effects of an escarpment compressing wind flow. Therefore, coastal winds gain the competence to transport exceptionally coarse aeolian material up escarpments to cliff-top locations.

Cliff-top aeolian deposition was documented on top of Muckish Mountain in Ireland (Wilson, 1989). Although 8km inland from the coast, Muckish Mountain is described as having maritime climate that receives up to 2m of annual precipitation and experiences exceptionally strong winds deriving from the coast. The aeolian deposits on Muckish Mountain lack a sand dune morphology and were described as sand sheets and sand islands along the crest of its north-facing escarpment (Wilson, 1989). Despite predominant winds originating from the south and west, Wilson (1989) suggested the aeolian deposits were produced by northwest winds. The northwest facing escarpment of Muckish Mountain contains friable quartzite beds, thus providing grains susceptible to

aeolian transport (Wilson, 1989). Wilson (1989) emphasized the importance of localized wind conditions in the transport and deposition of the deposits.

In an analogous humid maritime mountain environment located along the St. Lawrence Estuary of northern Gaspésie, Canada, aeolian processes were recorded along Mount Saint-Pierre. Mount Saint-Pierre is vegetated by boreal forest, but its windward facing northwest escarpment is dissected by unvegetated erosional "funnels" created by mass wasting events (e.g., rockfalls, debris flows) that produce talus deposits at its base (Hétu, 1992, pp. 96). During a 1988 blizzard, sustained winds of 72km/hr or greater were documented with the highest recorded velocity reaching 99.4km/hr. Resulting niveo-aeolian deposits were found in cliff-top positions covering snow that accumulated during the blizzard (Hétu, 1992). These deposits were poorly sorted, up to 14mm thick, covered $1200m^2$, were exceptionally coarse, and included flakes of shale with a mean area of $150.4mm^2$ (Hétu, 1992).

Cliff-top dunes can also incidentally be located within coastal environments, as their formation is unrelated to coastal processes. Within the Tuktoyaktuk Coastlands of northwestern Canada cliff-top dunes were documented along escarpments adjacent to lakes, rivers, and the coastline (Rampton, 1988; Bateman and Murton, 2006). Cliff-top dune formation was ascribed to aeolian erosion along exposed, eroding escarpments that possess "fine grained glaciofluvial sediments"(Rampton, 1988, pp.77). Coastal processes were not linked to escarpment erosion and resulting cliff-top dune formation. Instead, permafrost degradation within the escarpments provides loose sediment for deflation and transport to cliff-top locations (Bateman and Murton, 2006). The tundra environment of northwest Canada thus provides the geomorphic processes that allow for cliff-top dune

formation within the region. Consequently, there appears to be a poor correlation between cliff-top dune formation and coastal processes in the Tuktoyaktuk Coastlands.

The formation of coastal hybrid cliff-top dunes is related to sources of sand and geomorphic processes that are not necessarily specific to coastal environments. Instead, they are formed independently of coastal processes (Rampton, 1988; Bateman and Murton, 2006) or by a combination of inland and coastal processes (Jennings, 1967; Wilson, 1989; Hétu, 1992; Englebright et al., 2000). Thus, the model developed for hybrid coastal cliff-top dunes expands upon scenario A of the model produced by Jennings (1967). This adapted model also includes the driving variables (e.g., permafrost degradation, mass wasting, and coastal winds) ascribed to coastal hybrid cliff-top dune formation by subsequent literature (Fig. 12) (Rampton, 1988; Wilson, 1989; Hétu, 1992; Englebright et al., 2000; Bateman and Murton, 2006).

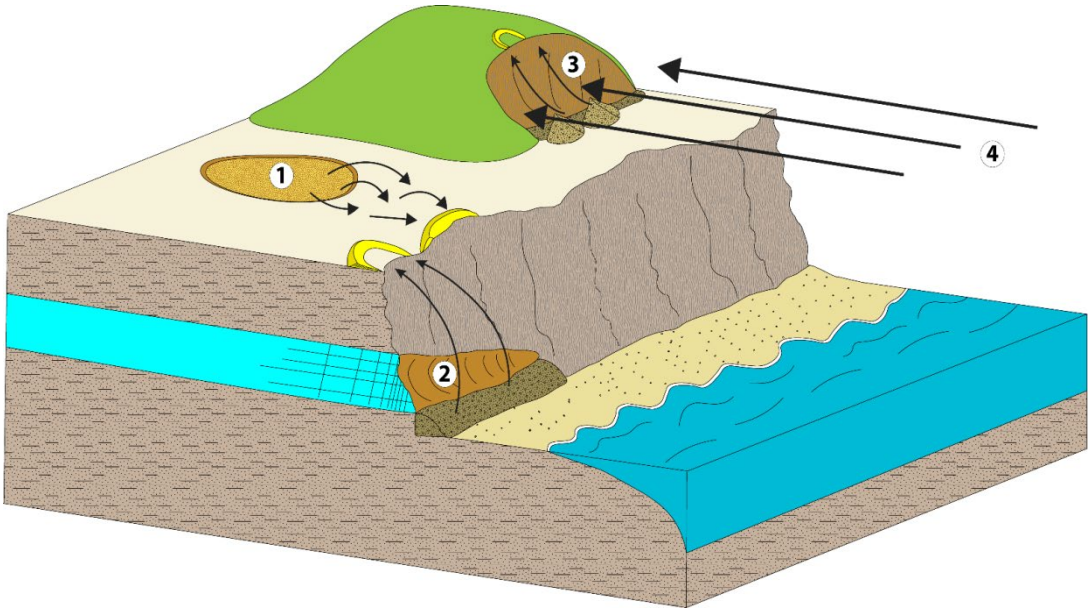

Fig. 12. An adatped model for coastal hybrid cliff-top dune formation. 1: Cliff-top dune built from sediment supplied from an inland source (e.g., lake, estuary), 2: Permafrost degradation undermines escarpment and provides unconsolidated material for deflation and cliff-top dune development, 3: Mass wasting on a windward facing upland slope provides unconsolidated colluvium, 4: Colluvium along upland slope exposed to exceptionally strong coastal fetch winds that transports sediment to cliff-top positions

2.5 Terrestrial Cliff-Top Dunes

Cliff-top dunes formed by terrestrial geomorphic processes were first recognized by researchers at the end of the 19th Century (Cowles, 1899; Howchin, 1923; Hack, 1941; White, 1960; Arbogast et al., 2017; Schaetzl et al., 2017). However, archaeological artifacts have been found within or adjacent to cliff-top dunes, which suggest they were recognized by previous peoples (Howchin, 1923; White, 1960; Valentine, Fladmark and Spurling, 1980; Beaudoin, Wright and Ronaghan, 1996). Research of terrestrial cliff-top dunes is underrepresented in comparison to coastal cliff-top dunes (Table 2, Appendix A). Moreover, little existing research synthesizes the complex and variable landscape-climate interactions required to produce cliff-top dunes in terrestrial settings. Consequently, researchers have made inconsistent statements concerning the status of terrestrial cliff-top dune research (Rawling, Fredlund and Mahan, 2003; Arbogast et al., 2017).

Terrestrial cliff-top dunes have been documented in semi-arid (White, 1960) to humid (Arbogast et al., 2017; Schaetzl et al., 2017) environments. Unlike coastal cliff-top dunes, which often have readily available littoral sources of sand, the formation of terrestrial cliff-top dunes is limited by sand supply and sand availability. Sand supply and sand availability are determined by escarpment stability, vegetative cover, and climate (Hack, 1941; White, 1960; Arbogast et al., 2017; Schaetzl et al., 2017). Therefore, cliff-top dunes have been used to constrain previous climatic changes (White, 1960; Rawling, Fredlund and Mahan, 2003) and geomorphic processes (Arbogast et al., 2017). Terrestrial normal cliff-top dunes are dependent upon the minimization of vegetative cover along escarpments or lowland sources of sand (Sharp, 1949; White, 1960; Rawling, Fredlund and Mahan, 2003) and thus can provide better records of

paleoclimates. In contrast, terrestrial fluvial cliff-top dune formation involves lateral and vertical stream erosion into and undermining a slope, thereby promoting removal of vegetation. Once vegetative cover on the escarpment is diminished, sediment is exposed and deflated by winds, allowing upslope aeolian transport and deposition (Hack, 1941; White, 1960; David, 1972; Larson et al., 2008; Arbogast et al., 2017; Schaetzl et al., 2017). In addition, fluvial incision must be concomitant with favorable conditions for aeolian activity, such as winds perpendicular to the escarpment (Arbogast et al., 2017) or increased aridity (David, 1972). Consequently, terrestrial fluvial cliff-top dune formation is dependent upon the complex interaction between climate and geomorphic processes at localized scales.

In order to remediate the inconsistencies in terrestrial cliff-top dunes research, a review of the primary literature on terrestrial cliff-top dunes is provided. Models for terrestrial normal and terrestrial fluvial cliff-top dune formation are then developed using descriptions from the literature.

2.5.1 Terrestrial Normal Cliff-Top Dune Research

In Hack's (1941) pivotal work "Dunes of Navajo Country", he detailed the intricate relationship between vegetative cover and type, and sand dune formation. He recognized climbing dunes occurring along de-vegetated escarpments (Hack, 1941, pp. 241). Additionally, he observed that climbing dunes could reach cliff-top position and are in part supplied by erosional processes along the escarpment such as gullying. Headward erosion of gullies limited growth of 'bound sand' vegetation (plants with deeper root systems) while maintaining 'loose sand' vegetation (plants with shallower root systems)

which promotes the deposition and stabilization of cliff-top dunes (Hack, 1941, pp. 259). Although a fluvial process, gullying was apparently not the primary mechanism for cliff-top formation. Hack (1941) understood the role of topography in limiting or fomenting aeolian processes. Sharp (1949) documented non-fluvial cliff-top dune formation by describing transport and deposition of unconsolidated, devegetated escarpment material upslope and atop cliffs. However, he did not indicate the morphology of the dunes or the means by which the escarpments were exposed (Sharp, 1949). Nonetheless, Sharp's (Sharp, 1949) work influenced White (1960), who developed formation models for terrestrial normal and terrestrial fluvial cliff-top dunes.

White (1960) described terrestrial normal and terrestrial fluvial cliff-top dunes within the White River Badlands of western South Dakota. Cliff-top dunes that formed independent of stream incision were documented atop buttes and nearby deeply incised devegetated gullies (White, 1960). Evidence of buried soils and pedogenic activity within the cliff-top dunes led White (1960) to conclude their formation was related to periods of increased aridity. A reinvestigation of White's (1960) work in the White River Badlands of South Dakota provided a brief review of cliff-top dune literature preclusive of coastal varieties that combined fluvial and terrestrial normal geomorphic processes (Rawling, Fredlund and Mahan, 2003). Rawling, Fredlund and Mahan (2003) radiocarbon dated buried soils within cliff-top dunes perched on mesas to constrain periods of dune activity and immobilization. Radiocarbon ages corroborated White's (1960) supposition of aeolian activity related to Holocene climatic variations such as increased aridity (Rawling, Fredlund and Mahan, 2003). Halfen and Johnson (2013) subsequently applied the results produced by Rawling, Fredlund and Mahan (2003) to construct a chronology of sand dune activity in the Great Plains.

A cliff-top dune located on top of Saskatoon Mountain in Alberta, Canada was used to constrain glacial retreat, and human habitation within the region (Beaudoin, Wright and Ronaghan, 1996). The southwest slope of Saskatoon Mountain provides an escarpment conducive to cliff-top dune deposition of sediment up to 2m thick (Beaudoin, Wright and Ronaghan, 1996). The subaerial lake beds produced by the draining of Glacial Lake Peace following the terminal Pleistocene served as the major sand supply for the cliff-top dune (Beaudoin, Wright and Ronaghan, 1996). The formation of this dune may have also been sustained by intermittent forest fires prior to its stabilization around 5,000 radiocarbon years before present (Beaudoin, Wright and Ronaghan, 1996). Archaeological artifacts within this dune were used to determine that Saskatoon Mountain was used as a game lookout. Ages derived from the artifacts indicate human occupation of Saskatoon Mountain occurred around 9,500 and 8,000 radiocarbon years before present (yrs B. P.). These ages helped constrain glacial retreat in the region, as conditions must have ameliorated sufficiently to attract game and human habitation. The cliff-top dune on Saskatoon Mountain was valuable for understanding the paleo-environmental conditions, landscape processes, and presence of human activity (Beaudoin, Wright and Ronaghan, 1996).

Cliff-top dunes consisting of coarse, poorly-sorted material were documented in the Palliser Triangle of southern Alberta and Saskatchewan (Lemmen et al., 1998). When storms produce high velocity winds, colluvium at the base of an escarpment is transported upslope to cliff-top positions (Lemmen et al., 1998). Deposition of these cliff-top dunes is intermittent, as their formation depends upon colluvium availability which occurs during dry periods (Lemmen et al., 1998).

2.5.1.1 Terrestrial Normal Cliff-Top Dune Model

Research on terrestrial normal cliff-top dunes describes aridity as a direct influence on their formation (White, 1960; Lemmen et al., 1998; Rawling, Fredlund and Mahan, 2003). Increased aridity affects vegetative cover and soil moisture content, which determines the availability of sediment for deflation and transport (Nickling and Neuman, 2009). Terrestrial normal cliff-top dunes are supplied by sediment that derives from escarpments (Hack, 1941; Sharp, 1949; White, 1960), colluvial deposits at the base of escarpments (Lemmen et al., 1998), and dry lake beds (Beaudoin, Wright and Ronaghan, 1996). Consequently, a model is developed for terrestrial cliff-top dune formation that utilizes the sources of sand described in the literature alongside a period of increased aridity (Fig. 13).

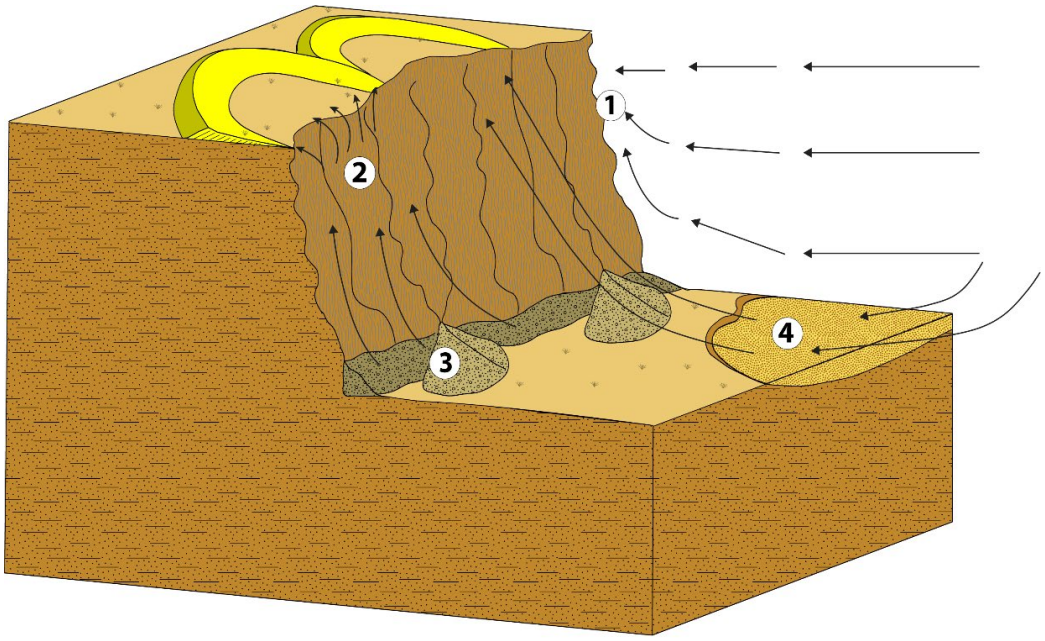

Fig. 13. An adapted model for terrestrial normal cliff-top dune formation. 1: Escarpment compression of airflow and strong offshore winds, 2: Cliff-top dune produced by deflation of escarpment material, 3: Cliff-top dune supplied by escarpment colluvial material, 4: Cliff-top dune

2.5.2 Terrestrial Fluvial Cliff-Top Dune Research

Fluvial cliff-top dunes are found in a landscape assemblage that consists of an incising stream and exposed escarpment (White, 1960; David, 1972; Arbogast et al., 2017; Schaetzl et al., 2017). The vertical stream incision that produces and mobilizes the escarpments has been ascribed to drops in their local base level (David, 1972; Bégin, Michaud and Filion, 1995; Arbogast et al., 2017; Schaetzl et al., 2017). Base level, according to Faulkner et al. (2016, pp. 75) is "a major external control or boundary condition for streams and the fluvial system that comprise them." Base level at the largest scale is the sea level (Schumm, 1993), but for tributary streams, base level can occur at local-scales and consists of lakes or larger rivers (Faulkner et al., 2016). The complex interactions between climate, topography, and fluvial processes that produce cliff-top dunes is described in recent publications (Arbogast et al., 2017; Schaetzl et al., 2017). Nontheless, it should be noted that White (1960) was the first to fully detail the means of fluvial cliff-top dune formation. He described cliff-top dunes located above steep devegetated escarpments produced by meandering streams (White, 1960). White (1960) suggested that cliff-top dune formation depended upon stream undercutting of an escarpment. Additionally, according to White (1960, pp.81) "[Cliff dunes] formed by meandering rivers or creeks may not be related to past climates. These cliff dunes could have been deposited whenever the stream undercut the high terrace to expose a new cliff to wind." Therefore, according to White (1960), fluvial cliff-top dune formation does not require an additional climatic input. Ostensibly, fluvial cliff-top dunes are affected by climate, as climate determines the wind regimes which are essential in cliff-top dune formation. Therefore, climate's influence on fluvial cliff-top dunes is investigated in terms of climatic change. Climatic change refers to a past climate that was different from

the present climate and influenced fluvial cliff-top dune formation. White's (1960) conclusion about the role of climatic change on fluvial cliff-top dunes is both corroborated (Arbogast et al., 2017) and contradicted (David, 1972; Bégin, Michaud and Filion, 1995) by subsequent research. The influence of climatic change on fluvial cliff-top dune formation will be discussed through observations within the literature and investigated within the LCRV case study.

David (1972) ascribed periods of greater aridity to the formation of an active fluvial cliff-top dune in the Great Sand Hills of Saskatchewan, Canada. The cliff-top dune parallels a meander bend of the South Saskatchewan River and it reaches its maximum size at the crest of the meander bend (David, 1972). The cliff-top dune is supplied by escarpment colluvium and sediments at the valley floor (David, 1972). A drop in base level related to the draining of glacial lake during the terminal Pleistocene caused vertical incision along South Saskatchewan River. Deposition of the cliff-top dune did not occur until increased aridity reduced vegetative cover along the escarpment. Buried soils within the cliff-top dune correspond to more humid conditions, when vegetative cover protected the escarpment from deflation. According to David (1972), the cliff-top dune records at least ten periods greater humidity during its formation throughout the Holocene.

In northwest Canada, Bégin, Michaud and Filion (1995) modeled the complex landscape evolutionary processes that produced a large cliff-top parabolic dune above an escarpment flanking the Mountain River. A drop in local base level caused by the breach of a natural fluvial dam along the Mountain River, resulted in the river's vertical incision and pattern change from a braided to a single channel. Vertical incision along the river produced an abandoned floodplain and newly-created escarpments consisting of fluvial

fill. The fluvial fill within the escarpment provided sediment susceptible to aeolian deflation and transport to cliff-top positions (Bégin, Michaud and Filion, 1995). In addition, katabatic winds from the nearby mountain ranges flow down the river valley and strike the exposed escarpment at a perpendicular angle, thus supplying wind velocities capable of entrainment and transport of colluvial deposits (Bégin, Michaud and Filion, 1995). The absence of other cliff-top dunes along Mountain River indicates that katabatic winds striking the escarpment at a perpendicular angle below cliff-top dune investigated by Bégin, Michaud and Filion (1995) was significant to its formation. Additionally, modern regional climatic warming was attributed to the activation of the cliff-top dune (Bégin, Michaud and Filion, 1995). Higher discharges and decreased permafrost further undermine and destabilize the escarpment, thereby inducing greater vegetation removal. Additionally, warmer winters increase the thermal gradient between alpine and lowland regions resulting in more intense katabatic winds with a greater capacity to transport aeolian material (Bégin, Michaud and Filion, 1995).

Recent research in Wisconsin (Schaetzl et al., 2017) and Michigan (Arbogast et al., 2017) have similarly provided comprehensive models for fluvial cliff-top dune formation. Vertical and lateral fluvial incision, sand supply, sand availability, and wind regime and wind fetch are described in the model developed by Arbogast et al. (2017) for cliff-top dune formation along Michigan's Au Sable River. A drop in base level along the Au Sable River caused it to vertically incise into its substrate and produce escarpments (Arbogast et al., 2017). A subsequent rise in base level caused the Au Sable to migrate laterally and undercut escarpments, thereby exposing their sediments to aeolian deflation and transport (Arbogast et al., 2017). Additionally, the distribution of cliff-top dunes along the Au Sable River was determined by the predominant wind regime (Arbogast et

al., 2017). They were formed along escarpments oriented perpendicular to the northwesterly paleo-wind wind regime (Arbogast et al., 2017). According to Arbogast et al. (2017), climatic change was not a driving factor for cliff-top dune formation, as vegetation was removed along the escarpment by intrinsic geomorphic processes (river adjustments base level changes) (Arbogast et al., 2017). Schaetzl et al. (2017) similarly describe cliff-top dune formation along the Chippewa River in relation to the river's response to changes in its base level. The cliff-top dune formation model and preliminary findings by Larson et al. (2008) and Schaetzl et al. (2017) will be discussed within the LCRV case study section.

2.5.2.1 Terrestrial Fluvial Cliff-Top Dune Formation Model

There is limited research on terrestrial fluvial cliff-top dunes and the role of climatic change is inconsistently applied to their formation. Nonetheless, there are consistent themes within the research involving geomorphic processes and sources of sand for fluvial cliff-top dune formation. A generalized terrestrial fluvial cliff-top dune model is developed from commonalities within the research and consists of: an incising stream, an exposed escarpment, and sediment supply deriving primarily from the escarpment (Fig. 14). This model is applied to cliff-top dunes identified along the LCRV.

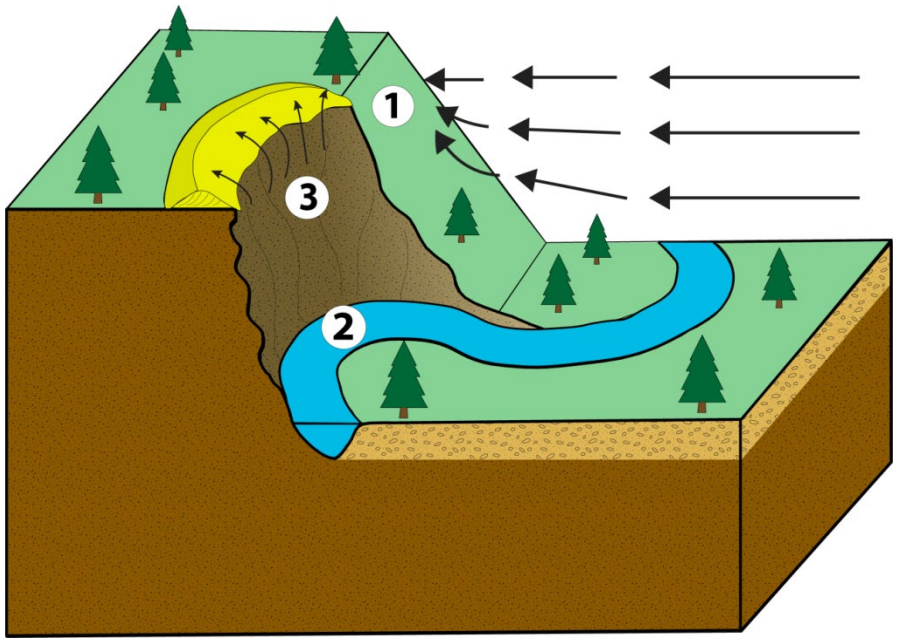

Fig. 14. An adapted model for terrestrial normal cliff-top dune formation. 1: Escarpment compression of airflow, 2: Fluvial erosion exposes escarpment material to deflation, 3: Cliff-top dune produced by deflation of escarpment material, 3: Cliff-top dune supplied by escarpment colluvial material.

2.6 Lower Chippewa River Valley Case Study

2.6.1 Introduction

Cliff-top dunes within the LCRV are located above the terrace escarpments of the Chippewa River that consist of fine to gravelly sand (Larson et al., 2008; Faulkner et al., 2016; Schaetzl et al., 2017). Previous research on these dunes has been limited to the Roy Street Dune (RSD) which was first

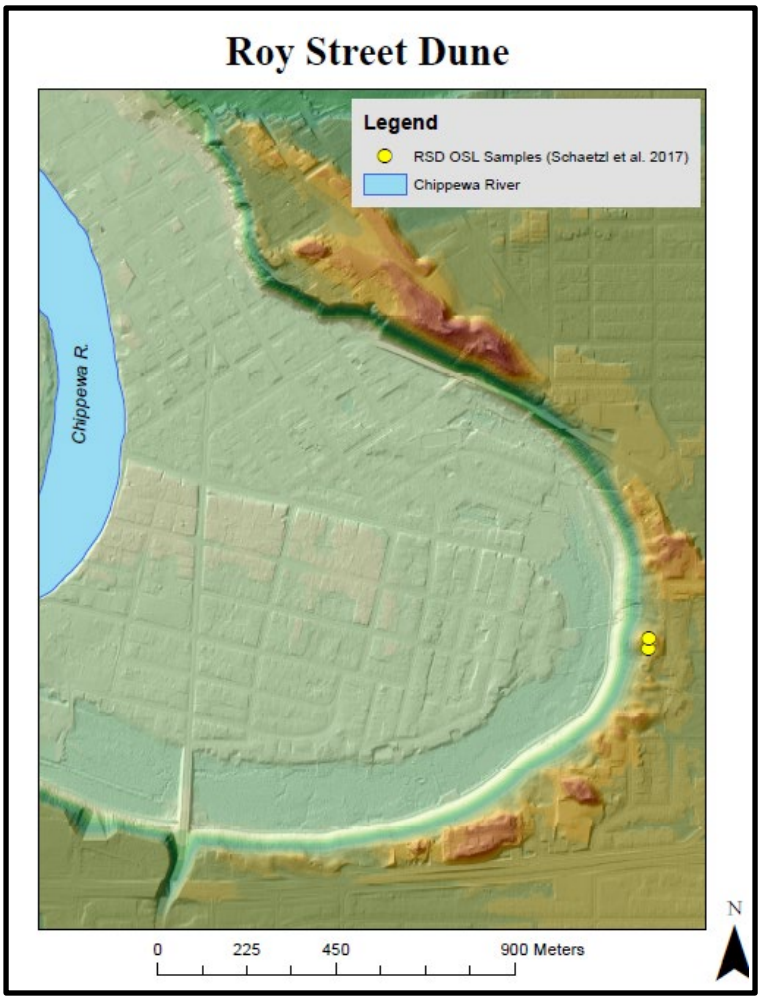

Fig. 15. Location of the Roy Street Cliff-top Dune in Eau Claire, Wisconsin.

identified by Larson et al. (2008) and then dated via OSL by Schaetzl et al. (2017). RSD is located along an abandoned meander within the city of Eau Claire, Wisconsin (Fig. 15) (Larson et al., 2008; Schaetzl et al., 2017). RSD is composed of medium sand (250-350 micrometers (μm)) and exhibits internal bedding with slip faces angled to the southeast which indicates it formed by northwest winds (Fig. 16) (Larson et al., 2008; Schaetzl et al., 2017). Winds were predominately from the northwest during the late Pleistocene and into the early to mid-Holocene (Schaetzl et al., 2017).

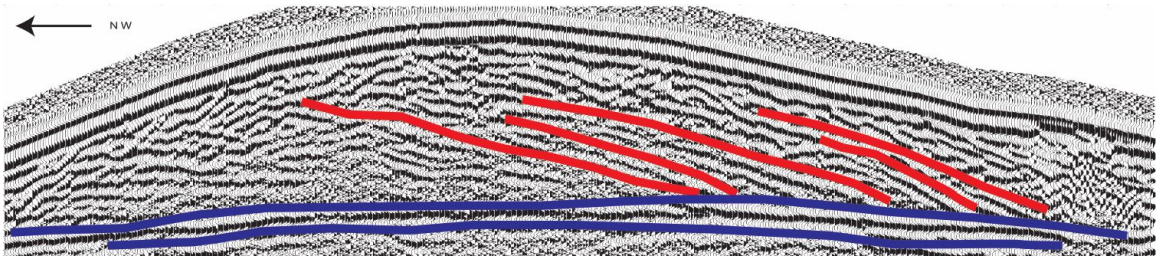

Fig. 16. A ground penetrating radar image of the cross bedding within RSD. It depicts slipfaces dipping to the southeast, which suggests a northwest wind regime Larson et al. (2008).

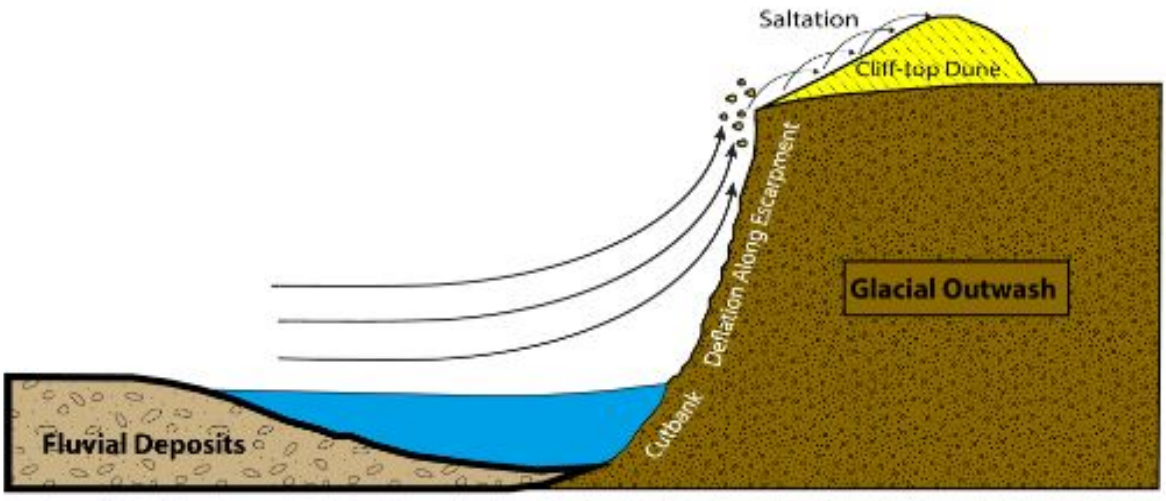

Fig. 17. Chippewa River of Wisconsin eroding into and undermining glacial outwash material of an escarpment thereby exposing material to deflation (Larson et al. 2008).

Larson et al. (2008) developed a model to describe the formation of RSD and other unidentified cliff-top dunes in the LCRV. They posit the Chippewa River erodes into glacio-fluvial fill, exposes material for deflation, which is transported and deposited immediately upslope to cliff-top locations (Fig. 17) (Larson et al., 2008; Schaetzl et al., 2017). This model requires cliff-top dunes postdate headward incision of the Chippewa River's adjustment to base level lowering events. OSL ages of RSD produced by are grouped closely around 6ka (Schaetzl et al., 2017) and correlate with a headward incision model for the Chippewa River (Faulkner et al., 2016). However, the arrival of headward incision along the Chippewa River at the location of the RSD is poorly constrained (Schaetzl et al., 2017). Therefore, given the limited age constraints on terraces near RSD and other cliff-top dunes along the Chippewa River, the cliff-top dune model has yet to be verified (Larson et al., 2008; Faulkner et al., 2016; Schaetzl et al., 2017). Alternatively, these cliff-top dunes may have been pre-existing parabolic dunes that were subsequently eroded into by the laterally moving Chippewa River. In this alternative hypothesis, parabolic dunes in cliff-top position would have formed independent of the Chippewa River (Schaetzl et al., 2017).

Immobilized sand dunes in cliff-top position along an active meander bend of the Chippewa River and downstream of RSD are identified within this chapter. These dunes are collectively known as the Kiwanis site due to the non-profit Kiwanis International who owned the property when they were found. Like RSD, the dunes at the Kiwanis site either formed as fluvial cliff-top dunes or their formation was independent of the Chippewa River and their cliff-top position is incidental. The Kiwanis site dunes are investigated through OSL ages, grain size analysis, and morphological analysis. The results from the Kiwanis site are compared to RSD and used to revise the model created

by Larson et al. (2008). Additionally, the results from the Kiwanis site and comparisons with RSD are used to classify cliff-top dunes at both locations as terrestrial fluvial cliff-top dunes. The terrestrial fluvial cliff-top dune model is then applied to the RSD as well as the Kiwanis site dunes. This model expands upon the model produced by Larson et al. (2008) by using supporting literature of terrestrial fluvial cliff-top dunes and introducing a climatic influence.

2.6.2 Methods

2.6.2.1 Grain Size Analysis

Four samples known as 2017-3, 2017-4, 2017-6, and 2017-8 were collected from the Kiwanis site for a preliminary grain size analysis. The sample 2017-3 was collected immediately above the Wissota terrace contact with overlying aeolian sand sheets. Samples 2017-4, 2017-6, and 2017-8 were collected at variable depths from cliff-top dunes at the Kiwanis site. The grain size samples were processed at the Saint Anthony Falls Laboratory in Minneapolis, Minnesota. The samples were dry sieved using a Rotap® sieve shaker. The samples were sieved into nine grain size fractions: <45μm, 45-90 μm, 90-125 μm, 125-250 μm, 250-425 μm, 425-710 μm, 71-1180 μm, 1180-2000 μm, and >2000 μm. The grain size fraction percentages were analyzed using the © GRADISTAT version 8.0 software developed by Blott and Pye (2001).

2.6.2.2 LiDAR Morphological Analysis

LiDAR data were used to analyze and compare the morphology and morphometry of RSD and cliff-top dunes at the Kiwanis site. The LiDAR data were provided by the county of Eau Claire, WI with average point spacing around 2m. The LiDAR data were

provided as LiDAR Data Exchange (LAS) files which were merged into LAS datasets. The LAS datasets were then converted to a high resolution raster digital elevation model (DEM). Slope, hillshade, and shaded relief raster surfaces were then derived from the DEM. Cliff-top dune morphology was interpreted from the hillshade and shaded relief rasters. Cliff-top dune morphometry (e.g., slope, elevation) was interpreted using the slope and DEM surfaces.

2.6.2.3 Luminescence Dating

OSL is an effective method for dating aeolian deposits (Rhodes, 2011). OSL dating has effectively used on fluvial (Faulkner et al., 2016) and aeolian deposits (Schaetzl et al., 2017) within the LCRV. Additionally, there is a lack of organic deposits for radiocarbon dating of aeolian deposits of the LCRV. Therefore, OSL dating was conducted on cliff-top dunes and the underlying Wissota terrace within the Kiwanis site. The OSL dating methodology determines an estimate length of burial for non-organic sedimentary material consisting of quartz or feldspar minerals (Rittenour, 2008; Rhodes, 2011; Nelson et al., 2015). When buried, grains of quartz and feldspar accumulate electrons deriving from cosmic radiation and radiation from the surrounding material that are collectively used to determine the dose rate (Nelson et al., 2015). When exposed to an external light or heat source, the electrons within quartz and feldspar grains are released, which produces a luminescence signal (Rittenour, 2008; Rhodes, 2011; Nelson et al., 2015). The luminescence signal's magnitude is affected by the length of burial, as sediments buried for a longer duration luminesce with greater intensity (Nelson et al., 2015). The luminescence signal from an OSL sample can be controlled, measured, and regenerated within an OSL lab to determine the equivalent dose (Rhodes, 2011; Nelson et al., 2015). The equivalent dose is the measured amount radiation needed for a sample to

reproduce a luminescence signal of the same intensity as when first exposed to light or heat (Nelson et al., 2015). An estimated length of burial is produced by dividing equivalent dose by the dose rate, assuming the dose rate accumulated at a regular or expected rate (Rittenour, 2008; Rhodes, 2011; Nelson et al., 2015). The feldspar and quartz grains accumulate electrons at different rates and thus need to be separated during sample processing. OSL dating is effective for exceptionally fine silts (7-11 μm) and fine sands (63-250 μm) (Nelson et al., 2015). OSL samples need to be taken from depths greater than 1m to avoid volatility in cosmic contribution to the dose rate at shallower depths and bioturbation. Bioturbation affects OSL results by introducing grains recently exposed to light to the samples resulting in anomalously young ages (Hanson et al., 2015). Additionally, effective OSL dating requires sediment within the samples were sufficiently exposed to sunlight prior to burial and were subsequently never exposed to light or contaminated by material that was exposed to light prior to extraction (Rittenour, 2008; Rhodes, 2011; Nelson et al., 2015). Consequently, issues in the accuracy of OSL ages arise when proper precautions are not taken during sampling.

Ten OSL samples were taken from the Kiwanis site at depths ranging from 1.45 to 3.45 meters. Eight samples named USU-2605, USU-2606, USU-2607, USU-2608, USU-2609, USU-26012, USU-2866, and USU-2867 were taken at different locations within cliff-top dunes (Fig. 18). A single sample named USU-2868 one was taken from an interpreted sand sheet beneath the cliff-top dunes. The final sample known as USU-2869 was extracted from the underlying Wissota terrace fill (Fig.18).

OSL sampling was conducted using the protocol described by Nelson et al. (2015). Separate dose rate and soil moisture samples were collected from the surrounding material of each OSL sample. The dose rate samples were used to determine each OSL

sample's exposure to isotopic radiation that emanated from the surrounding material. The soil moisture content samples were used to determine the degree to which water attenuated the amount of isotopic radiation the OSL sample received when buried. Additionally, coordinates and elevation data for were acquired for each OSL sample using the Trimble Geo 7x™. The coordinates, elevation, and depth of each sample were used to determine the cosmic radiation contribution to the dose rate.

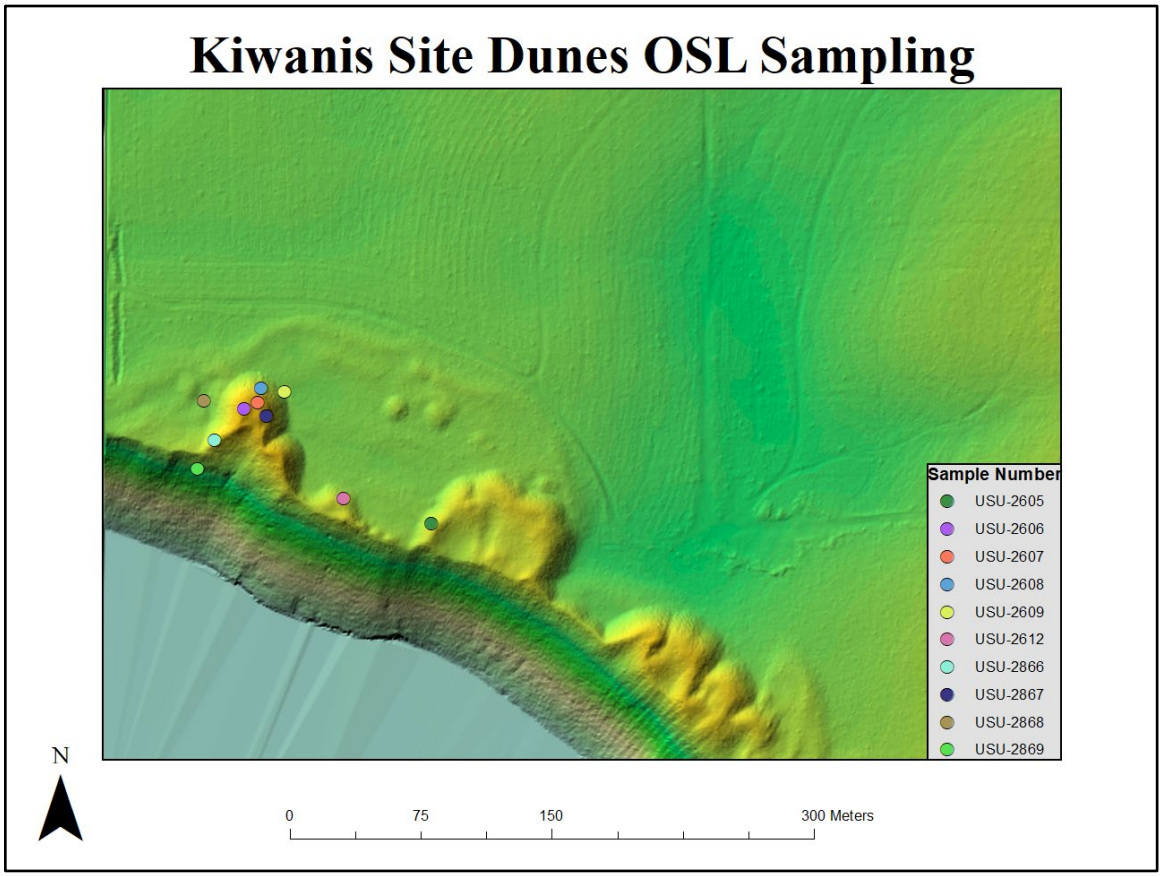

Fig. 18. OSL sampling locations and their affiliate sample numbers from the Kiwanis site.

The OSL samples extracted from the Kiwanis site were processed and analyzed at Utah State's Luminescence Lab. The samples were wet sieved to isolate the desired grain sizes at 125-250µm and 150-250µm. Carbonates were removed from each sample using 10% HCl concentration. Hydrogen peroxide was used to remove any organic material present within the samples. Quartz grains were the target mineral to be analyzed and were

isolated from the samples using a float of 2.7g cm^{-3} of sodium polytungstate. Quartz grains were then etched using a 47% concentration of hydrofluoric acid. The OSL samples were analyzed using the small aliquot regenerative dose (SAR) methodology (Murray and Wintle, 2000; Rittenour, 2008). The quartz grains were place on 2mm diameter aliquots discs and loaded into the Risø TL/OSL Reader Model DA-20. The Risø TL/OSL Reader produced blue-green wavelengths of .47µm to stimulate luminescence within the quartz grains. The samples then underwent preheat plateau and dose recover tests to determine their appropriate preheat temperatures and equivalent dose rates. At least nine to 25 aliquots were processed for each sample to derive the equivalent dose.

2.6.3 Results

2.6.3.2 Grain Size Analysis

Grains size analysis from cliff-top dunes within the Kiwanis site indicates they are composed primarily of moderately sorted medium sand. The grain size fractions containing the largest constituent portion of each sample were 125-250µm, 250-410µm, and 425-710µm (Appendix B). Each of the four grain size samples were composed of at least 97% sand (63-2000µm) (Appendix B). The samples 2017-3, 2017-4, 2017-6 were composed of 48-53% medium sand and 2017-8 contained 23.5% medium sand (Appendix B). The samples ranged from moderately sorted to moderately well-sorted. The mean grain size values were calculated using the Folk and Ward method which is the sum of the grain sizes in phi units at 16%, 50%, and 84% of the sample by weight divided by three (Blott and Pye, 2001). Phi units are logarithmic values derived from the grain diameter (Blott and Pye, 2001). Samples 2017-3, 2017-4, and 2017-6 had mean grain size

values of 249.2µm, 284.8µm, and 304.3µm respectively. Sample 2017-8 had a considerably larger mean grain size value of 666.6µm. The grain size distribution from the samples collected at the Kiwanis site correlate well with the grain sizes recorded at RSD by Schaetzl et al. (2017). However, sample 2017-8 had a more significant composition of coarser grain sizes, which could have been the consequence of inherent issues with the dry sieving method. Dry sieving grain sizes finer than 50µm is less effective as clays and fine silts can conglomerate thus causing samples to have a misrepresentative coarseness (Gee and Or, 2002; Rodríguez and Uriarte, 2009). Consequently, future grain size analysis using alternative methods such as laser diffraction are needed to produce conclusive results (Rodríguez and Uriarte, 2009).

2.6.3.1 LiDAR Morphological Analysis

LiDAR analysis of cliff-top dunes at Kiwanis site and RSD indicates they exhibit significantly different morphologies and orientations. Cliff-top dunes at the Kiwanis site have parabolic dune morphology and are oriented perpendicular to the terrace escarpment in a north-northeasterly direction. The Kiwanis site dunes have well-preserved morphologies with identifiable slipfaces, trailing arms, and deflation hollows (Fig. 19). Additionally, they are up to 9.8 m high and have a maximum slope of 31 degrees (Fig. 20). According to Schaetzl et al. (2017), RSD is a parabolic dune, however its morphology is significantly modified where it is more diffuse of form and its orientation is inconclusive (i.e., more rounded, eroded) (Fig. 19). The maximum height of RSD is 6m (Schaetzl et al., 2017) and its maximum slope is 7.1 degrees (Fig. 20). As a result, the Kiwanis site dunes have better preserved morphology and a different orientation than RSD.

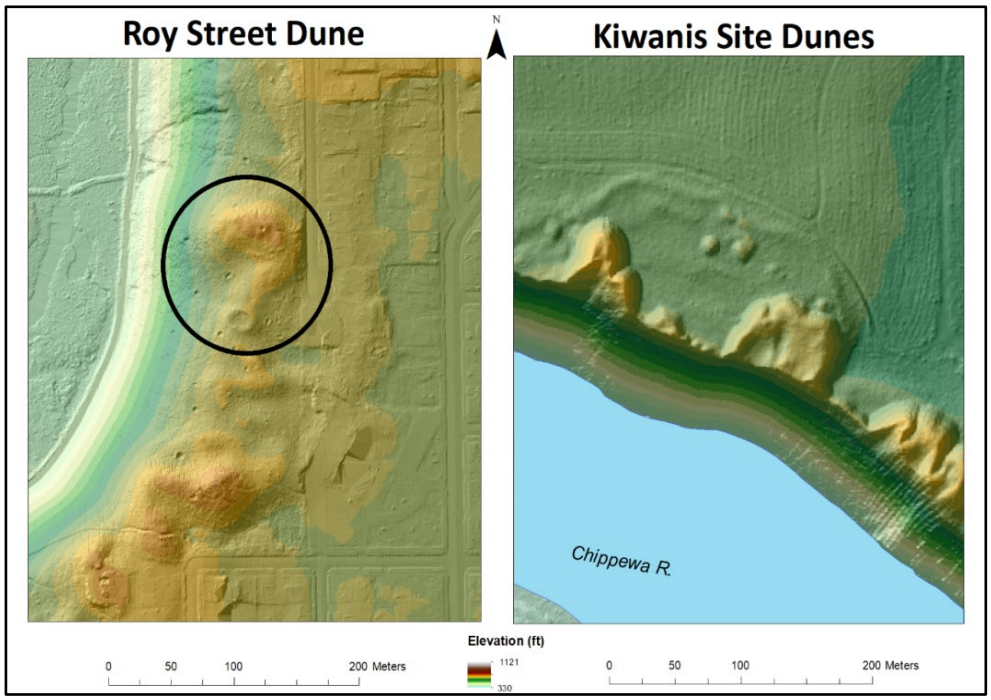

Fig. 19. Comparison of RSD and the Kiwanis site dunes' morphology using a shaded relief map derived from LiDAR data.

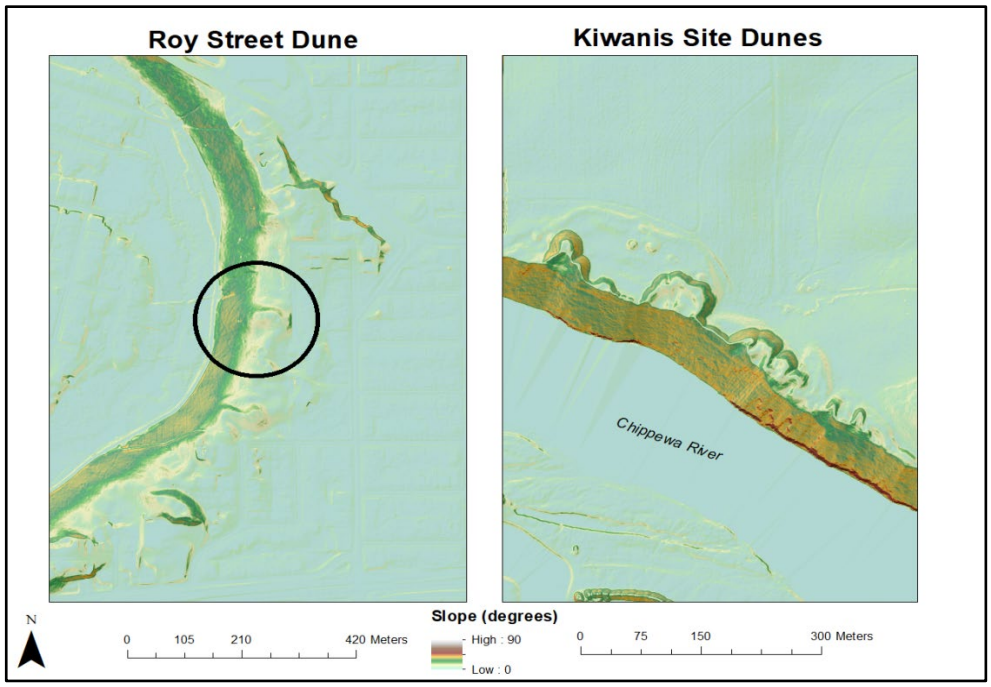

Fig. 20. Comparison of RSD and the Kiwanis site dunes' morphology using a slopeshade relief map derived from LiDAR data.

2.6.3.3 Luminescence Dating

In the present, seven of the 10 OSL samples collected from the Kiwanis site have a sufficient number of 15 or more aliquots run in order to produce a reliable age estimate (Table 3). However, the remaining three OSL samples have close to15 aliquots and have ages consistent with the other seven OSL samples. Moreover, the dose rates and equivalent doses of these samples are consistent have a small margin of error (Table 3; Appendix C).

The eight samples taken from the cliff-top dunes have ages ranging from .45ka to .96ka (Table 3) (Fig. 21). Five of these samples cluster around .5ka and the other three are grouped around .9ka. Consequently, there were either two periods of dune formation between .96ka and .45ka, or dune activity persisted for this entire period. OSL sample USU-2868, which was interpreted to be a sand sheet, has a preliminary age of 96ka. The sand sheet is located immediately above the Wissota terrace and has an age similar to the estimated period Chippewa River incision below the Wissota terrace at this reach (Fig. 21) (Faulkner et al., 2016). The Wissota terrace OSL sample (USU-2869) has a preliminary age of about 19ka. This age is considerably older than the Wissota terrace ages determined by Faulkner et al. (2016) along the same reach of the Chippewa River. However, this OSL age describes when the Wissota terrace material was deposited, not when it was abandoned by incision along the Chippewa River. Therefore, the Wissota terrace at the Kiwanis site may have been an inactive part of the Chippewa River after 19ka.

Sample Number	Depth	Number of Aliquots Run	Dose Rate (Gy/ka)	Preliminary DE	OSL Age
USU-2605	1.97m	16	1.56±.06	1.49±0.19	.96±0.14
USU-2606	1.51m	24	1.66±.06	1.38±0.21	0.84±0.14
USU-2607	1.46m	22	1.63±.06	.82±0.21	0.50±0.13
USU-2608	1.49m	17	1.60±.06	.88±0.20	0.55±0.13
USU-2609	1.49m	17	1.59±.06	.72±0.14	0.45±0.09
USU-2612	1.45m	17	1.72±.07	1.60±0.22	0.93±0.15
USU-2866	2.54m	16	1.80±.07	1.15±0.12	0.64±0.08
USU-2867	3.35m	10	1.57±.06	.95±0.19	.60±0.13
USU-2868	2.25m	11	1.47±.06	13.31±1.43	9.07±1.22
USU-2869	2.12m	9	1.74±.07	33.03±3.54	18.95±2.53

Table 3. OSL results from the Kiwanis site that include the sample number, depth, number of aliquots, dose rate, equivalent dose, and age

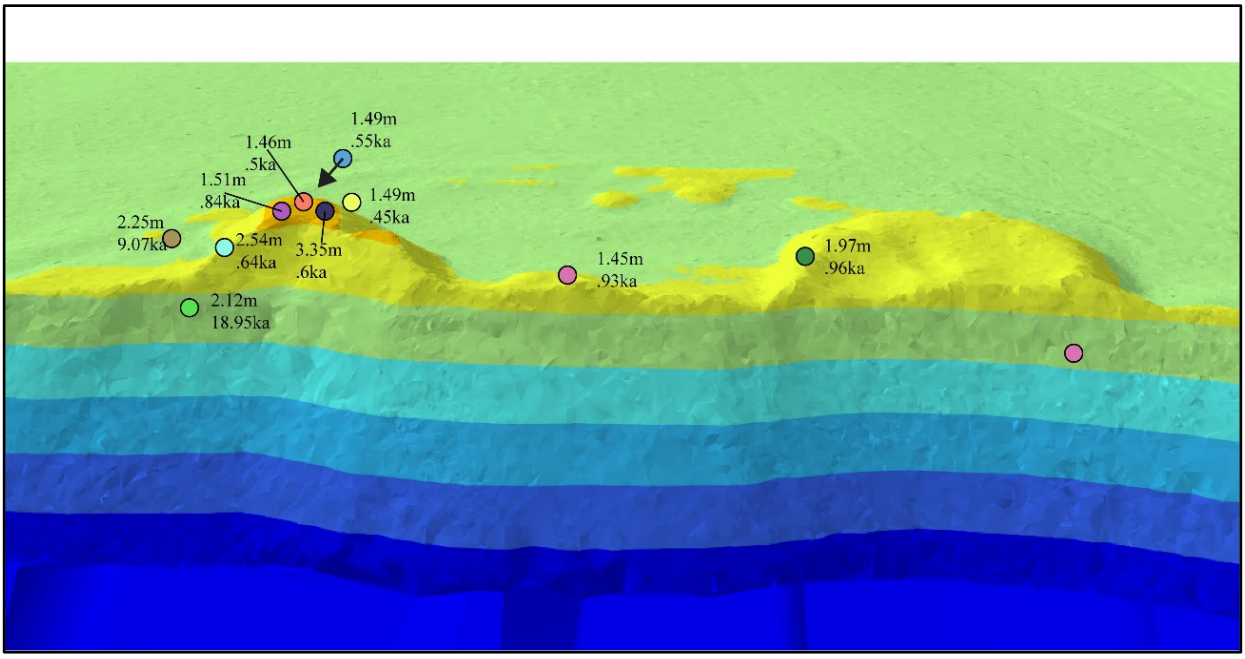

Fig. 21. Profile view of OSL sample depths and ages at the Kiwanis site.

2.6.4 Discussion

2.6.4.1 Grain Size Analysis

The grain size samples from cliff-top dunes the Kiwanis site exhibit similar characteristics as RSD. Three of the four samples taken from the Kiwanis site have mean grain sizes (249-304μm) that correspond to the texture described for RSD (250-350 μm) (Schaetzl et al., 2017). Additionally, the moderate degree of sorting and presence of a coarser sand fraction within all four samples from the Kiwanis site dunes indicate the dunes transported a short distance from their source of sand. Collectively, the Kiwanis site dunes' grain distribution, size, and sorting suggest they were formed as fluvial cliff-top dunes. However, more grain size analysis is needed to elucidate conclusive results.

2.6.4.2 Morphological Analysis

The morphological analysis of the Kiwanis cliff-top dunes indicates they formed during a south-southwest wind regime which was perpendicular to the terrace escarpment along the Chippewa River's meander trend. Winds perpendicular to the escarpment are regularly described for cliff-top dune formation (Olson, 1958a; David, 1972; Bégin, Michaud and Filion, 1995; Arbogast et al., 2017). RSD and the Kiwanis dunes possess different orientations and thus were formed by contrasting wind regimes. Additionally, Kiwanis site dunes exhibit greater relief and are better-preserved forms than RSD. Furthermore, the Kiwanis site dunes position along an active meander of the Chippewa River along with their morphology (Jennings, 1957) indicates them having formed recently. In contrast, RSD is located on a terrace escarpment of an abandoned meander far removed vertically and laterally from the present course of the Chippewa River. Therefore, the escarpment below the RSD has not recently been eroded by the Chippewa

River. RSD was likely separated from its sediment supply (i.e., terrace escarpment) when the Chippewa River abandoned the meander along which the dune is located. RSD's diffuse form and age around 6ka (Schaetzl et al., 2017) support the hypothesis that it has been removed from its sediment supply and was subsequently deteriorated by erosional processes within west-central Wisconsin's humid climate.

2.6.4.3 Luminescence Analysis and Kiwanis Site Dune Classification

The OSL ages for the Kiwanis site dunes indicate they were deposited between 1ka and .4ka, which corresponds to the morphological analysis of them forming recently. The Kiwanis site dunes have different orientations, morphological preservation, and OSL ages than RSD. Therefore the RSD and Kiwanis site dunes formed asynchronously under different wind regimes. However, their similar grains size distribution and location perpendicular to terrace escarpments suggests they were formed by the same or similar morphological processes. The apparent relationship between cliff-top dune formation and active river incision into the escarpments that underlie the dunes within the LCRV is supported by similar observations in fluvial cliff-top dune research (David, 1972; Bégin, Michaud and Filion, 1995; Arbogast et al., 2017). Therefore, the Kiwanis site dunes are classified as fluvial cliff-top dunes.

2.6.4.4 Contradictions to the Cliff-Top Dune Formation Model

There are locations along the LCRV where the Chippewa River is actively eroding and devegetating terrace escarpments (Fig. 22) which include the Kiwanis site. The stabilized Kiwanis cliff-top dunes' location along an active meander contradicts the model proposed by Larson et al. (2008), where cliff-top dune formation is directly linked to Chippewa River incision. In other words, there is not a causal relationship between

river erosion into a terrace escarpment and cliff-top dune formation at the Kiwanis site. Therefore, cliff-top dune formation at the Kiwanis site is likely dependent upon river incision and its interaction with previously unrecognized variables. As mentioned above, research on fluvial cliff-top dunes ascribes their formation to the interactions between stream erosion and perpendicular wind regimes (Arbogast et al., 2017) and/or climate change (David, 1972; Bégin, Michaud and Filion, 1995). As mentioned in Chapter 1, the LCRV has wind regime capable of aeolian transport that ranges from predominately northwesterly in the winter to southeasterly in the summer. The south-southwest facing terrace escarpment at the base of the Kiwanis site cliff-top dunes is therefore likely exposed to seasonal wind velocities capable of transporting its unconsolidated fine to gravelly sand (Iowa Environmental Mesonet, 2019). Thus, if the model proposed by Larson et al. (2008) is valid, then cliff-top dunes should be actively forming at the Kiwanis site.

2.6.4.5 Limitations to Present Day Aeolian Transport

The present humid climate of the LCRV which supports dense vegetative cover and a higher soil moisture contents appear to be the limiting factor for aeolian transport and deposition. Dense vegetation cover increases surface roughness, which significantly increases the required wind velocity threshold for aeolian transport (Nickling and Neuman, 2009). Vegetation also stabilizes soil, which makes it more resistant to wind erosion (Hack, 1941). Vegetative cover ranging from 17.5% (Lancaster and Baas, 1998) to 20% (Yan and Baas, 2015) can significantly reduce or prevent aeolian activity on sand dunes. Lateral fluvial incision along the LCRV may not be removing sufficient vegetative cover on terrace escarpments to allow for cliff-top dune formation (Fig. 22).

Conversely, aeolian activity could be limited by relatively high soil moisture content of the terrace escarpments within the LCRV. Soil moisture produces matric bonds consisting of capillary and adsorptive forces that cause individual grains to cohere (Nickling and Neuman, 2009). According to Nickling and Neuman (2009, pp. 539) the "gravimetric moisture content [mass of water per mass of dry soil] of approximately .6% can more than double the threshold velocity of medium sized sands." Moreover, when the gravimetric soil moisture content exceeds 5%, sand sized material becomes impervious to aeolian deflation and transport. The gravimetric soil moisture content of dose rate OSL samples taken from cliff-top dunes at the Kiwanis site ranged from 4.26% to 5.95%.

Fig. 22. An escarpment devegetated by lateral erosion of a cutbank along the Lower Chippewa River Valley.

However, the dose rate OSL samples were taken at depths greater that 1m, whereas the surficial soil moisture content affects aeolian transport. Nonetheless, the Chippewa River

likely increases the soil moisture content of the lower terrace escarpment fill along the LCRV. The humid climate also promotes greater discharges along the Chippewa River which would raise the water table and provide increased soil moisture to higher locations along the terrace escarpments. As a result, cliff-top dune formation along the LCRV likely requires stream erosion concomitant with conditions drier than the present.

2.6.4.6 Investigation of Increased Aridity in the LCRV

Aridity denotes a time period spanning several years or decades with a sustained precipitation regime lesser than recorded in the present (Beaudoin, 2002). When a location's climate is investigated on century and millennial time scales, periods of increased aridity become commonplace and affect the average precipitation regime (Beaudoin, 2002). Conversely, according to Beaudoin (2002), droughts are typically described as lasting less than five years. Droughts ostensibly occur during periods of increased aridity, but they can also occur interstitial to periods of increased moisture. Therefore, the legacy of a drought may not be recorded in a climate as its effect is counteracted by a periods of increased moisture. Moreover, the shorter temporal scale of droughts may not be sufficient to initiate dune building processes in humid climates, which require sustained periods of aridity to reduce soil moisture contents and remove vegetative cover (Wolfe et al., 2001; Beaudoin, 2002). Wolfe et al. (2001) suggested that drought succeeded by sustained aridity allowed for dune mobilization in the Great Sand Hills of Saskatchewan. Contrastingly, drought interstitial to moist periods would have been ineffective in causing aeolian activity (Wolfe et al., 2001). As a result, cliff-top dune formation in the LCRV could correspond to droughts within longer periods of increased aridity or perhaps are a signature of longer term landscape change resulting from aridity.

As of the present, buried soils have not been recorded within RSD or the Kiwanis site cliff-top dunes. The absence of buried soils indicates that cliff-top dune formation within the LCRV was relatively uninterrupted by periods of dune stabilization perhaps caused by more humid conditions. Nonetheless, the Kiwanis site OSL ages appear to group around two separate periods of dune activity at ~.9ka and ~.5ka. Additionally, the location and ages of the OSL samples correspond to the timing of cliff-top dune formation indicated by the morphology. The significantly truncated and less morphologically preserved cliff-top dunes at the Kiwanis site exhibit the oldest OSL ages (Fig. 23). The youngest ages are located along the slip face of the best preserved cliff-top dune, which is a location that should record the last period of deposition. Additionally, the OSL sample USU numbers 2867 and 2866 appear to be anomalously young, as samples at shallower depths within the same dune have a similar age or are older. However, there appears to be a secondary morphological modification to the best preserved cliff-top dune represented by a deflation hollow with a slightly different orientation (Fig. 23). As a result, the young OSL age from USU 2866 and 2867 are potentially recording the reactivation period indicated by the deflation hollow. Perhaps evidence of vegetative cover and/or pedogenic activity between ~.9ka and ~.5ka was removed during the second period of activity. Alternatively, cliff-top dune formation was continuous from ~.9ka to ~.5ka and terminated with a slightly altered wind regime represented by the deflation hollow.

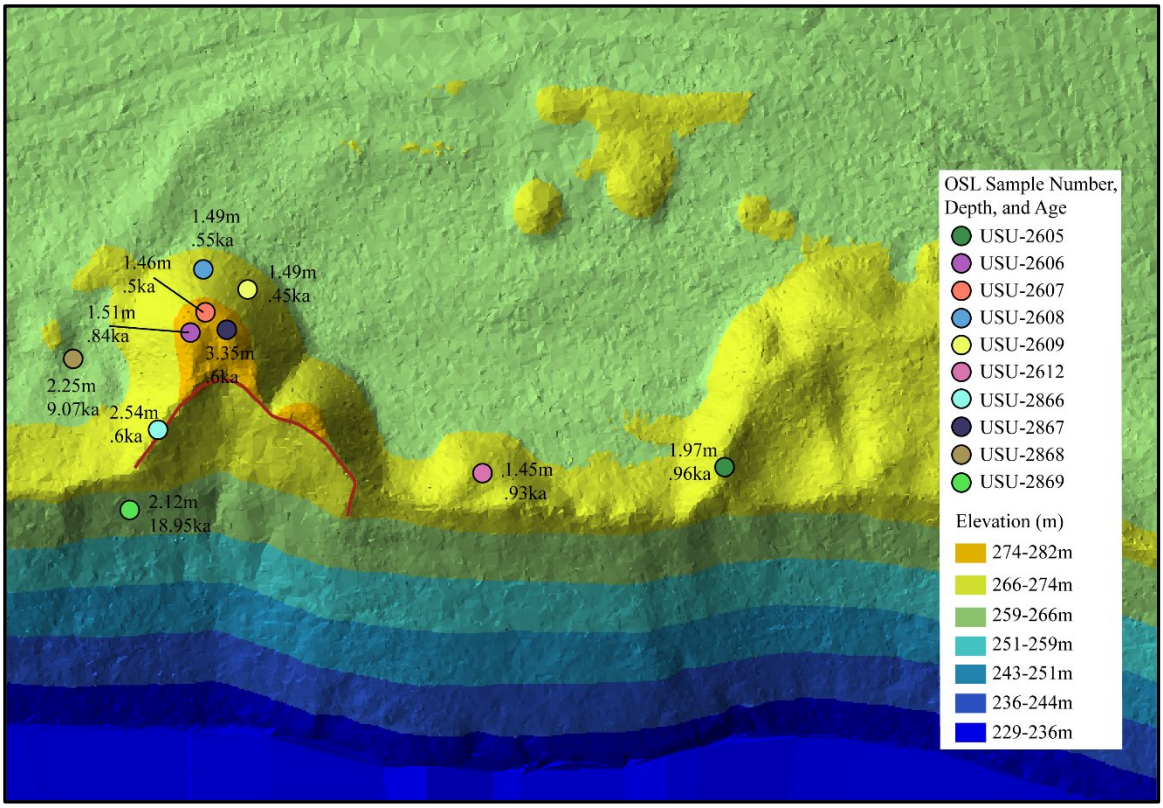

Fig. 23. OSL ages and depths related to cliff-top dune morphology at the Kiwanis site. The red line indicates a deflation hollow from a potential remobilization event.

2.6.4.7 Holocene Aridity

OSL ages from RSD and the Kiwanis site correspond to the Mid-Holocene Climatic Optimum and the Medieval Climatic Anomaly respectively. The Mid-Holocene Climatic Optimum is a period of increased aridity with warmer temperatures and decreased precipitation in the northern hemisphere (Bryant, 1997). In North America the Mid-Holocene Climatic Optimum has been recorded at varying time intervals (Running, 1995), however they generally overlap at 6ka (Bryant, 1997; Harrison et al., 2003). The Medieval Climatic Anomaly (MCA) also known as the Medieval Warm Period (Beaudoin, 2002) and Medieval Climatic Optimum (Mann, 2002), is a period of increased temperatures across Europe and North America from about 1.0 to .750ka (Mann et al., 2009). The MCA was succeeded by the Little Ice Age around .5ka (Tian,

Nelson and Hu, 2006; Jacques, Cumming and Smol, 2008; Wahl, Diaz and Ohlwein, 2012). The Little Ice Age in the upper Midwest is characterized by overall cooler and more humid conditions than the present (Tian, Nelson and Hu, 2006; Jacques, Cumming and Smol, 2008; Wahl, Diaz and Ohlwein, 2012).

Unfortunately, there is minimal research concerning Holocene paleoenvironmental conditions along the LCRV (Schaetzl et al., 2017). Moreover, given that some research on fluvial cliff-top dunes suggests they form independent of climatic changes (White, 1960; Arbogast et al., 2017), it would be unwise to assume cliff-top dune in the LCRV formed in response to increased aridity without other corroborating evidence (Williams, 2009). Therefore, Holocene climatic records from the Upper Midwest regions of North Dakota (Running, 1995; Cook et al., 2016), Michigan (Jacques, Cumming and Smol, 2008), Minnesota (Wright, Winter and Patten, 1963; Grigal, Severson and Goltz, 1976; Keen and Shane, 1990; Dean et al., 1996; Jacques, Cumming and Smol, 2008; Shuman et al., 2009), Iowa (Denniston et al., 1999), and Wisconsin (Denniston et al., 1999; Wahl, Diaz and Ohlwein, 2012) are used as proxies for aridity during the Mid-Holocene Climatic Optimum and MCA in the LCRV.

2.6.4.7.1 Mid-Holocene Climatic Optimum

Aridity during the middle Holocene in the regions surrounding the LCRV was periodic, yet it coincides around 6ka (Grigal, Severson and Goltz, 1976; Keen and Shane, 1990; Running, 1995; Dean et al., 1996; Denniston et al., 1999). Carbon and oxygen isotopic records from speleothems in caves within Iowa, Minnesota, and Wisconsin indicated increased prairie vegetation was affiliated with aridity, which was most

prevalent from 6,500 to 5,500 radiocarbon yrs B. P. (Denniston et al., 1999). The speleothem records also exhibited a sharp west to east increase in the moisture gradient during this period that demarcated a prairie-forest ecotone west of the Mississippi River (Denniston et al., 1999). Pollen records from lakes in southeastern Minnesota record an influx of prairie vegetation between 7,100 and 5,100 radiocarbon yrs B. P. (Wright, Winter and Patten, 1963). This influx of prairie vegetation was attributed to increased aridity within the region during the mid-Holocene climatic optimum. Dune records in southeastern North Dakota suggest aeolian activity occurred 8,000 to 4,925 radiocarbon yrs B. P. and again 3,000 to 1,500 radiocarbon yrs B. P. (Running, 1995). Moreover, Running (1995) indicated a west to east temporal delay in aridity as it transited the eastern Great Plains and upper Midwest.

Pollen and radiocarbon ages from Lake Ann in east central Minnesota exhibited three periods of increased aridity, decreased vegetation, and increased aeolian activity. The first period occurred from 9.1ka to 6.5ka with maximum aridity occurring 8ka and 7.4ka. The second period occurred at 6.5ka to 5.1ka with the most intense aridity occurring around 6ka. The final period recorded greatest aridity around 4.9ka which ameliorated during the late Holocene (Keen and Shane, 1990). Pollen records from Elk Lake in north western Minnesota indicate a period of decreased precipitation and increased warmth from 7.5ka to 4.5ka (Dean et al., 1996). Carbon dating of charcoals within buried soils of a dune field southeast of Lake Winnibigoshish in north central Minnesota similarly indicate increased aridity from 7.9 to 5radiocarbon yrs B. P. (Grigal, Severson and Goltz, 1976). Thus, the 6ka ages from RSD correspond to a period of aridity indicated by a variety of proxy records within the Upper Midwest and Northern Plains.

2.6.4.7.2 Medieval Climatic Anomaly

Research of the MCA in regions surround the LCRV provides a more disjointed record of aridity that spans from 1k to .35ka (Booth et al., 2006; Shuman et al., 2009). The late Holocene ages of increased aridity may indicate the MCA occurred for a prolonged period or post-MCA period was interrupted by periodic aridity.

In the Central Plains there have been investigations that used aeolian, alluvial, and lacustrine records to indicate a period of aridity at .966-.985ka (Cook et al., 2016). Radiocarbon dating from stabilized parabolic dunes in the Minot dune field of North Dakota indicates they were activated between 1.170ka to .940ka and around .5ka (Muhs et al., 1997). In west-central Wisconsin, pollen records from lake cores indicate a sustained period of warmth from about .8 to .5ka, which produced a higher PE and increased aridity (Wahl, Diaz and Ohlwein, 2012). Booth et al. (2006) used radiocarbon dates from peatlands in eastern Michigan and west central Minnesota to correlate periods of increased aridity to lowered water tables. Booth et al. (2006) recorded an extended period of increased aridity from 1ka-.6ka with distinct periods occurring at 1ka, .8ka, and .7ka. Shuman et al. (2009) suggested that the onset of deciduous trees in the Big Woods forest of east central Minnesota was related to a period of increased aridity that began around .660ka and lasted until .350ka. Jacques, Cumming and Smol (2008) used pollen records from Lake Mina in west central Minnesota to indicate a period of increased aridity from .7ka to .6ka. Dean (1997) used lake cores from Elk Lake in north central Minnesota to indicate increased aeolian activity from .8ka-.6ka.

Research by Sridhar et al. (2006) of a dune field in the Nebraska Sand Hills indicates increased aridity and an altered wind regime from 1ka to.8ka. Sridhar et al. (2006) used the orientation of the sand dunes to suggest summer winds during the MCA had a more significant southwest component and were of greater velocity than in the

present. Additionally, increased southwesterly wind directions brought warmer and drier air thereby reducing moisture availability during the summer (Sridhar et al., 2006). The increased southwesterly winds that occurred in the Nebraska Sand Hills during the MCA (Sridhar et al., 2006) correspond to the oldest cliff-top dune ages and their orientation at the Kiwanis site. Additionally, ages from the Kiwanis site cliff-top dunes correspond to periods of aridity during the MCA which are recorded throughout the upper Midwest and the Great Plains. Consequently, periods of increased aridity were likely needed to in order to cross a geomorphic threshold (Schumm, 1973; Schumm, 1979) that allowed the Kiwanis site cliff-top dunes to form. Moreover, the Kiwanis site dunes can potentially be used to contribute to the chronology of increased aridity and also indicate an altered wind regime in the LCRV during the MCA.

2.6.4.8 Fluvial Cliff-Top Dune Model for the LCRV

Research in the regions surrounding the LCRV describe periods of aridity that correspond to OSL ages from RSD and the Kiwanis site dunes. Moreover, there is a present absence of cliff-top dune formation in the LCRV, which is a humid environment with active fluvial incision and a wind regime capable of supporting aeolian transport (Iowa Environmental Mesonet, 2019; Young, 2019). A new complex fluvial-aeolian cliff-top dune formation model for the LCRV is proposed, and builds upon the model by Larson et al. (2008) by including aridity as an additional and necessary environmental control on cliff-top dune formation in the LCRV (Fig. 24).

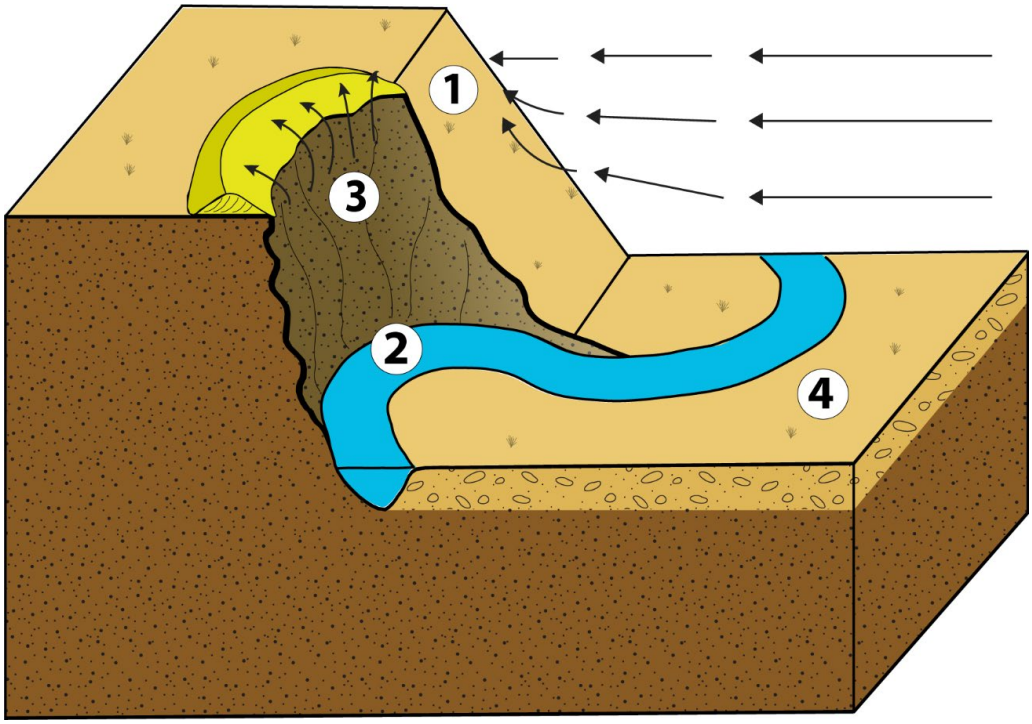

Fig. 24. A new complex fluvial-aeolian cliff-top dune formation model for RSD and the Kiwanis site cliff-top dunes. 1: Escarpment compression of airflow, 2: Fluvial erosion exposes escarpment material to deflation, 3: Cliff-top dune produced by deflation of escarpment material, 4; Increased aridity decreases vegetative cover and/or soil moisture to allow deflation of escarpment material.

2.7 Conclusion

RSD and the Kiwanis site cliff-top dunes formed at different periods of the Holocene that likely exhibited similar conditions. Research of fluvial cliff-top dunes describes interactions between several environmental processes is required for their formation. Correspondingly, the results and research of paleoenvironmental conditions in regions surrounding the LCRV indicate RSD and the Kiwanis site cliff-top dunes were formed by concomitant fluvial erosion, aridity, and wind regimes perpendicular to terrace escarpments. Evidence of fluvial cliff-top dune formation in the LCRV in relation to climatic change thus contradicts the findings of White (1960) and Arbogast et al. (2017). However, simple models of cliff-top dune formation processes are limited because a multitude of local-scale factors are involved. Models are useful in describing and

categorizing cliff-top dunes in all environmental settings, but cannot fully describe the various processes that contribute to the formation of an individual cliff-top dune.

Chapter 3

3.1 Introduction

Sandy aeolian deposits have been identified within the LCRV (Schaetzl et al., 2017) and surrounding regions including southeastern Minnesota (Keen and Shane, 1990; Zanner, 1999; Hanson et al., 2015), northeastern Iowa (Zanner, 1999; Mason, 2015), northwestern Illinois, and central Wisconsin (Rawling et al., 2008) (Fig. 25). However, the chronology of aeolian deposition within the LCRV and surrounding region is poorly constrained due to insufficient dating and analysis (Mason, 2015). Parabolic and cliff-top

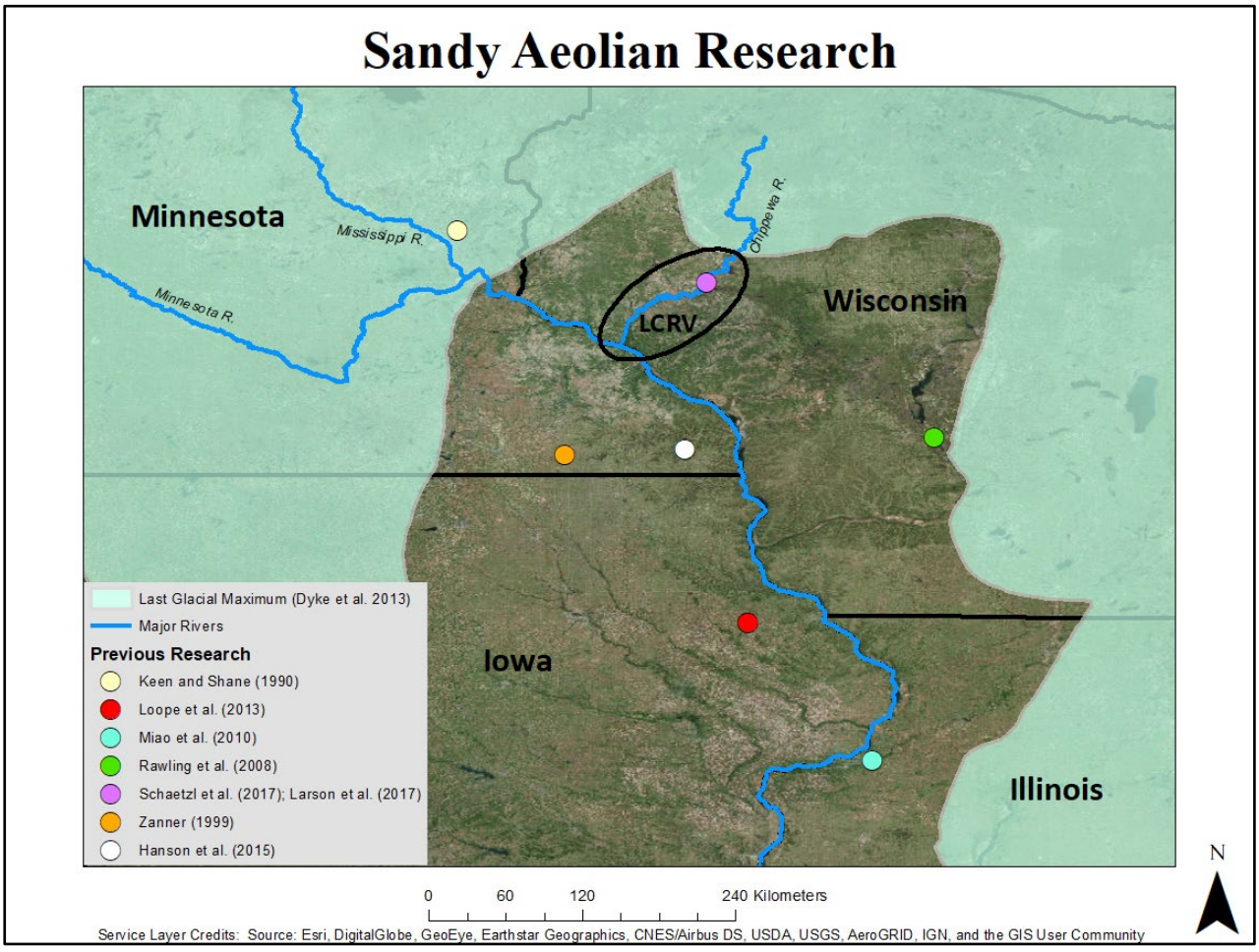

Fig. 25. Locations of research concerning sandy aeolian deposition surrounding the LCRV.

dune mapping, grain size analysis, and OSL dating are used to contribute to the chronology of aeolian deposition within the LCRV and the surrounding region.

The results from RSD and the Kiwanis site indicate cliff-top dune formation in the LCRV was episodic and potentially linked to periods of increased aridity during the mid to late Holocene. From these results a model for cliff-top dune formation in the LCRV was developed which integrates an intrinsic geomorphic process (i.e., fluvial erosion) with an extrinsic forcing mechanism (i.e., increased aridity). This model accounts for the asynchronous cliff-top dune formation at RSD and Kiwanis site and describes why cliff-top dune formation does not occur during present fluvial erosion into terrace escarpments within the LCRV. This model is tested via OSL and grain size analysis at a new location that exhibits a cliff-top dune along an active meander of the Chippewa River.

OSL dating and grain size analysis are conducted on parabolic dunes removed from the cliff-top position in the LCRV, which are previously undated. The ages from these parabolic dunes contribute to the chronology of aeolian deposition within the LCRV. Moreover, the OSL ages elucidate a poor correlation between cliff-top and parabolic dune formation in the LCRV, which supports the validity of the cliff-top dune model. Discordant parabolic and cliff-top dune ages provide support for the model because they indicate there were different formation processes involved. Additionally, the spatial distribution of parabolic and cliff-top dunes in the LCRV is determined via a mapping process. The mapping process ascribes orientations and confidence values to the sand dunes. The distribution and attributes for parabolic and cliff-top are used to determine appropriate location for field investigations and further describe the disassociation between the dune types.

3.1.1 *Research of Sandy Aeolian Deposits in the LCRV and Surrounding Region*

Research of sandy aeolian deposits in the LCRV and surrounding regions indicate the majority of aeolian activity occurred during the late and Terminal Pleistocene between ~17.5ka to ~10ka (Zanner, 1999; Rawling et al., 2008; Miao et al., 2010; Loope et al., 2013; Hanson et al., 2015; Schaetzl et al., 2017). This period of aeolian activity succeeded the last glacial maximum for the LCRV and the surrounding region, which was not synchronous across Wisconsin, but generally lasted from 20-18ka (Clayton, Attig and Mickelson, 2001; Syverson and Colgan, 2011; Faulkner et al., 2016; Schaetzl et al., 2017). Aeolian deposition is recorded by sand ramps (Hanson et al., 2015; Schaetzl, Forman and Attig, 2017), linear-shaped deposits (Zanner, 1999; Schaetzl, Forman and Attig, 2017), and parabolic dune fields (Rawling et al., 2008; Miao et al., 2010).

3.1.1.1 Sand Ramps

In addition to RSD, Schaetzl et al. (2017) identified linear shaped aeolian deposits, sand ramps, and parabolic dunes along the LCRV. Schaetzl et al. (2017) conducted preliminary OSL dating on a sand ramp located along the westward side of a bedrock outcrop east of the Chippewa River within the city of Eau Claire, Wisconsin. Three samples were extracted for OSL dating at variable depths that produced closely grouped ages ranging from 10.67-10.12ka (Schaetzl et al., 2017). The OSL ages, in addition to sedimentological analysis, led Schaetzl et al. (2017) to conclude that the sand ramp was deposited prior to headward incision of the Chippewa River reaching its location. During the terminal Pleistocene, the Chippewa River was a broad, aggrading glacial outwash stream with high sediment loads (Faulkner et al., 2016; Schaetzl et al., 2017). Therefore, the sand ramp was likely supplied by the glacial outwash sediments of

the Chippewa River, which were deflated and transported by northwest winds (Schaetzl et al., 2017).

In southeastern Minnesota, aeolian sand on ridgetops that were deposited by sand ramps along the Root River produced variable OSL ages ranging from 1.5-14.8ka (Hanson et al., 2015). These OSL ages however, were contaminated by bioturbation, thus producing anomalously young dates for samples taken at depths less than 1m (Hanson et al., 2015). As a result, only the ages from samples taken at depths greater than 1m meter were used to indicate that deposition of the ridgetop aeolian sands occurred during the terminal Pleistocene prior to 10.1ka (Hanson et al., 2015). The Root River was the source of the sandy aeolian deposits, which like the sand ramp in Eau Claire, were supplied by locally-sourced alluvial deposits (Hanson et al., 2015).

3.1.1.2 Linear-Shaped Aeolian Deposits

Schaetzl et al. (2017) identified northwest to southeast trending, elongate linear-shaped aeolian deposits marginal to the LCRV. These deposits are identified above glacial till instead of the glacial outwash of the Chippewa River (Schaetzl et al., 2017). Schaetzl et al. (2017) concluded that deposition of the linear aeolian deposits occurred when the glacial outwash of the Chippewa River was still active during the late Pleistocene. However, there are currently no ages for the linear-shaped deposits in the LCRV.

Zanner (1999) investigated sand stringers within southeastern Minnesota and northeastern Iowa that possess a similar morphology and orientation as the linear shaped-deposits described by Schaetzl et al. (2017). The sand stringers described by Zanner (1999) overlie glacial till and exhibit sand wedges indicative of thermal contractions due

to exceptionally cold conditions. Thermoluminescence dating (TL) of a sand stringer in southeastern Minnesota indicate it was deposited between 13.7-11.2ka (Zanner, 1999).

3.1.1.3 Parabolic Dunes

A dune field along the Green River in northwestern Illinois consisting of parabolic and transverse dunes was investigated by Miao et al. (2010). OSL and radiocarbon dating were used to indicate the dune field was formed around 17.5ka and was subsequently periodically reactivated during the Holocene (Miao et al., 2010). Miao et al. (2010) linked the timing of dune formation to an increased sand supply produced by the draining of a glacial lake. Therefore, dune formation in the Green River was similarly unrelated to climatic change (Miao et al., 2010).

There has been no previous investigation on parabolic dunes in the LCRV. Nonetheless, research of parabolic dune fields in central Wisconsin (Rawling et al., 2008) and northwestern Illinois (Miao et al., 2010) indicates dune formation occurred during the late Pleistocene. A dune field within the Central Sand Plain of former glacial Lake Wisconsin that consists of parabolic and transverse dunes was investigated by Rawling et al. (2008). Rawling et al. (2008) used 21 OSL samples taken at variable depths to constrain the chronology of sand dune activity. They found that the majority of the transverse and parabolic dunes were active from 14-10ka, and attributed the period of dune formation to the local sand availability from the Central Sand Plain as opposed to increased aridity or climatic change. The sand availability was determined either by an influx of outwash material deriving from the draining of Glacial Lake Wisconsin or by permafrost degradation and water table lowering (Rawling et al., 2008).

Loope et al. (2013) produced 29 OSL dates from aeolian deposits in southwestern Wisconsin and northeastern Iowa that were primarily grouped around 16ka. They indicated that this period of aeolian activity in this region was controlled by sand availability likely related to permafrost degradation within the region, which increased soil drainage capacity and exposed unconsolidated sand to deflation (Loope et al., 2013). Consequently, sand availability and sand supply appear to have been major limiting factors for sand dune formation during the late Pleistocene. Sand availability and sand supply were determined by geomorphic processes inherent to a periglacial environment (e.g., permafrost degradation and glacial lake outbursts).

3.1.2 *Study Sites*

In order to identify suitable (e.g., possessing a well-preserved representative morphology, and is accessible) sand dunes for analysis, parabolic and cliff-top dunes within the counties surrounding the LCRV were mapped and ascribed a confidence score. Consequently, sand dunes marginal to the LCRV, such as those along the major tributaries of the Chippewa River, were also identified. Additionally, the mapping process was used to delineate spatial relationships of the parabolic and cliff-top dunes. This led to the identification of a cliff-top dune known as the Steffes and Zanoni site and a parabolic dune field known as the Hurlburt site for field investigation using OSL and grain size analysis. The Steffes and Zanoni site is located in Dunn County approximately 11km down valley of the Kiwanis site (Fig. 26), and is situated along a meander of the Chippewa River that is actively eroding into the northern valley terrace escarpment. The Hurlburt site is located in Buffalo County further down valley of the Steffes and Zanoni

site, in close proximity to the Chippewa River, and approximately 17km upstream of the Mississippi River confluence (Fig. 27). It is located on the east side of the Chippewa River, as the river has changed from a west southwest trend to a southwest trend at this reach (Fig. 27).

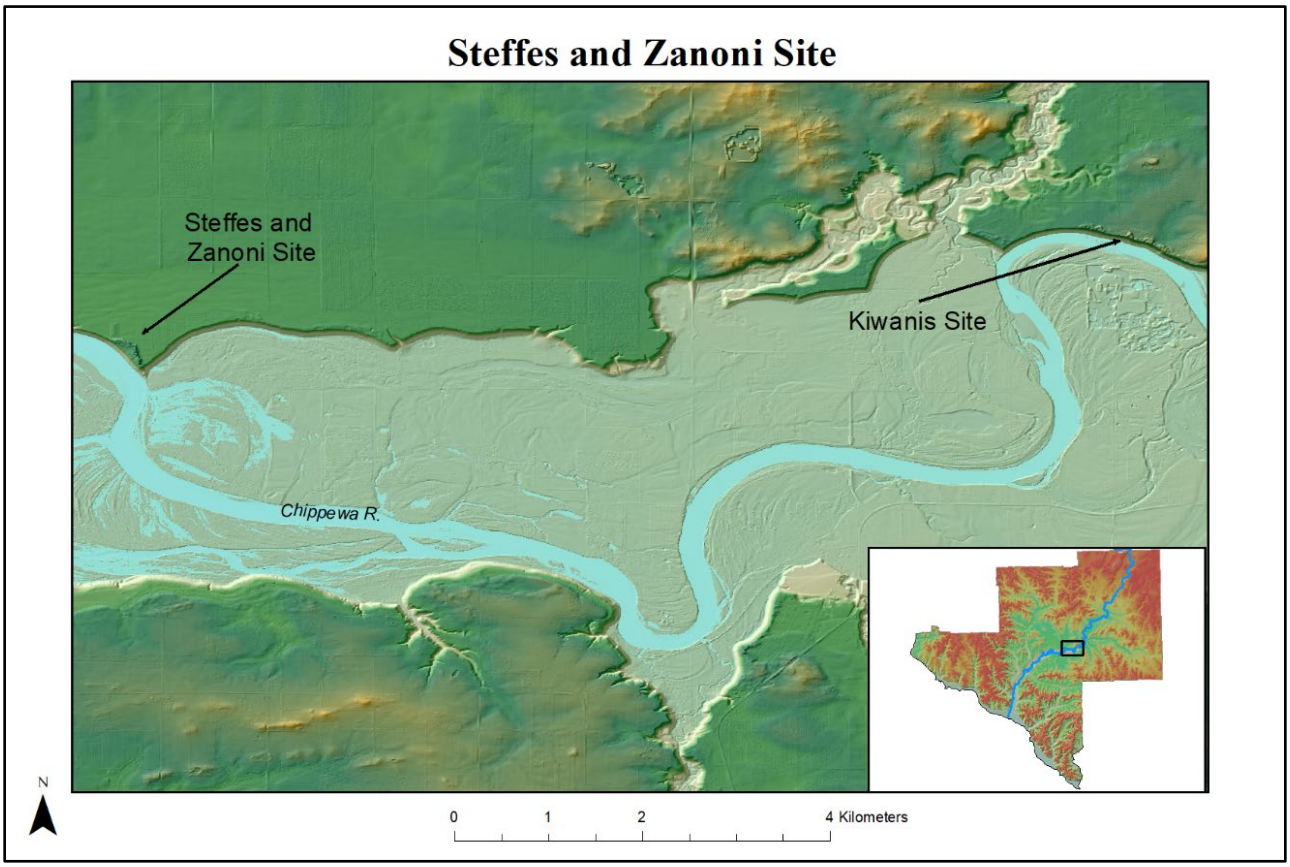

Fig. 26. The Location of the Steffes and Zanoni site in relation to the Kiwanis site. Both are located along meandering reaches of the Chippewa River.

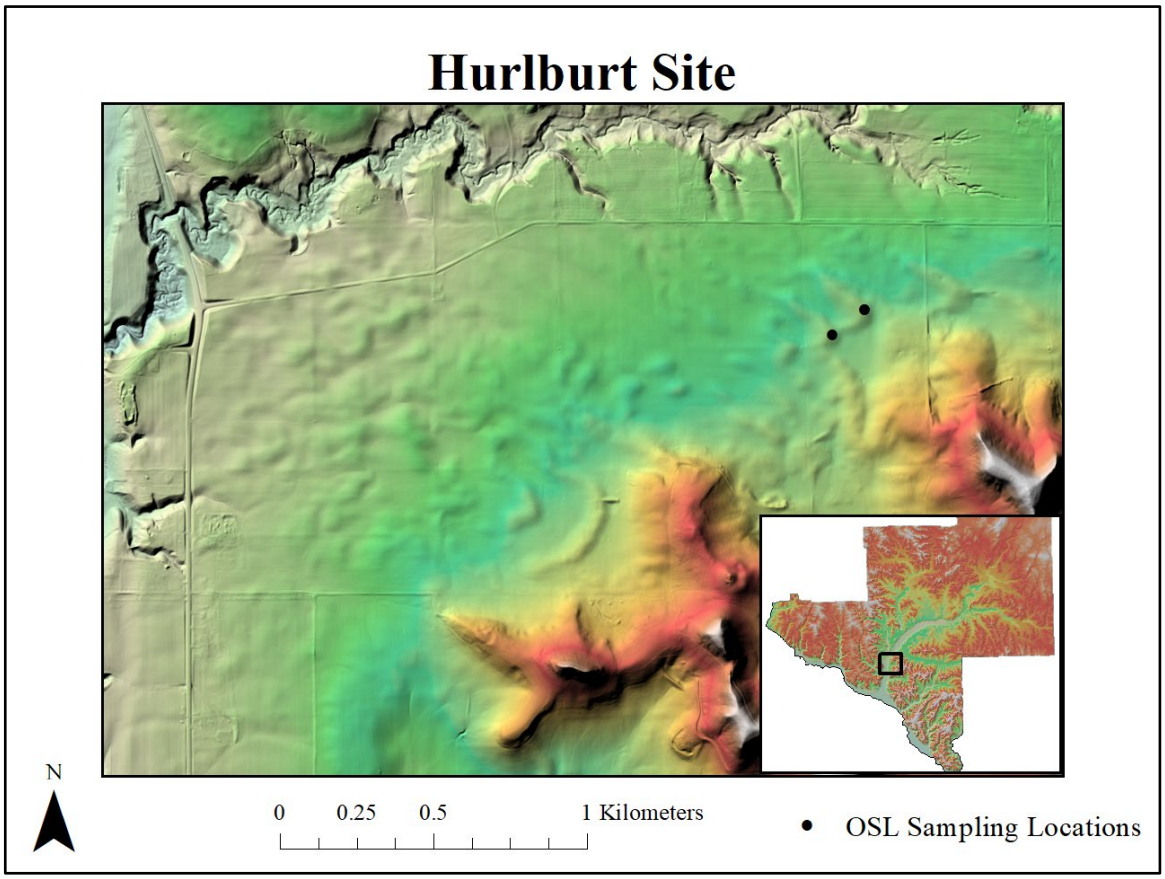

Fig. 27 The location of the Hurlburt site and the OSL sampling locations within the Hurlburt site.

3.2 Methods

3.2.1 *Parabolic and Cliff-Top Dune Mapping*

Sand dunes described as either parabolic dunes or cliff-top dunes were mapped within the counties surrounding the LCRV, including Chippewa County, Eau Claire County, Dunn County, Pepin County, Buffalo County, and Pierce County (Fig. 5). For mapping purposes, parabolic dunes in cliff-top positions were described as cliff-top dunes and parabolic dunes removed from cliff-top position were simply described as parabolic dunes. A confidence score was created in order to address the uncertainty deriving from an inconsistent DEM spatial resolution across counties within the LCRV and the variability in parabolic and cliff-top dune forms. The spatial distribution of cliff-top and parabolic dunes was analyzed using the mean center, median center, and directional

distribution tools within ArcMap 10.6 Copyright © 1995-2018. The mean center tool averaged the coordinate values of the sand dunes to find a central coordinate value. The median center tool placed coordinate values for all sand dunes in numeric order to find a centrally located sand dune within the LCRV and its surrounding counties. The directional distribution tool used an ellipse to display the direction in which the sand dunes were oriented.

County	Spatial Resolution	Point Spacing
Chippewa	3 meter	N/A
Eau Claire	3 meter	2 meter
Dunn	10 meter	N/A
Pepin	5 meter	N/A
Buffalo	2 meter	N/A
Pierce	3 meter	N/A

Table 4. The spatial resolution of the LiDAR data for each county within the LCRV.

3.2.2 *Confidence Score*

The confidence score is based upon a ten point scale consisting of LiDAR data, soil survey geographic databases (SURRGO), aerial imagery, and field investigations criteria (Figs. 28, 29, 30, and 31) (Table 5). The LiDAR data criterion was most useful for identifying sand dunes and determining their morphology, and thus was given a value up to five. The SSURGO data, and satellite imagery were ascribed a value of 0 or 1 if they contradicted or supported the LiDAR analysis. The field investigation criterion was given a value of 0 or 3 depending if the sand were analyzed in the field or supported/contradicted the LiDAR data.

LiDAR Data	SSURGO Data	Aerial Imagery	Field Investigation
0-5	0 or 1	0 or 1	0 or 3

Table 5. The confidence criteria and their affiliated point values for cliff-to and parabolic dunes in the LCRV.

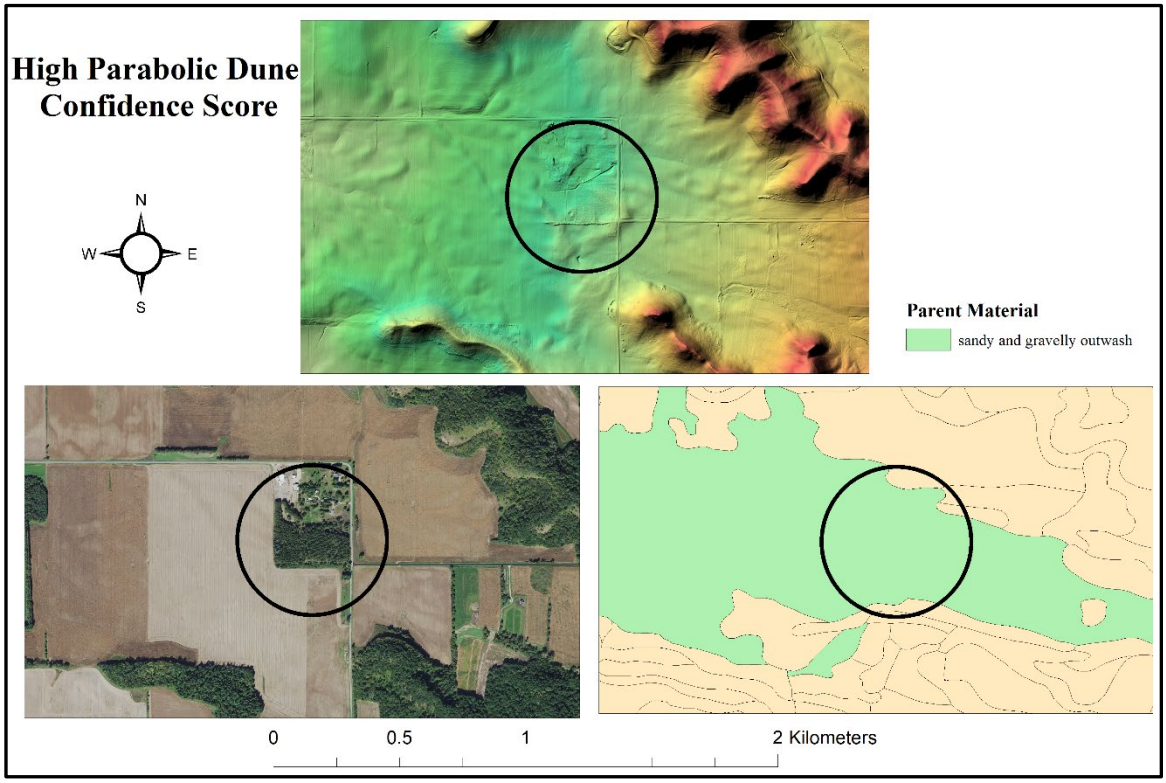

Fig. 28. Parabolic dunes that received a high confidence score of 6. The respective criteria values were: LiDAR (5pts), aerial imagery (1pt), SSURGO data (0pt), and Field analysis (0pts).

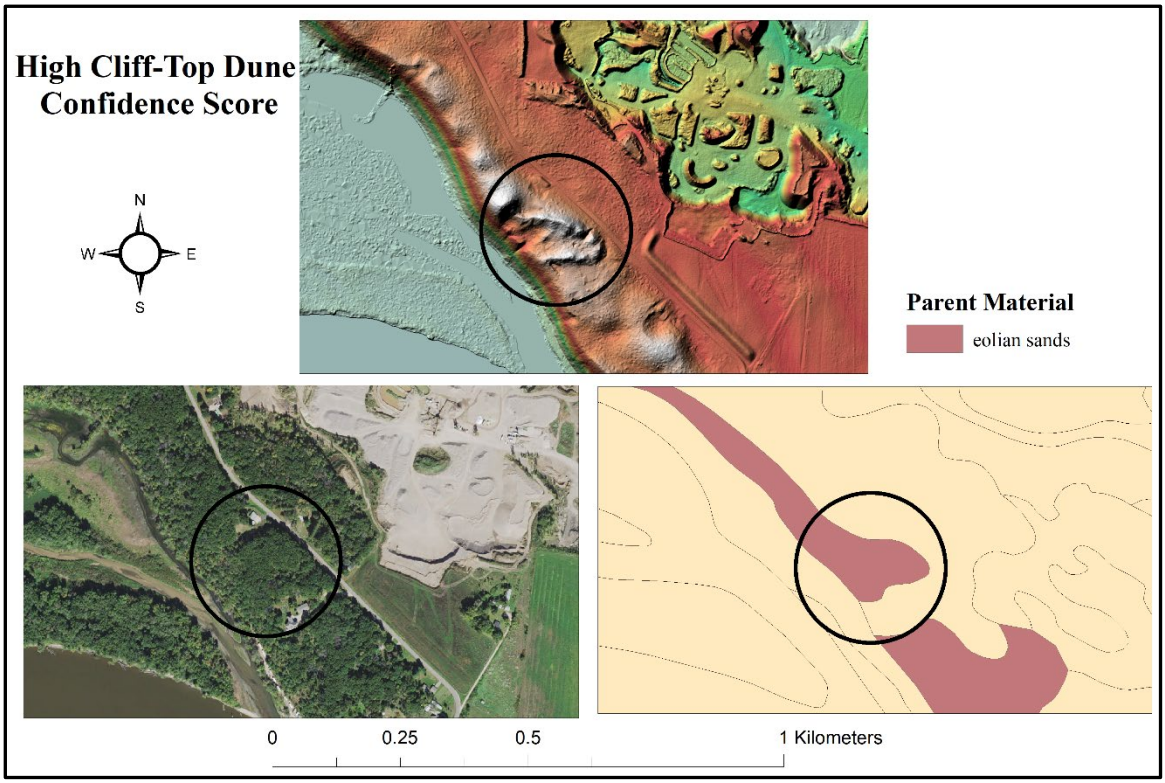

Fig. 29. A cliff-top dune that received a high confidence score of 7. The respective criteria values were: LiDAR (5pts), aerial imagery (1pt), SSURGO data (1pt), and Field analysis (0pts).

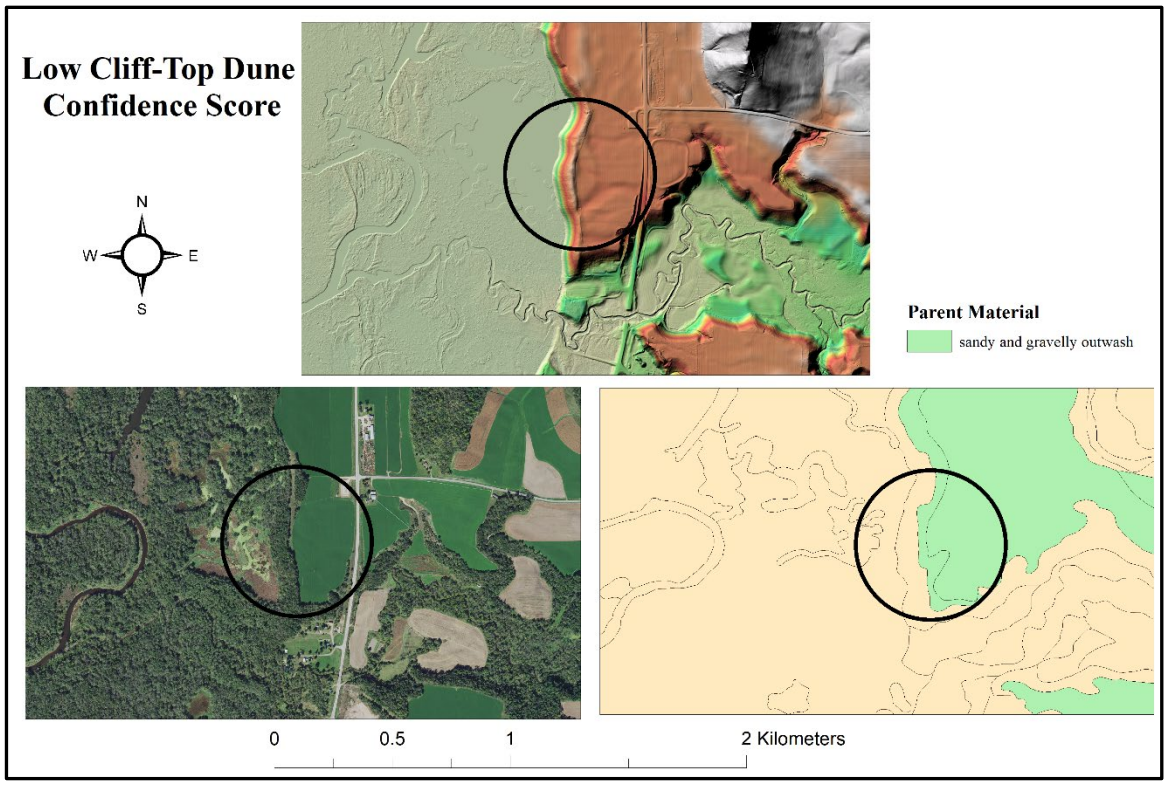

Fig. 30. A cliff-top dune that received a low confidence score of 3. The respective criteria values were: LiDAR (2pts), aerial imagery (1pt), SSURGO data (0pt), and Field analysis (0pts).

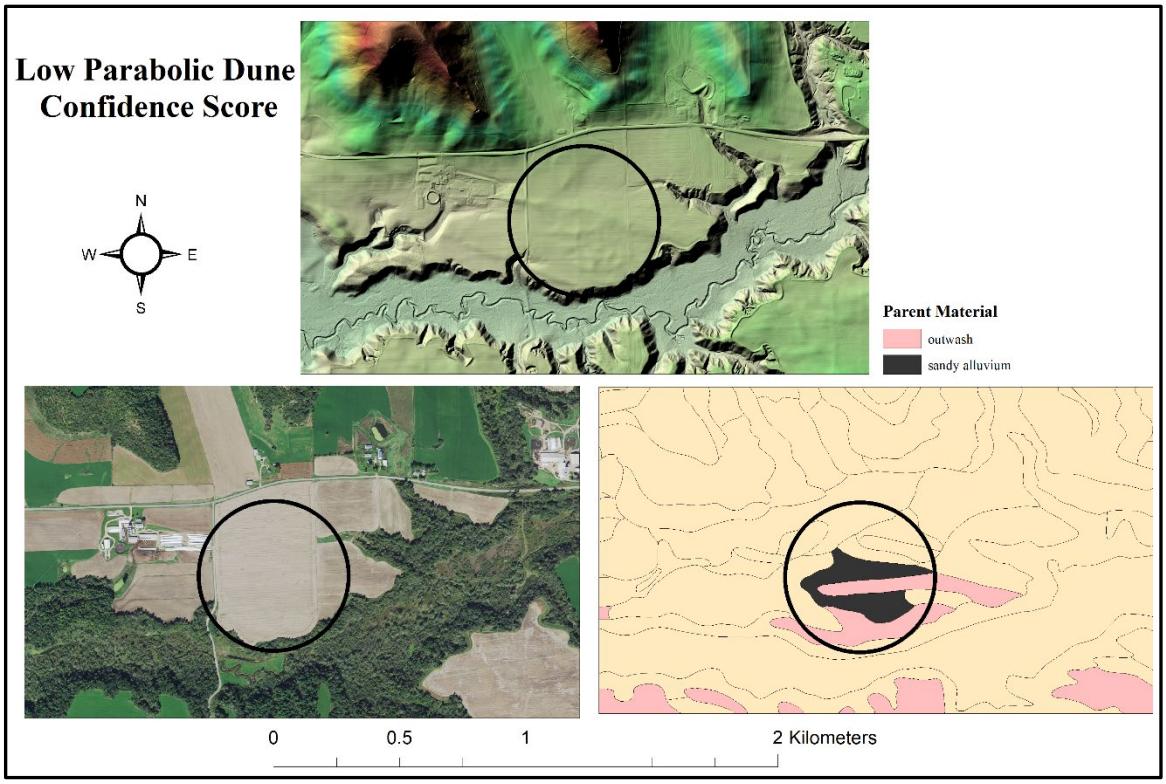

Fig. 31. A parabolic dune that received a low confidence score of 2. The respective criteria values were: LiDAR (1pt), aerial imagery (1pt), SSURGO data (0pt), and Field analysis (0pts).

3.2.2.1 LiDAR Analysis

Parabolic dunes were identified using greyscale hillshades derived from LiDAR DEMs. The LiDAR data were provided by the local government of each county. Unfortunately, only the DEMs derived from LiDAR were provided, with the exception of Eau Claire County, which supplied the LAS files. Consequently, the DEMs' spatial resolution could not be standardized and thus varied according to each county (Table 4). Parabolic and cliff-top dunes were identified based upon their characteristic morphology (e.g., U-shape, trailing arms, crest). The relief alongside the completeness and regularity of form for parabolic and cliff-top dunes were used to assign a value to the LiDAR morphological criterion. Cliff-top and parabolic dunes with well-preserved and an identifiable morphology were given higher confidence scores (Figs 28, 29, 30, and 31).

3.2.2.2 SSURGO Data

SSURGO data from each county's soil survey were downloaded from the United States Depart of Agriculture's National Resources Conservation Service Geospatial Data Gateway (Soil Survey Staff, 2017). The data were then linked to geographic information system software ArcMap 10.5 Copyright © 1995-2017 Esri using the Soil Data View tool downloaded from the National Resources Conservation Service (Soil Survey Staff, 2017). The SSURGO data were broken into three sub-categories consisting of the soil type, parent material, and texture for the parabolic and cliff-top dunes. Soil types described as udipsamments or quartzipsamments, which are great groups of the Entisol soil order, were composed the soil type criteria (Soil Survey Staff, 2015). Udipsamments are sandy Entisols found in humid regions and are typically of late Pleistocene or younger in age (Soil Survey Staff, 2015). Quartzipsamments are sandy Entisols consisting of more than

90% resistant minerals that are typically represented as quartz (Soil Survey Staff, 2015). The parent material types included, but were not restricted to eolian sand, outwash, and sandy outwash. The texture sub-criterion consisted of fine to medium sand and sandy loam. Two of the three sub-criteria needed to be met in order for the SSURGO data criterion to receive a value of one.

3.2.2.3 Aerial Imagery

The aerial imagery used for each county were acquired by the national agriculture imagery program (NAIP) between June 6th and August 31st of 2015 (Space Science & Engineering Center, 2019). The aerial imagery is orthorectified, consists of three band true color, and has 1m spatial resolution (Space Science & Engineering Center, 2019). The aerial imagery data were downloaded from the WisconsinView Data Portal geodatabase. The aerial imagery criterion was used as a reference to the LiDAR data, which occasionally produced erroneous artifacts resembling parabolic morphologies. Thus, if the aerial imagery did not contradict the findings from the morphology criterion, it was given a value of one.

3.2.2.4 Field Investigations

The field investigation criterion was based upon morphological and textural analysis of proposed parabolic and cliff-top dunes within the field. The field investigation criterion was given a value of 3 if it supported that the identified landform was a sand dune. Otherwise, a field investigation value of 0 was given to sand dunes/landforms that were not analyzed in the field. Additionally, the orientation was recorded for each parabolic and cliff-top dune.

3.2.3 *Grain Size Analysis*

Three samples were taken from the Hurlburt and Steffes and Zanoni site for grain size analysis. Two samples retrieved from the Hurlburt site were taken from the crests of two different parabolic dunes and known as Hurlburt site exploratory hole and Hurlburt site 2A. A single sample from the Steffes and Zanoni site was taken from the cliff-top dune and known as Steffes and Zanoni site auger hole 2018-1. These samples were processed using the dry sieving method and therefore are only considered preliminary. See Chapter 2 for the grain size lab processing protocol.

3.2.4 *Luminescence Dating*

A total of four OSL samples were taken at variable depths from the Hurlburt and Steffes and Zanoni sites using the OSL sampling protocol described in Chapter 2. The two OSL samples from the Steffes and Zanoni site were extracted from the cliff-top dunes at depths of 1.67m and 2.48m (Fig. 32). The two samples from the Hurlburt site were taken from the crests of two adjacent parabolic dunes at depths of 1.75 and 3.02m (Fig. 27). The OSL samples were processed and analyzed using the SAR methodology described in Chapter 2 at Utah State's Luminescence Lab.

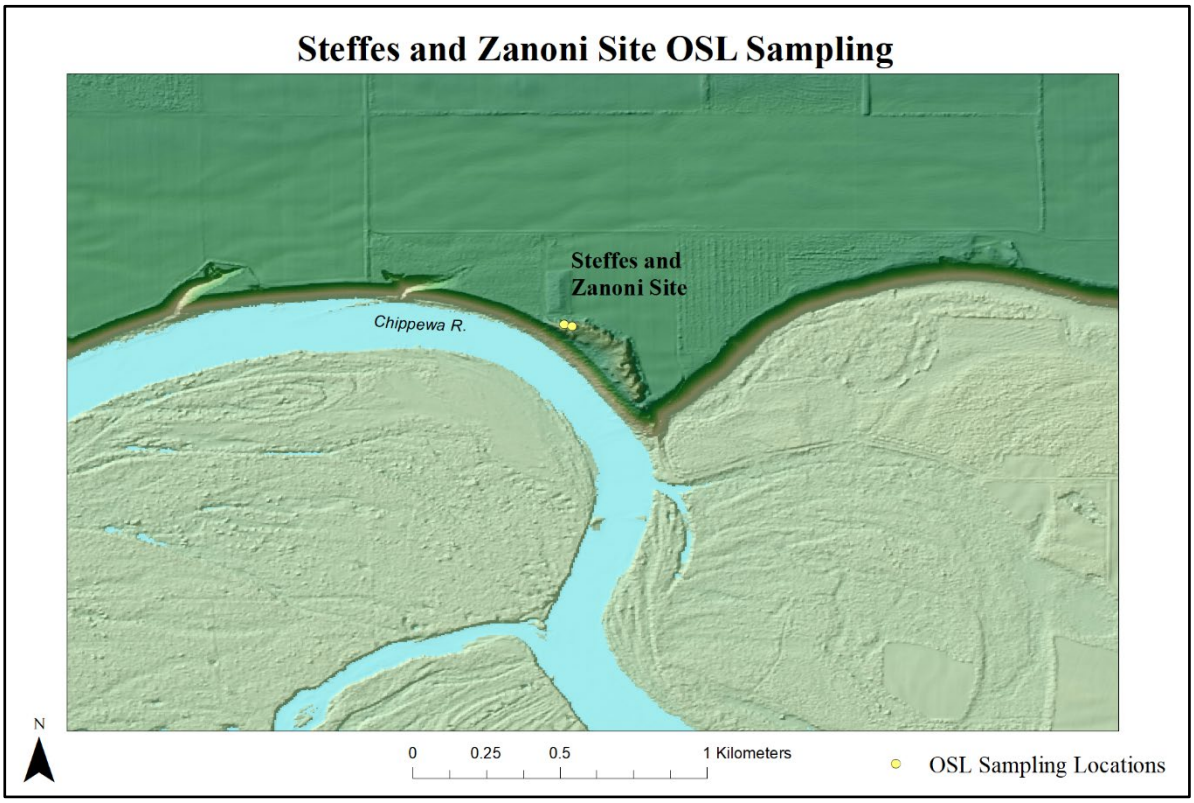

Fig. 32. OSL sampling locations at the Steffes and Zanoni site, .which is located along an active meander of the Chippewa River.

3.3 Results

3.3.1 *Parabolic and Cliff-Top Dune Mapping*

A total of 136 parabolic and cliff-top parabolic dunes were identified and assigned a confidence value within the counties surrounding the LCRV (Fig. 33). Forty-three were identified as cliff-top dunes and the remaining 93 are parabolic dunes. Thirty cliff-top and parabolic dunes were assigned a confidence of 3, which comprised the largest confidence class. Eighteen parabolic and cliff-top dunes received a confidence of 7, which is the highest score possible without field analysis. The Hurlburt and Steffes and Zanoni sites were among the 18 sand dunes that received a confidence score of 7. These two sites were selected for subsequent OSL and grain size analysis based upon their representative

form (i.e., possessing a typical morphology), accessibility, and land owner permission. It should be noted that the confidence scores for these two sites were changed to 10 following field analysis. The mean confidence score for cliff-top dunes was 5.49, whereas the mean confidence score for parabolic dunes was 4.44. The mean confidence score for all identified cliff-top and parabolic dunes was 4.77.

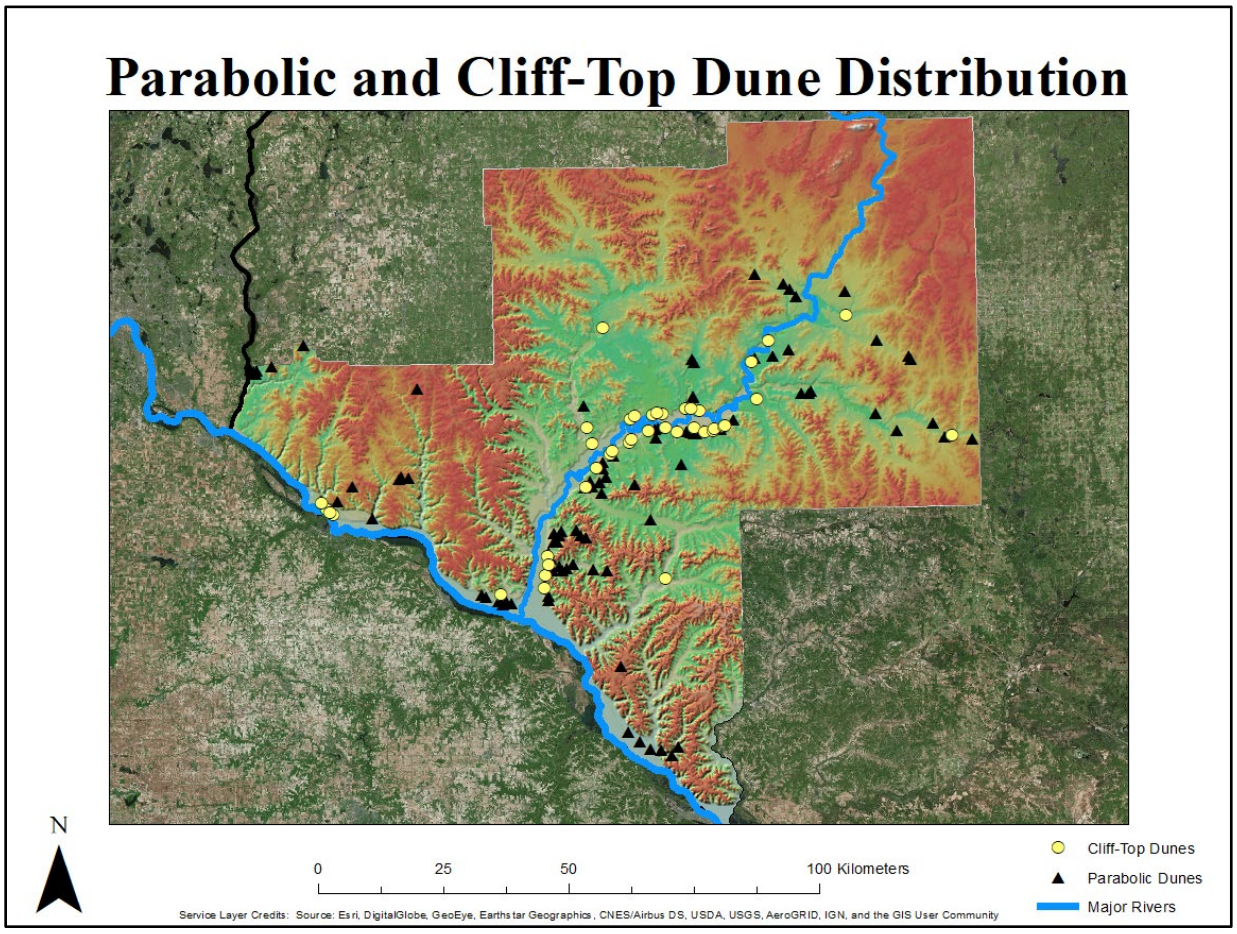

Fig. 33. The distribution of cliff-top dunes (yellow dots) and parabolic dunes (black triangles) within the LCRV.

Multiple orientations and morphologies for both parabolic and cliff-top dunes were identified from the mapping process. Orientations ranged from northeast to southeast indicating alternating northwest to southwest wind regimes. The mean orientation for parabolic dunes sand dunes was 110.69 degrees or east southeast. The mean orientation for cliff-top dunes was 85.29 degrees or east northeast. When combined, the mean orientation for cliff-top dunes and parabolic dunes was 102.66 degrees or east southeast. Consequently, the predominant dune forming wind regime in the LCRV and its surrounding counties was from the west. However, there was a 25.4 degree difference in mean orientation between cliff-top dunes and parabolic dunes. A total of 54.7% of cliff-top dunes had a northerly orientation, whereas only 16.8% of parabolic dunes were oriented in a north direction. Cliff-top dunes in the LCRV and its surrounding counties were formed by winds with a more significant southerly component whereas parabolic dunes were formed by winds with a more significantly northerly component. The different wind regimes indicate cliff-top and parabolic dunes formed asynchronously in the LCRV.

The parabolic and cliff-top dunes exhibit a similar spatial distribution within the LCRV and its surrounding counties. The mean and median center tools for the parabolic and cliff-top dunes were in similar locations (Fig. 34). Results from the directional distribution tool were also similar for parabolic and cliff-top dunes (Fig. 35). The directional distribution tool also indicated a spatial relationship between sand dune distributions and the Chippewa River. Cliff-top and parabolic sand dunes are distributed in a southwest to northeast orientation which parallels the trend of the northeast to southwest flowing Chippewa River (Fig. 35).

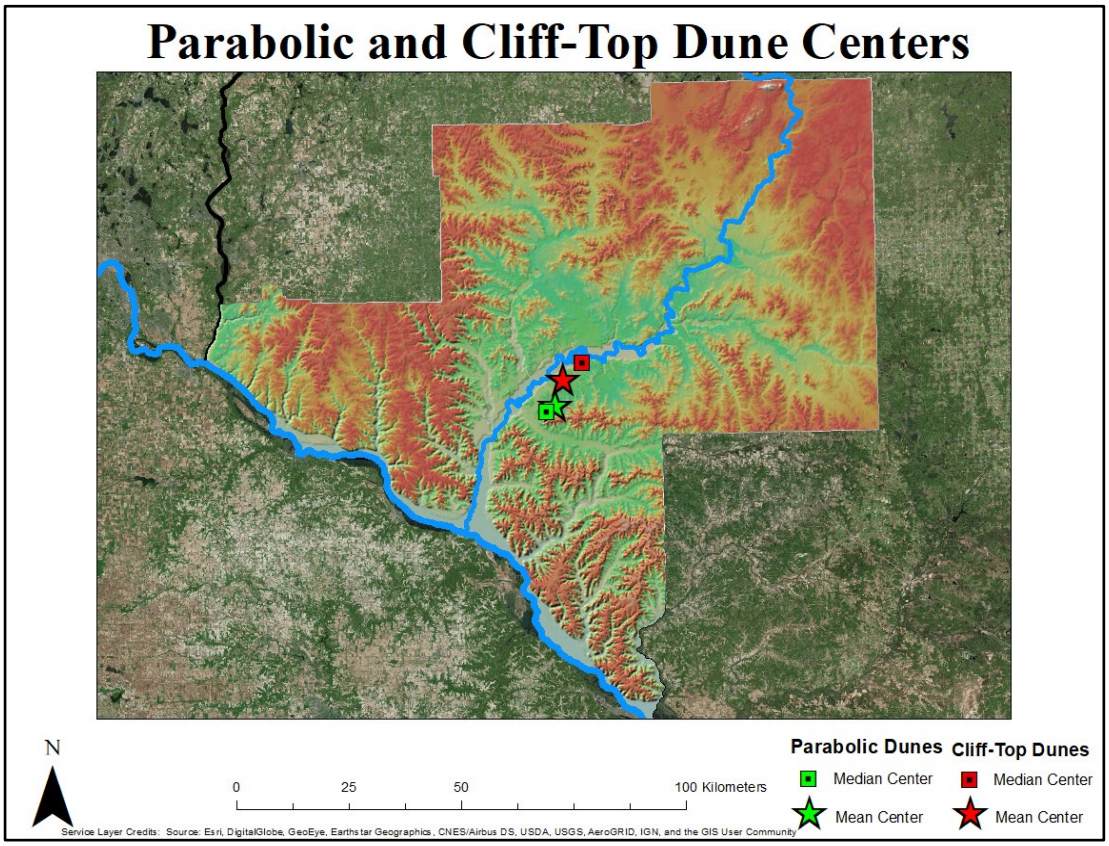

Fig. 34. The median and mean location for cliff-top and parabolic dunes within the LCRV.

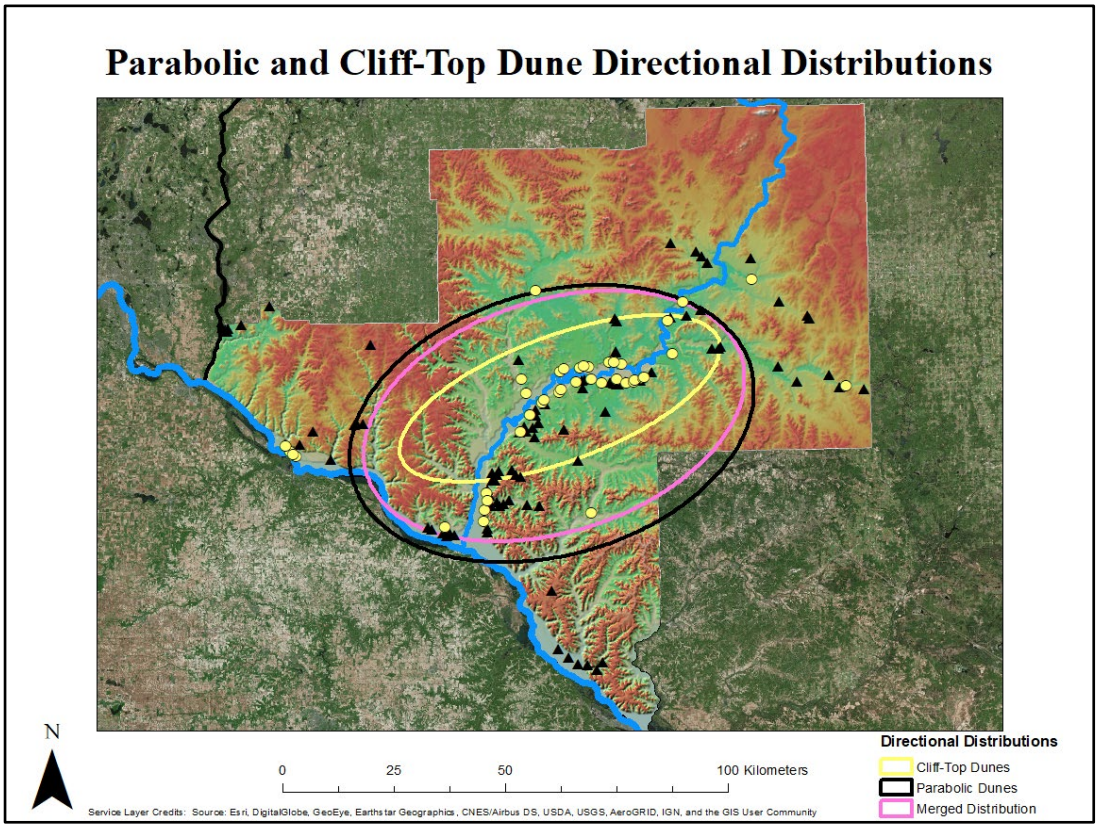

Fig. 35. The directional distribution for parabolic, cliff-top, and a composite of parabolic and cliff-top dunes

The morphology of parabolic and cliff-top dunes varied from degraded to well-preserved (Figs. 36 and 37). Aerial imagery indicated that all identified sand dunes are vegetated and stabilized. Sand dunes adjacent to the Chippewa River and its major tributaries were found exclusively above terrace escarpments and thus are in cliff-top position. In other words, sand dunes are not adjacent to the Chippewa River and its major tributaries at reaches where terrace escarpments are absent (i.e., locations where headward incision has not yet reached). Most cliff-top dunes do not exhibit complete morphologies, as their trailing arms have been truncated by previous or present erosion of their underlying terrace scarp. Some parabolic dunes were situated near the terrace escarpments of the Chippewa River. Therefore, some cliff-top dunes could represent pre-existing parabolic dunes that were subsequently placed in cliff-top position by a laterally incising Chippewa River.

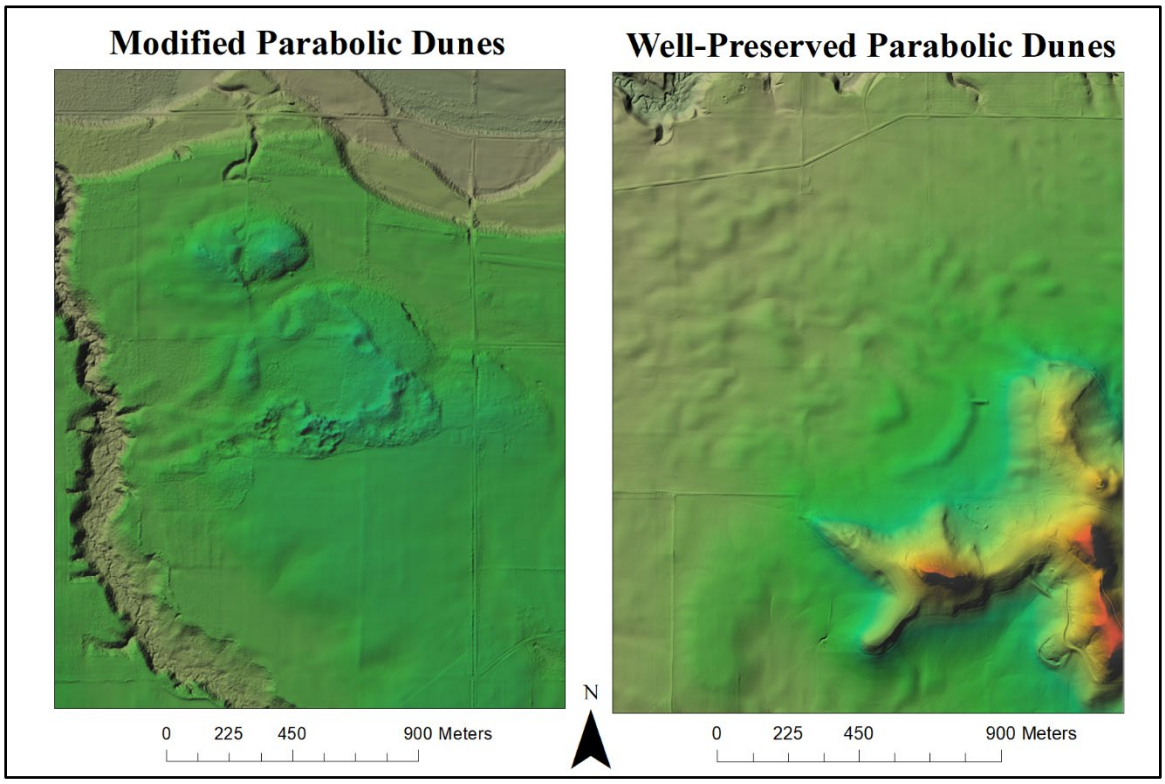

Fig. 36.A Comparison between modified and well-preserved parabolic dunes within the LCRV.

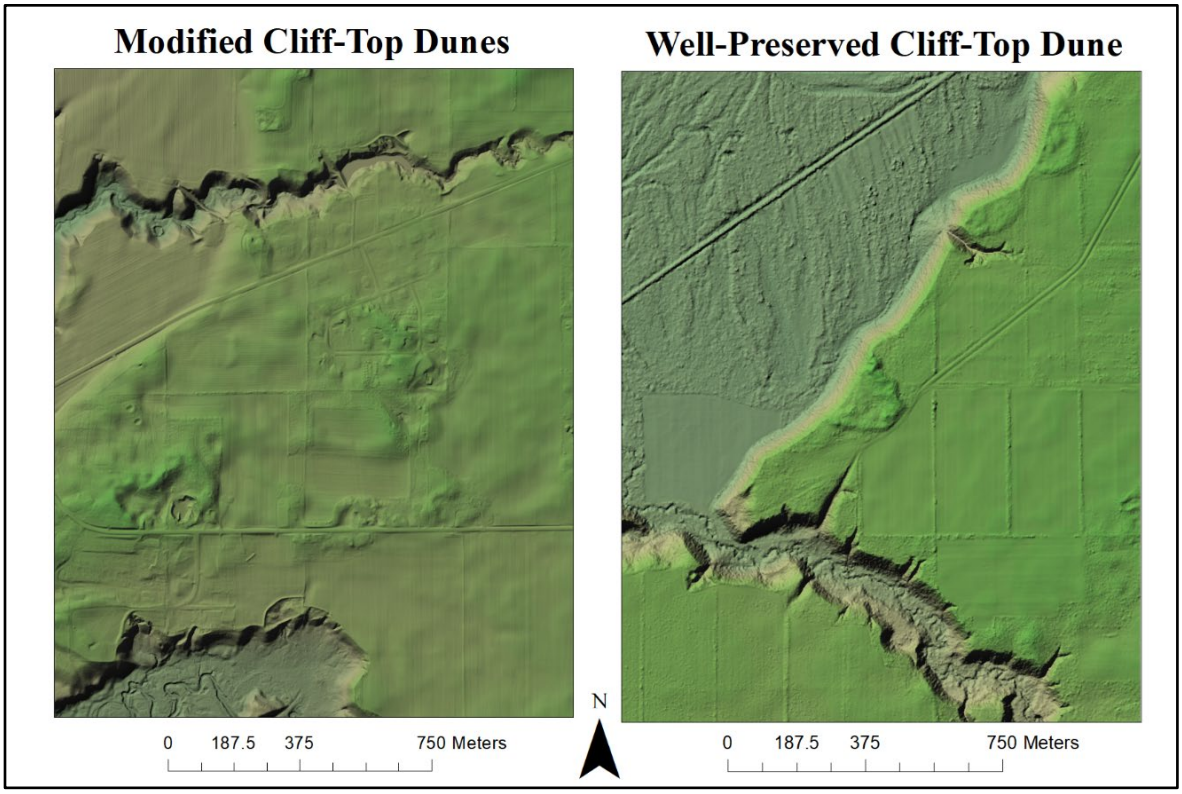

Fig. 37. A comparison between modified and well-preserved cliff-top dunes in the LCRV.

3.3.2 *Grain Size Analysis*

Grain sized analysis indicated minor differences between the two samples taken from the Hurlburt parabolic dunes and the single sample taken from the Steffes and Zanoni cliff-top dune. All three samples had remarkably similar grain size distributions, with Steffes and Zanoni site auger hole 2018-1 exhibiting a slightly greater contribution of coarser sediment at 410-710µm and 710-1180µm (Appendix D). The mean grain size values were calculated using the Folk and Ward method (see Chapter 2 for description) (Blott and Pye, 2001). The mean grain size values for the Hurlburt site exploratory hole and Hurlburt site 2A were 314.6µm and 314.9µm respectively. The Steffes and Zanoni site auger hole 2018-1 sediments were slightly coarser with a mean grain size value of

342.3µm. All three samples were described as medium sands and moderately sorted (Appendix D).

3.3.3 *Luminescence Dating*

In the present there are insufficient aliquots run on the Hurlburt and Steffes and Zanoni site OSL samples to derive final ages. Ten aliquots have been run on Hurlburt site OSL sample number USU-2896 and only seven aliquots have been run on sample number USU-2897 (Table 6). Twelve aliquots were run on the Steffes and Zanoni OSL sample number USU-2899 and ten aliquots have been run on the USU-2898 sample (Table 6). Therefore, the current OSL ages are considered to be preliminary. However, the ages from the Hurlburt and Steffes and Zanoni site dunes are consistent with other aeolian deposits in the region (Rawling et al., 2008; Hanson et al., 2015; Schaetzl et al., 2017) and/or the Kiwanis site dunes. Moreover, the dose rate and equivalent dose errors affiliated with each sample are consistent and relatively small (Appendix E), thus indicating the OSL ages are accurate.

Sample Number	**Depth**	**Number of Aliquots Run**	**Dose Rate (Gy/ka)**	**Preliminary DE**	**Preliminary OSL Age**
USU-2898	1.67	10	1.72±0.07	0.89±0.09	0.52±0.07
USU-2899	2.48	12	1.65±0.06	0.87±0.22	0.53±0.14
USU-2896	1.75	10	1.43±0.06	14.42±2.2	10.07±1.74
USU-2897	3.02	7	1.37±0.05	12.77±2.20	9.29±1.77

Table 6. OSL results for the Hurlburt and Steffes and Zanoni Sites that include the sample number, depth, number of aliquots, dose rate, equivalent dose, and preliminary ages.

The OSL samples from Hurlburt site parabolic dunes exhibit ages corresponding with the late Pleistocene to early Holocene transition at 10.1ka ± 1.7ka and 9.6ka ± 1.8ka. The OSL ages from two different parabolic dunes at the Hurlburt site are closely grouped and within the margin of error. The OSL samples from Steffes and Zanoni site cliff-top dune exhibits ages at .5ka ±.1ka and .6ka ± .1ka. These ages are remarkably close to one another and within the margin of error. Additionally, the OSL ages from the Steffes and Zanoni site correspond to the youngest ages from the Kiwanis site. Comparison between the Hurlburt and Steffes and Zanoni site dunes indicates there was over a 9ka gap between periods of deposition (Table 6).

3.4 Discussion

3.4.1 *Parabolic and Cliff-Top Dune Mapping and Distribution*

The difference between the mean confidence values for parabolic (4.44) and cliff-top dunes (5.49) was likely caused by them possessing a characteristically different morphology. All identified cliff-top dunes had a parabolic dune morphology, but with closer spacing between trailing arms, more pronounced crests, and overall greater relief than non-cliff-top parabolic dunes. In contrast, parabolic dunes were more diffused and exhibited a less preserved morphology (e.g., absent trailing arms, indiscernible crests). Consequently, parabolic dunes commonly received a lower morphology criterion value within the confidence score.

Parabolic and cliff-top dunes also exhibit different orientations, which alongside their morphology, indicates they formed asynchronously. The parabolic dunes' orientation corresponds to the findings of sandy aeolian research in the LCRV and

surrounding region (Zanner, 1999; Rawling et al., 2008; Miao et al., 2010; Mason, 2015; Schaetzl et al., 2017). This research indicates that most aeolian deposition took place during the Late Pleistocene under a predominant northwesterly wind regime (Zanner, 1999; Rawling et al., 2008; Mason, 2015; Schaetzl et al., 2017). In contrast, the mean orientation of cliff-top dunes in the LCRV indicates they formed by west southwest winds, which corresponds to the Kiwanis site dunes. This wind regime is previously unrecognized as forming sand dunes in the LCRV and surrounding region.

Cliff-top dunes within the LCRV are more common along a reach of the Chippewa River characterized by channel meandering (Andrews, 1965) and anastomosing (Faulkner et al., 2016)(Fig. 38). In contrast, cliff-top dunes are relatively absent at the lowest and upper reaches of the LCRV that exhibit less lateral incision (Andrews, 1965; Faulkner et al., 2016). Consequently, the spatial distribution of cliff-top

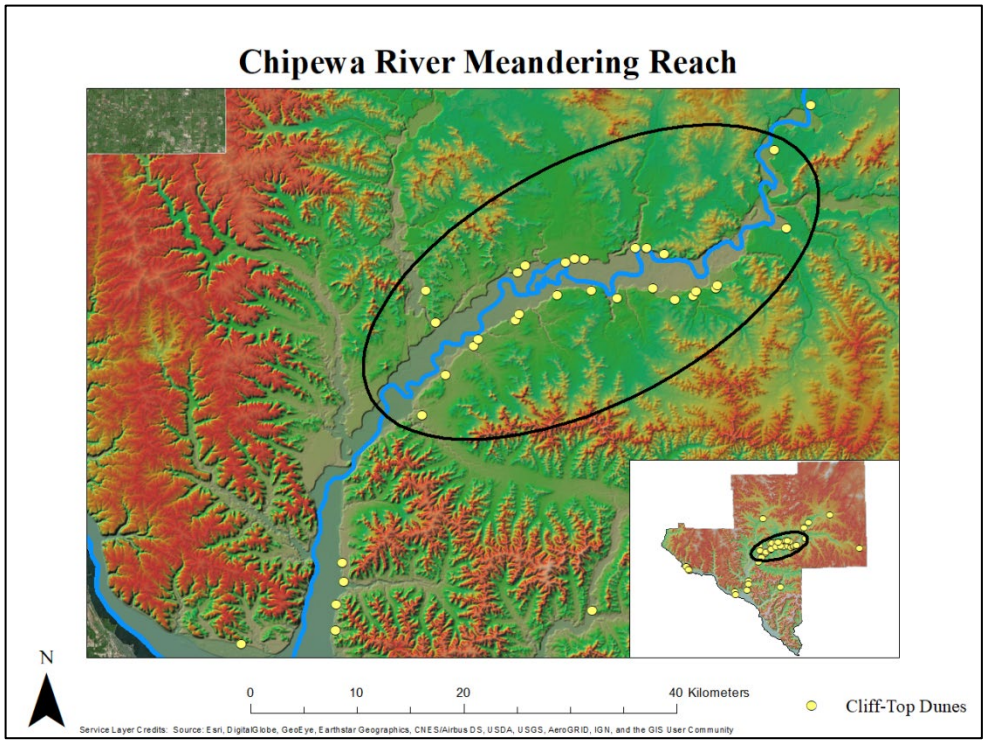

Fig. 38. Cliff-top dunes are preferentially located within the central reach of the lower Chippewa River, which is characterized by meandering.

dunes along the LCRV supports the cliff-top dune formation model proposed in Chapter 2.

3.4.2 *Grain Size Analysis*

There are insubstantial differences between grain size values at the Hurlburt and Steffes and Zanoni sites. The mean grain sizes from the samples at these two sites were generally coarser than the samples taken from the Kiwanis site. Overall the grain sizes and degree of sorting from samples taken from all sites within the LCRV indicate a short period of transport and/or exceptionally strong paleowinds. Yet additional grain size analysis of parabolic and cliff-top dunes within the LCRV is needed to determine more significant correlations.

3.4.3 *OSL Analysis*

3.4.3.1 Steffes and Zanoni Site

The OSL ages from the Steffes and Zanoni site at .6ka-.5ka correspond the youngest ages from cliff-top dunes at the Kiwanis site. Moreover, cliff-top dune formation at the Steffes and Zanoni site correlate with periods of increased aridity recorded in eastern Michigan (Jacques, Cumming and Smol, 2008), Minnesota (Dean, 1997; Shuman et al., 2009), and west-central Wisconsin (Wahl, Diaz and Ohlwein, 2012). More OSL ages are needed at the Steffes and Zanoni site in order to obtain an entire chronology of aeolian deposition. Nonetheless, it appears that cliff-top dune formation took place at this site during a period that exhibited increased aridity within the surrounding region. The OSL ages from RSD, the Kiwanis site, and the Steffes and Zanoni site indicate there were at least two and perhaps three periods of cliff-top dune

formation (6ka; 1ka-.8ka; .6ka-.4ka?) within the LCRV during the mid to late Holocene. These periods correspond to increased aridity recorded within regions surrounding the LCRV. Consequently, the correlation between aeolian cliff-top deposition at the Steffes and Zanoni site and a period of aridity supports the complex fluvial-aeolian cliff-top dune formation model for the LCRV proposed in Chapter 2. This model is used to represent the cliff-top dune forming stage within a time transgressive model that describes the aeolian landscape evolution of the LCRV throughout the Holocene (Fig. 39). The time transgressive model brackets the various stages of cliff-top dune evolution within the LCRV represented by RSD, the Kiwanis site, and the Steffes and Zanoni site.

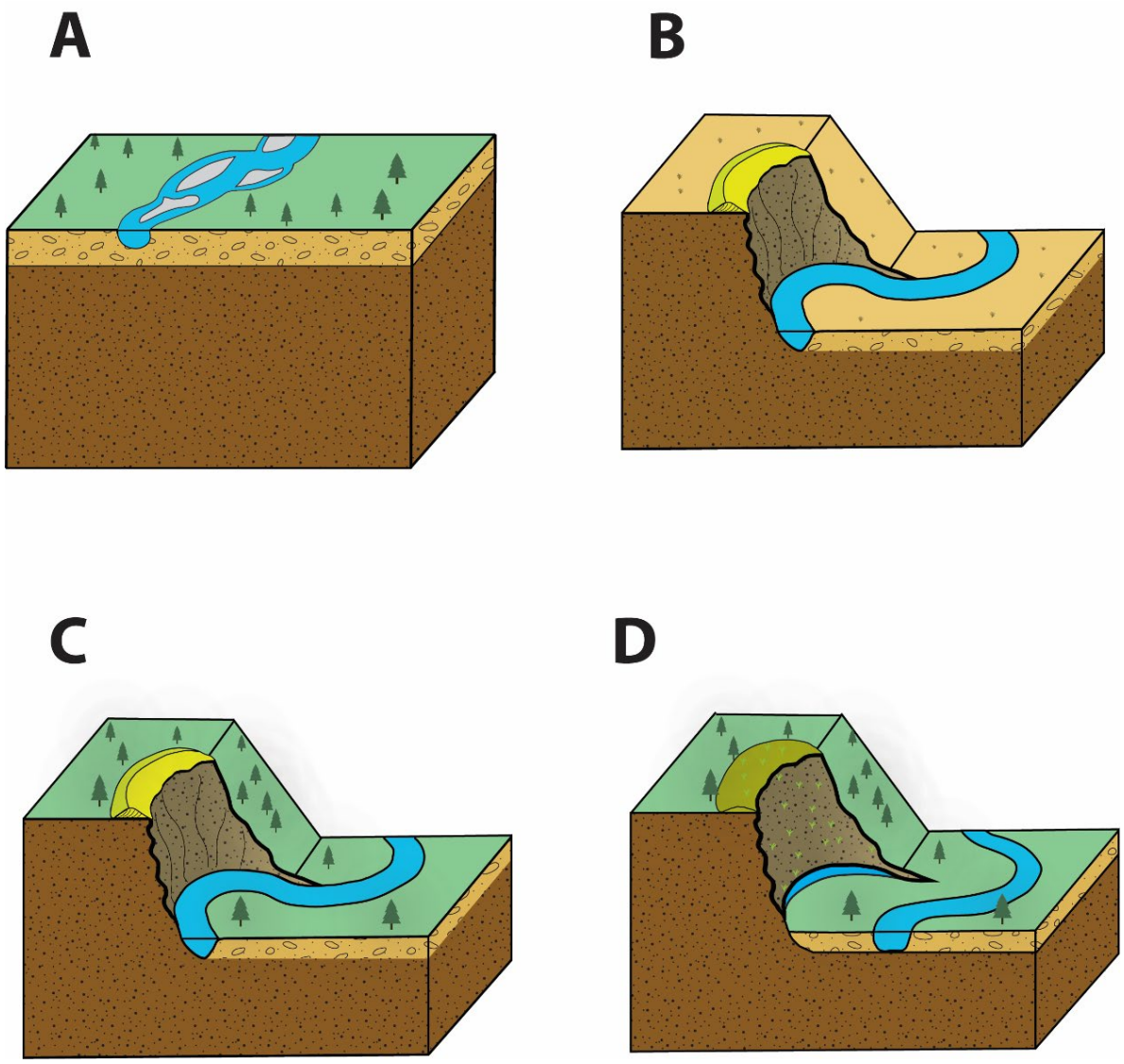

Fig. 39. Time series description of cliff-top dune evolution in the LCRV. A: Chippewa River prior to headward incision. B: Increased aridity while the Chippewa River incises vertically and laterally into outwash fill allows for cliff-top dune formation. C: Humid climate inhibits cliff-top dune formation during active fluvial incision (corresponds to Kiwanis and Steffes and Zanoni site cliff-top dunes). D: The Chippewa River abandons its meander and the cliff-top dune's morphology is degraded (corresponds to RSD).

3.4.3.2 Hurlburt Site

The 9.6ka-10.1ka OSL ages from the parabolic dunes at the Hurlburt site correspond well with previous records of aeolian deposition within the LCRV (Schaetzl et al., 2017), southeastern Minnesota (Hanson et al., 2015), and central Wisconsin (Rawling et al., 2008). The 17.5ka -10ka period of the late Pleistocene is identified as a period of overall climatic warming in the upper Midwest following the last glacial maximum (Rawling et al., 2008). Research of aeolian activity deposition during this period consistently affiliates sand dune formation to local sand supply/availability (Rawling et al., 2008; Miao et al., 2010; Loope et al., 2013; Schaetzl et al., 2017). Sand availability has been ascribed to permafrost degradation following the last glacial maximum in the region (Rawling et al., 2008; Loope et al., 2013). The parabolic dunes at the Hurlburt site were not likely affiliated with permafrost degradation, as permafrost had retreated from southern Wisconsin by 14ka and from northern Wisconsin by 10ka (Clayton, Attig and Mickelson, 2001). Nonetheless, the corresponding ages between the Hurlburt site parabolic dunes and nearby aeolian deposits indicates there was a broader signal of aeolian activity around 10ka.

Alternatively, these aeolian deposits could be recording the terminal period of continuous aeolian activity during the late Pleistocene as climatic conditions ameliorated and vegetative cover increased. OSL dating records the minimum ages on depositional features, meaning the Hurlburt dunes may have been active prior to their final deposition around 10ka. OSL ages will not record earlier periods of deposition if the material has been remobilized and re-exposed to sunlight. Therefore, instead of recording a period of increased aeolian activity, the Hurlburt dunes age may actually indicate a period during which aeolian activity was subsiding. Future OSL analysis is needed from samples taken

greater depths from parabolic dunes in the Hurlburt site and in other locations within the LCRV.

3.4.3.3 Parabolic Dune Sand Supply

Regardless of environmental conditions at 10ka, the Hurlburt parabolic dunes were likely supplied by sands from west northwest locations. The sand supply for the sand ramp along the LCRV in Eau Claire, Wisconsin is ascribed to the outwash sediments of the Chippewa River (Schaetzl et al., 2017). The sand ramp and the Hurlburt site parabolic dunes exhibit similar ages and were formed under a similar northwest wind regime. Additionally, parabolic dunes in close proximity to the Chippewa River are more common to its south and east including those investigated at the Hurlburt site. Consequently, the preferential location, orientation, and ages of the Hurlburt parabolic dunes suggests they were supplied by sediment within the Chippewa River as described for the sand ramp in the city of Eau Claire (Schaetzl et al., 2017). Yet the Hurlburt site is located several kilometers down valley of the sand ramp where headward incision along the Chippewa River may have already been active by ~10ka. If, the Chippewa River had already incised into the LCRV in response to local base level fall, it would likely have functioned as a sink for sand as opposed to a source (Mason et al., 1999). Mason et al. (1999) suggested the distribution of aeolian sand and loess deposits in northeastern Iowa and southeastern Minnesota was related to incised valleys that would limit sand transport and thus promote downwind loess deposition.

The Hurlburt site is located approximately 17km upstream from the confluence of the Chippewa River and Mississippi River. To constrain headward incision along the Chippewa River, Faulkner et al. (2016) OSL dated terraces located 10km and 19km

upstream of the Mississippi River confluence. The OSL ages from the terrace 10km upstream of the Mississippi River confluence indicate ~5m of incision occurred between 18.5 and 13.5ka, with subsequent incision occurring after 13.5ka. The OSL ages from the terrace 19km upstream of the Mississippi River confluence indicate ~5m of incision occurred between 17.5ka and 12.3ka, with subsequent incision occurring after 12.3ka. Consequently, headward incision along the Chippewa River reached the Hurlburt site prior to dune formation around 10ka. However, the vertical depth of incision may not have been significant enough to produce an obstruction to sand transport. Moreover, the terraces along the Chippewa River were formed by cut-fill-cut processes, meaning there were periods of flood plain development and sediment aggradation prior to terrace abandonment (Faulkner et al., 2016). The formation period for parabolic dunes at the Hurlburt site could correspond to a period of aggradation at the lower reach of the Chippewa River. Additionally, headward incision along the Chippewa River eventually reached and rejuvenated its largest tributary, the Red Cedar River, which is located approximately 20km upstream of the Hurlburt site. The rejuvenation of the Red Cedar likely increased sediment supply to the Chippewa River, which promoted aggradation in its downstream reaches (e.g., Hurlburt site). According the headward incision model proposed by Faulkner et al. (2016), rejuvenation of the Red Cedar River was occurring while the Hurlburt dunes formed ~10ka and had diminished by around 9ka. As a result, the current understanding of headward incision along the Chippewa River does not confirm or deny the hypothesis that parabolic dunes such as those at the Hurlburt site, were supplied by the river's sediment. Future OSL dating of parabolic dunes throughout different reaches of the LCRV is needed to determine if there is a broader signal of aeolian activity around 10ka.

3.5 Conclusion

Results from the Steffes and Zanoni site cliff-top dune indicate aeolian activity occurred in the LCRV during the late Holocene. In contrast, OSL ages from the Hurlburt site parabolic dunes record aeolian activity during the late Pleistocene to early Holocene transition. The different morphology, orientation, and OSL ages from the Hurlburt and Steffes and Zanoni site collectively suggest parabolic and cliff-top dunes formed asynchronously and under different conditions within the LCRV. Additionally, OSL ages from the Steffes and Zanoni site correlate with a period of aridity recorded in surrounding regions, thus supporting the cliff-top dune formation model proposed in Chapter 2. Analysis of parabolic and cliff-top dunes in the LCRV contributes to the chronology of sand aeolian deposition in the region. It provides supporting evidence for late Pleistocene aeolian activity and indicates a previously unrecognized period of late Holocene aeolian activity.

Chapter 4

The LCRV is a relict aeolian landscape with stabilized sand ramps, sand stringers, parabolic dunes and cliff-top dunes. Cliff-top dunes are valuable features for reconstructing paleoenvironmental conditions within a landscape because they preserve past climatic and climatic and geomorphic processes. Their utility is exemplified in the LCRV, whereby fluvial cliff-top dunes record vertical and lateral incision along the Chippewa River coupled with past wind regimes and periods of increased aridity. OSL ages of cliff-top dunes from RSD, the Kiwanis site, and the Steffes and Zanoni site indicate at least two periods of aeolian activity in the LCRV over the past 6ka. In contrast, the morphology, orientations, and initial OSL ages from parabolic dunes in the LCRV suggest they formed around 10ka under different environmental conditions than cliff-top dunes. Therefore, cliff-top and parabolic dunes in the LCRV record a chronology of periodic aeolian deposition since the end of the Pleistocene and throughout the Holocene. The periodicity of aeolian activity within the LCRV over the past 10ka indicates this landscape's intrinsic geomorphic processes make is susceptible to aeolian activity when exposed to external variables such as climatic change.

References

Anderton, J. B. and Loope, W. L., 1995. Buried Soils in a Perched Dunefield as Indicators of Late Holocene Lake Level Change in the Lake Superior Basin. Quaternary Research 44, 190-199.

Andrews, G. W., 1965. Late Quaternary geologic history of the lower Chippewa valley, Wisconsin. Geological Society of America Bulletin 76, 113-124.

Arbogast, A. F., Hansen, E. C. and Van Oort, M. D., 2002. Reconstructing the geomorphic evolution of large coastal dunes along the southeastern shore of Lake Michigan. Geomorphology 46, 241-255.

Arbogast, A. F. and Loope, W. L., 1999. Maximum-limiting ages of Lake Michigan coastal dunes: Their correlation with Holocene lake level history. Journal of Great Lakes Research 25, 372-382.

Arbogast, A. F., Luehmann, M. D., William Monaghan, G., Lovis, W. A. and Wang, H., 2017. Paleoenvironmental and geomorphic significance of bluff-top dunes along the Au Sable River in Northeastern Lower Michigan, USA. Geomorphology 297, 112-121.

Bateman and Murton, 2006. The Chronostratigraphy of late Pleistocene glacial and periglacial aeolian activity in the Tuktoyaktuk Coastlands, NWT, Canada. Quaternary Science Reviews 2552-2568.

Beaudoin, A., 2002. On the identification and characterization of drought and aridity in postglacial paleoenvironmental records from the northern great plains. Géographie physique et Quaternaire 56, 229-246.

Beaudoin, A. B., Wright, M. and Ronaghan, B., 1996. Late quaternary landscape history and archaeology in the 'Ice-Free Corridor': Some recent results from Alberta. Quaternary International 32, 113-126.

Bégin, C., Michaud, Y. and Filion, L., 1995. Dynamics of a Holocene cliff-top dune along Mountain River, Northwest Territories, Canada. Quaternary Research 44, 392-404.

Blott, S. J. and Pye, K., 2001. GRADISTAT: a grain size distribution and statistics package for the analysis of unconsolidated sediments. Earth surface processes and Landforms 26, 1237-1248.

Booth, R. K., Notaro, M., Jackson, S. T. and Kutzbach, J. E., 2006. Widespread drought episodes in the western Great Lakes region during the past 2000 years: geographic extent and potential mechanisms. Earth and Planetary Science Letters 242, 415-427.

Bowden, A. J. and Lindley, D., 1977. A wind-tunnel investigation of the wind speed and turbulence characteristics close to the ground over various escarpment shapes. 12, 259-271.

Bullard, J. E. and Nash, D. J., 2000. Valley-marginal sand dunes in the south-west Kalahari: their nature, classification and possible origins. Journal of Arid Environments 45, 369-383.

Carter, R. and Wilson, P., 1993. Aeolian processes and deposits in northwest Ireland. Geological Society, London, Special Publications 72, 173-190.

Clayton, L., Attig, J. W. and Mickelson, D. M., 2001. Effects of late Pleistocene permafrost on the landscape of Wisconsin, USA. Boreas 30, 173-188.

Cook, B. I., Cook, E. R., Smerdon, J. E., Seager, R., Williams, A. P., Coats, S., Stahle, D. W. and Díaz, J. V., 2016. North American megadroughts in the Common Era: Reconstructions and simulations. Wiley Interdisciplinary Reviews: Climate Change 7, 411-432.

Costas, S., Brito, P., Ferraz, M., González-Villanueva, R., Novo, A. and Rebêlo, L., 2010. The cliff-top dune of Costa da Caparica: possible scenarios of formation and evolution. Coastal Hope 27-28.

Cowles, H. C., 1899. The Ecological relations of the vegetation on the sand dunes of Lake Michigan. Part I.-geographical relations of the dune floras. Botanical Gazette 95-117.

David, P. P., 1977. Sand Dune Occurrences of Canada: A Theme and Resource Inventory Study of Eolian Landforms of Canada. Géographie physique et Quaternaire 32, 375-375.

Dean, W. E., 1997. Rates, timing, and cyclicity of Holocene eolian activity in north-central United States: Evidence from varved lake sediments. Geology 25, 331-334.

Dean, W. E., Ahlbrandt, T. S., Anderson, R. Y. and Platt Bradbury, J., 1996. Regional aridity in North America during the middle Holocene. The Holocene 6, 145-155.

Denniston, R. F., González, L. A., Baker, R. G., Asmerom, Y., Reagan, M. K., Edwards, R. L. and Alexander, E. C., 1999. Speleothem evidence for Holocene fluctuations of the prairie-forest ecotone, north-central USA. The Holocene 9, 671-676.

Dow, K. W., 1937. The origin of perched dunes on the Manistee moraine, Michigan. Michigan Academy of Science, Arts, and Letters 23, 427-440.

Englebright, S. C., Hanson, G. N., Rasbury, T. and Lamont, E. E., 2000. On the origin of parabolic dunes near Friar's Head, Long Island, New York. Long Island Botanical Society Quarterly 10, 1-12.

Faulkner, D. J., Larson, P. H., Jol, H. M., Running, G. L., Loope, H. M. and Goble, R. J., 2016. Autogenic incision and terrace formation resulting from abrupt late-glacial base-level fall, lower Chippewa River, Wisconsin, USA. Geomorphology 266, 75-95.

Gates, F. C., 1950. The Disappearing Sleeping Bear Dune. Ecology 31, 386-392.

Gee, G. W. and Or, D., 2002. 2.4 Particle-size analysis. Methods of soil analysis. Part 4, 255-293.

Goudie, A., 2011. Parabolic dunes: distribution, form, morphology and change. Annals of Arid Zone 50, 1-7.

Grigal, D., Severson, R. C. and Goltz, G., 1976. Evidence of eolian activity in north-central Minnesota 8,000 to 5,000 yr ago. Geological Society of America Bulletin 87, 1251-1254.

Hack, 1941. Dunes of the western Navajo Country. Dunes of the Western Navajo Country 240-263.

Halfen, A. F. and Johnson, W. C., 2013. A review of Great Plains dune field chronologies. Aeolian Research 10, 135-160.

Hanson, P. R., Mason, J. A., Jacobs, P. M. and Young, A. R., 2015. Evidence for bioturbation of luminescence signals in eolian sand on upland ridgetops, southeastern Minnesota, USA. Quaternary International 362, 108-115.

Harrison, S. P., Kutzbach, J. E., Liu, Z., Bartlein, P. J., Otto-Bliesner, B., Muhs, D., Prentice, I. C. and Thompson, R. S., 2003. Mid-Holocene climates of the Americas: a dynamical response to changed seasonality. Climate Dynamics 20, 663-688.

Haslett, 2000. Geomorphologic and Palaeoenvironmental Development of Holocene Perched Coastal Dune Systems in Brittany, France. 79-88.

Hétu, B., 1992. Coarse cliff-top aeolian sedimentation in northern Gaspésie, Québec (Canada). Earth surface processes and Landforms 17, 95-108.

Ho, L.-D., Lüthgens, C., Wong, Y.-C., Yen, J.-Y. and Chyi, S.-J., 2017. Late Holocene cliff-top dune evolution in the Hengchun Peninsula of Taiwan: Implications for palaeoenvironmental reconstruction. Journal of Asian Earth Sciences 148, 13-30.

Howchin, W., 1909. Geological observations on some of the localities visited by the 'Governor Musgrave'Party. January, 1907, Proc. Roy. Geogrl. Soc. Australasia (S. Aust.) 10, 204-219.

Howchin, W., 1923. A geological sketch section of the sea cliffs on the eastern side of Gulf St Vincent from Brighton to Sellicks Hill, with descriptions. Trans. Roy. Soc. S. Aust 47, 279-315.

Isard, S. A., 1987. The effect of slope-aspect on turbulent transfer in an alpine fellfield: Niwot Ridge, Front Range, Colorado. Physical Geography 8, 133-147.

Jacques, J.-M. S., Cumming, B. F. and Smol, J. P., 2008. A 900-year pollen-inferred temperature and effective moisture record from varved Lake Mina, west-central Minnesota, USA. Quaternary Science Reviews 27, 781-796.

Jennings, J., 1957. On the orientation of parabolic or U-dunes. The Geographical Journal 123, 474-480.

Jennings, J. N., 1967. Cliff-top dunes. Australian Geographical Studies 5, 40-49.

Keen, K. and Shane, L. C., 1990. A continuous record of Holocene eolian activity and vegetation change at Lake Ann, east-central Minnesota. GSA Bulletin 102, 1646-1657.

Lancaster, N., 2009. Dune morphology and dynamics Geomorphology of Desert Environments 557-590.

Lancaster, N. and Baas, A., 1998. Influence of vegetation cover on sand transport by wind: field studies at Owens Lake, California. Earth Surface Processes and Landforms: The Journal of the British Geomorphological Group 23, 69-82.

Larson, P. H., J. Mcdonald, Baker, A., Dryer, W. P., Running, G. L., Faulkner, D. J. and Jol., H. M., 2008. Geomorphology of cliff-top parabolic dunes within the lower Chippewa River valley, upper Putnam Park, Eau Claire, Wisconsin. American Association of Geographers Abstracts with Programs.

Loope, W. L. and Arbogast, A. F., 2000. Dominance of an ~150-year cycle of sand-supply change in late Holocene dune-building along the eastern shore of Lake Michigan. Quaternary Research 54, 414-422.

Mann, M. E., 2002. Medieval climatic optimum. Encyclopedia of Global environmental change 1, 514-516.

Mann, M. E., Zhang, Z., Rutherford, S., Bradley, R. S., Hughes, M. K., Shindell, D., Ammann, C., Faluvegi, G. and Ni, F., 2009. Global signatures and dynamical origins of the Little Ice Age and Medieval Climate Anomaly. Science 326, 1256-1260.

Marsh, W. M., 1990. Nourishment of perched sand dunes and the issue of erosion control in the Great Lakes. Environmental Geology and Water Sciences 16, 155-164.

Marsh, W. M. and Marsh, B. D., 1987. Wind Erosion and Sand Dune Formation on High Lake Superior Bluffs. Geografiska Annaler. Series A, Physical Geography 69, 379-391.

Mason, J. A., 2015. Up in the refrigerator: Geomorphic response to periglacial environments in the Upper Mississippi River Basin, USA. Geomorphology 248, 363-381.

Mason, J. A., Nater, E. A., Zanner, C. W. and Bell, J. C., 1999. A new model of topographic effects on the distribution of loess. Geomorphology 28, 223-236.

Miao, X., Hanson, P. R., Wang, H. and Young, A. R., 2010. Timing and origin for sand dunes in the Green River Lowland of Illinois, upper Mississippi River Valley, USA. Quaternary Science Reviews 29, 763-773.

Muhs, D. R., Been, J., Mahan, S. A., Burdett, J., Skipp, G., Rowland, Z. M. and Stafford Jr, T. W., 1997. Holocene eolian activity in the Minot dune field, North Dakota. Canadian Journal of Earth Sciences 34, 1442-1459.

Murray, A. S. and Wintle, A. G., 2000. Luminescence dating of quartz using an improved single-aliquot regenerative-dose protocol. Radiation measurements 32, 57-73.

Nelson, M. S., Gray, H. J., Johnson, J. A., Rittenour, T. M., Feathers, J. K. and Mahan, S. A., 2015. User guide for luminescence sampling in archaeological and geological contexts. Advances in Archaeological Practice 3, 166-177.

Olson, J. S., 1958a. Lake Michigan dune development 1. Wind-velocity profiles. The Journal of Geology 66, 254-263.

Olson, J. S., 1958b. Lake Michigan dune development 2. Plants as agents and tools in geomorphology. The Journal of Geology 66, 345-351.

Olson, J. S., 1958c. Lake Michigan dune development. 3. lake-level, beach, and dune oscillations. The Journal of Geology 66, 473-483.

Olson, J. S., 1958. Rates of succession and soil changes on southern Lake Michigan sand dunes. Botanical Gazette 119, 125-170.

Pain, C. F., 1976. Late quaternary dune sands and associated deposits near Aotea and Kawhia Harbours, north island, New zealand. New Zealand Journal of Geology and Geophysics 19, 153-77.

Rampton, V. N., 1988. Quaternary geology of the Tuktoyaktuk coastlands, Northwest Territories. 1-98.

Rawling, J. E., Fredlund, G. G. and Mahan, S., 2003. Aeolian cliff-top deposits and buried soils in the White River Badlands, South Dakota, USA. The Holocene 13, 121-129.

Rawling, J. E., Hanson, P. R., Young, A. R. and Attig, J. W., 2008. Late Pleistocene dune construction in the Central Sand Plain of Wisconsin, USA. Geomorphology 100, 494-505.

Rhodes, E. J., 2011. Optically stimulated luminescence dating of sediments over the past 200,000 years. Annual Review of Earth and Planetary Sciences 39, 461-488.

Rittenour, T. M., 2008. Luminescence dating of fluvial deposits: applications to geomorphic, palaeoseismic and archaeological research. Boreas 37, 613-635.

Rodríguez, J. G. and Uriarte, A., 2009. Laser diffraction and dry-sieving grain size analyses undertaken on fine-and medium-grained sandy marine sediments: a note. Journal of Coastal Research 257-264.

Running, 1995. Archaeological geology of the Rustad Quarry. Geoarchaeology: An International Journal 183-204.

Sansò, P., Gianfreda, F., Leucci, G. and Mastronuzzi, G., 2016. Cliff evolution and late Holocene relative sea level change along the Otranto coast (Salento peninsula, southern Apulia, Italy). GeoResJ 9-12, 42-53.

Saye, S. E., Pye, K. and Clemmensen, L. B., 2006. Development of a cliff-top dune indicated by particle size and geochemical characteristics: Rubjerg Knude, Denmark. Sedimentology 53, 1-21.

Schaetzl, R. J., Forman, S. L. and Attig, J. W., 2017. Optical ages on loess derived from outwash surfaces constrain the advance of the Laurentide Ice Sheet out of the Lake Superior Basin, USA. Quaternary Research 81, 318-329.

Schaetzl, R. J., Larson, P. H., Faulkner, D. J., Running, G. L., Jol, H. M. and Rittenour, T. M., 2017. Eolian sand and loess deposits indicate west-northwest paleowinds during the Late Pleistocene in western Wisconsin, USA. Quaternary Research 1-17.

Schumm, S., 1973. Geomorphic thresholds and complex response of drainage systems. Fluvial geomorphology 6, 69-85.

Schumm, S., 1993. River response to baselevel change: implications for sequence stratigraphy. The Journal of Geology 101, 279-294.

Schumm, S. A., 1979. Geomorphic thresholds: the concept and its applications. Transactions of the Institute of British Geographers 4, 485-515.

Sharp, R. P., 1949. Pleistocene ventifacts east of the Big Horn Mountains, Wyoming. The Journal of Geology 57, 175-195.

Short, A. D., 1988. Holocene coastal dune formation in southern Australia: A case study. Sedimentary Geology 55, 121-142.

Shuman, B., Henderson, A. K., Plank, C., Stefanova, I. and Ziegler, S. S., 2009. Woodland-to-forest transition during prolonged drought in Minnesota after ca. AD 1300. Ecology 90, 2792-2807.

Sloss, C. R., Hesp, P. and Shepherd, M., 2012. Coastal Dunes: Aeolian Transport. Nature Education Knowledge 3, 1-6.

Sridhar, V., Loope, D. B., Swinehart, J. B., Mason, J. A., Oglesby, R. J. and Rowe, C. M., 2006. Large wind shift on the Great Plains during the Medieval Warm Period. Science 313, 345-347.

Thornthwaite, C. W., 1961. The Task Ahead. Annals of the Association of American Geographers 51, 345-356.

Tian, J., Nelson, D. M. and Hu, F. S., 2006. Possible linkages of late-Holocene drought in the North American midcontinent to Pacific Decadal Oscillation and solar activity. Geophysical Research Letters 33, 1-6.

Valentine, K. W., Fladmark, K. and Spurling, B., 1980. The description, chronology and correlation of buried soils and cultural layers in a terrace section, Peace River Valley, British Columbia. Canadian Journal of Soil Science 60, 185-197.

Wahl, E. R., Diaz, H. F. and Ohlwein, C., 2012. A pollen-based reconstruction of summer temperature in central North America and implications for circulation patterns during medieval times. Global and Planetary Change 84, 66-74.

White, E. M., 1960. Conditions for cliff dune formation and the climatic implications. Anthropologist 5, 80-82.

Wilson, P., 1989. Nature, origin and age of Holocene aeolian sand on Muckish Mountain, Co. Donegal, Ireland. Boreas 18, 159-168.

Wolfe, S. A. and David, P., 1997. Parolbolic dunes: Examples form the Great Sand Hills Southwestern Saskatchewan. The Canadian Geographer 2, 207-213.

Wolfe, S. A., Huntley, D. J., David, P. P., Ollerhead, J., Sauchyn, D. J. and MacDonald, G. M., 2001. Late 18th century drought-induced sand dune activity, Great Sand Hills, Saskatchewan. Canadian Journal of Earth Sciences 38, 105-117.

Wright, H. E., Winter, T. C. and Patten, H. L., 1963. Two pollen diagrams from southeastern Minnesota: problems in the regional late-glacial and postglacial vegetational history. Geological Society of America Bulletin 74, 1371-1396.

Yan, N. and Baas, A. C. W., 2017. Environmental controls, morphodynamic processes, and ecogeomorphic interactions of barchan to parabolic dune transformations. Geomorphology 278, 209-237.

Yan, N. and Baas, A. C. W., 2015. Parabolic dunes and their transformations under environmental and climatic changes: Towards a conceptual framework for understanding and prediction. Global and Planetary Change 124, 123-148.

Appendix A

A Table of Compiled Cliff-Top Dune Research

Table 2. A compiled list of research pertaining cliff-top dunes that were available to the author.

YEAR	AUTHOR	TITLE	CLIFF-TOP DUNE CLASSIFICATION
1879	Tate, R.	*The natural history of the country around the head of the Great Australian Bight*	Coastal Normal
1899	Cowles, H. C.	The ecological relations of the vegetation on the sand dunes of Lake Michigan. Part I.- geographical relations of the dune floras	Coastal Normal
1923	Howchin, W.	A geological sketch section of the sea cliffs on the eastern side of Gulf St Vincent from Brighton to Sellicks Hill, with descriptions.	Coastal Hybrid
1936	Bergquist, S. G.	The Grand Sable Dunes on Lake Superior, Alger County, Michigan	Coastal Normal
1937	Dow, K. W.	The origin of perched dunes on the Manistee moraine, Michigan	Coastal Normal
1941	Hack, J. T.	Dunes of the western Navajo country	Terrestrial Fluvial and Terrestrial Normal
1949	Sharp, R. P.	Pleistocene ventifacts east of the Big Horn Mountains, Wyoming	Terrestrial Normal
1950	Gates, F. C.	The disappearing Sleeping Bear Dune	Coastal Normal
1954	Brothers, R.	*A physiographical study of recent sand dunes on the Auckland west coast*: New Zealand	Coastal Normal
1958	Olson, J. S.	Rates of succession and soil changes on southern Lake Michigan sand dunes	Coastal Normal
1958	Olson, J. S.	Lake Michigan dune development 1. Wind-velocity profiles	Coastal Normal
1958	Olson, J. S.	Lake Michigan dune development 2. Plants as agents and tools in geomorphology	Coastal Normal
1958	Olson, J. S.	Lake Michigan Dune Development. 3. Lake-level, beach, and dune oscillations	Coastal Normal
1960	White, E. M.	Conditions for cliff dune formation and the climatic implications	Terrestrial Fluvial and Terrestrial Normal

1967	Jennings, J. N.	Cliff-top dunes	Coastal Normal and Coastal Hybrid
1972	David, P. P.	Great Sand Hills Saskatchewan	Terrestrial Fluvial
1976	Pain, C. F.	Late quaternary dune sands and associated deposits near Aotea and Kawhia Harbours, north island, New Zealand	Coastal Normal
1982	Pye, K.	Morphological development of coastal dunes in a humid tropical environment, Cape Bedford and Cape Flattery, North Queensland	Coastal Normal
1986	Snyder, F. S. 1986	*A Spatial and Temporal Analysis of the Sleeping Bear Dunes Complex, Michigan: (a Contribution to the Geomorphology of Perched Dunes in Humid Continental Regions)*	Coastal Normal
1987	Marsh, W. M., and B. D. Marsh.	Wind erosion and sand dune formation on high Lake Superior bluffs	Coastal Normal
1988	Short	Holocene coastal dune formation in southern Australia: A case study	Coastal Normal
1989	Wilson, P.	Nature, origin and age of Holocene aeolian sand on Muckish Mountain, Co. Donegal, Ireland	Coastal Hybrid
1990	Marsh, W. M.	Nourishment of perched sand dunes and the issue of erosion control in the Great Lakes	Coastal Normal
1992	Jackson, D., and G. H. Nevin	Sand transport in a cliff top dune system at Fonte-De-Telha, Portugal	Coastal Normal
1992	Hetu, B.	Coarse cliff-top aeolian sedimentation in northern Gaspesie, Quebec (Canada)	Coastal Hybrid
1993	Carter, R. and P. Wilson.	Aeolian processes and deposits in northwest Ireland	Coastal Hybrid
1993	Vreeken	Loess and Associated Paleosols in Southwestern Saskatchewan and Southern Alberta	Terrestrial Fluvial
1995	Anderton, J. B., and W. L. Loope.	Buried soils in a perched dunefield as indicators of late Holocene lake-level change in the Lake Superior basin	Coastal Normal
1995	Bégin, C., Y. Michaud, and L. Filion	Dynamics of a Holocene cliff-top dune along Mountain River, Northwest Territories, Canada	Terrestrial Fluvial
1996	Beaudoin, A. B., M. Wright, and B. Ronaghan.	Late quaternary landscape history and archaeology in the 'Ice-Free Corridor': Some recent results from Alberta	Terrestrial Fluvial and Terrestrial Normal
1996	Livinston, I., and A. Warren	*Aeolian Geomorphology*	Coastal Normal, and Terrestrial Normal
1998	Lemmen, D. S., I. A.	Geomorphic systems of the Palliser Triangle,	Terrestrial

	Vance, P. P. Campbell, D. J. David, D. J. Pennock, D. J. Sauchyn, and S. A. Wolfe	southern Canadian Prairies: descripiton and response to changing climate	Normal
1999	Arbogast, A. F. and W. L. Loope	Maximum-limiting ages of Lake Michigan coastal dunes: Their correlation with Holocene lake level history	Coastal Normal
2000	Bullard, J. E and D. J. Nash	Valley-marginal sand dunes in the south-west Kalahari: Their nature, classification and possible origins	Terrestrial Fluvial
2000	Englebright, S. C., G. N. Hanson, T. Rasbury, and E. E. Lamont	On the Origin of Parabolic Dunes	Coastal Hybrid
2000	Haslett, S.K, P. Davies, and R. H. Curr.	Geomorphologic and palaeoenvironmental development of Holocene perched coastal dune systems in Brittany, France	Coastal Normal
2000	Loope and A. F. Arbogast	Dominance of an ~150-year cycle of sand-supply change in late Holocene dune-building along the eastern shore of Lake Michigan	Coastal Normal
2002	Arbogast, A. F., E. C. Hansen, and M. D. Van Oort	Reconstructing the geomorphic evolution of large coastal dunes along the southeastern shore of Lake Michigan	Coastal Normal
2002	Wilson, P.	Holocene coastal dune development on the South Erradale peninsula, Wester Ross, Scotland.	Coastal Normal
2002	Wolfe, S. A., J. Ollerhead, and O. B. Lian	Holocene eolian activity in south-central Saskatchewan and the southern Canadian Prairies	Terrestrial Fluvial
2003	Rawling, J. E., G. G. Fredlund, and S. Mahan	Aeolian cliff-top deposits and buried soils in the White River Badlands, South Dakota, USA	Terrestrial Normal
2006	Bateman, M. D. and J. B. Murton	Chronostratigraphy of sate Pleistocene glacial and periglacial aeolian activity in the Tuktoyaktuk coastlands, NWT, Canada	Coastal Hybrid
2006	Saye, S. E., K. Pye, and L. B. Clemmensen.	Development of a cliff-top dune indicated by particle size and geochemical characteristics: Rubjerg Knude, Denmark	Coastal Normal
2008	Forman, S. L., L. Marín, J. Gomez, and J. Pierson	Late Quaternary eolian sand depositional record for southwestern Kansas: Landscape sensitivity to droughts	Terrestrial Fluvial
2009	Germain, D., M. Lavoie, and L. Filion	Cliff-Top eolian sedimentation reflecting mid- to late-Holocene environmental changes at Anticosti Island, Gulf of St. Lawrence, eastern	Coastal Normal

		Canada	
2010	Arbogast, A. F., M. E. Bigsby, M. H DeVisser, S. A. Langley, P. R Hanson, T. A. Daly, and A. R. Young	Reconstructing the age of coastal sand dunes along the northwestern shore of Lake Huron in lower Michigan: Paleoenvironmental implications and regional comparisons	Coastal Normal
2010	Costas, S., P. O. Brito, M. Ferraz, R. González-Villanueva, A. Novo, and L. Rebêlo	The cliff-top dune of Costa da Caparica: possible scenarios of formation and evolution	Coastal Normal
2012	Blumer, B. E., A. F. Arbogast, and S. L. Forman	The OSL chronology of eolian sand deposition in a perched dune field along the northwestern shore of lower Michigan	Coastal Normal
2012	Costas, S., S. Jerez, R. M. Trigo, R. Goble, and L. Rebêlo	Sand invasion along the Portuguese coast forced by westerly shifts during cold climate events	Coastal Normal
2013	Halfen, A. F., and W. C. Johnson	A review of Great Plains dune field chronologies	Terrestrial Normal
2013	Richter, A., D. Faust, and H. G Maas	Dune cliff erosion and beach width change at the northern and southern spits of Sylt detected with multi-temporal Lidar	Coastal Normal
2015	Hanson, P. R., J. A Mason, P. M. Jacobs, and A. R. Young	Evidence for bioturbation of luminescence signals in eolian sand on upland ridgetops, southeastern Minnesota, USA	Terrestrial Fluvial
2016	Sansò, P., F. Gianfreda, G. Leucci, and G. Mastronuzzi.	Cliff evolution and late Holocene relative sea level change along the Otranto coast (Salento peninsula, southern Apulia, Italy)	Coastal Normal
2016	Van Vliet-Lanoë, B., J. A. Goslin, B. Hénaff, C. Hallégouët, E. Delacourt, Le Cornec, and M. Meurisse-Fort	Holocene formation and evolution of coastal dunes ridges, Brittany (France)	Coastal Hybrid

2017	Arbogast, A. F., A. F., M. D. Luehmann, G. William Monaghan, W. A. Lovis, and H. Wang	Paleoenvironmental and geomorphic significance of bluff-top dunes along the Au Sable River in northeastern Lower Michigan, USA	Terrestrial Fluvial
2017	Ho, L.-D., C. Lüthgens, Y.-C. Wong, J.-Y. Yen, and S.-J. Chyi	Late Holocene cliff-top dune evolution in the Hengchun Peninsula of Taiwan: Implications for palaeoenvironmental reconstruction	Coastal Normal
2017	Schaetzl, R. J., P. H. Larson, D. J. Faulkner, G. L. Running, H. M. Jol, and T. M. Rittenour	Eolian sand and loess deposits indicate west-northwest paleowinds during the Late Pleistocene in western Wisconsin, USA	Terrestrial Fluvial

Appendix B

Grain Size Distributions from the Kiwanis Site

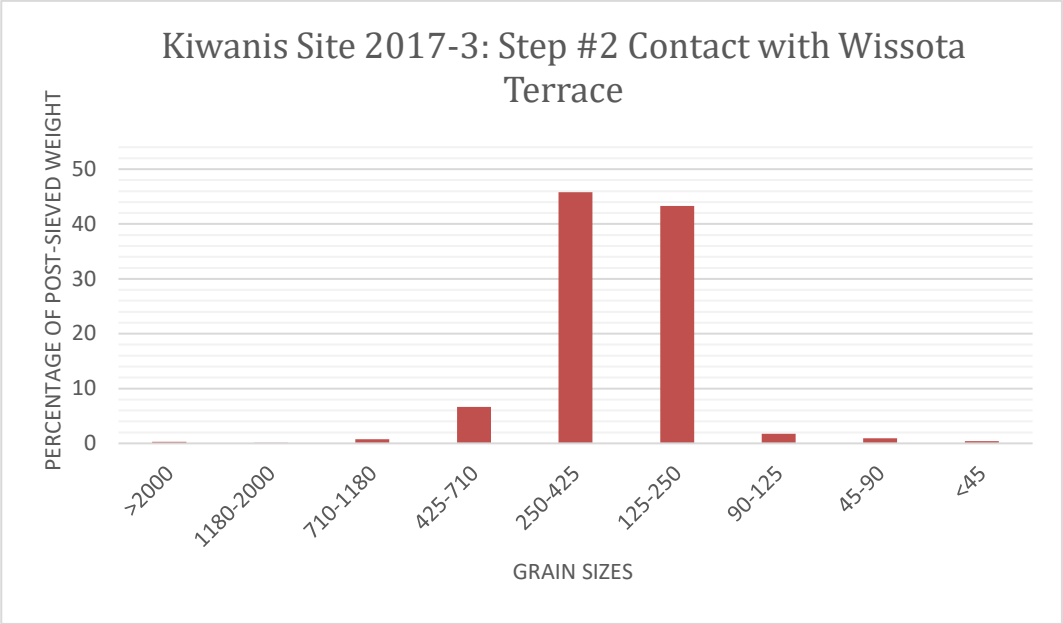

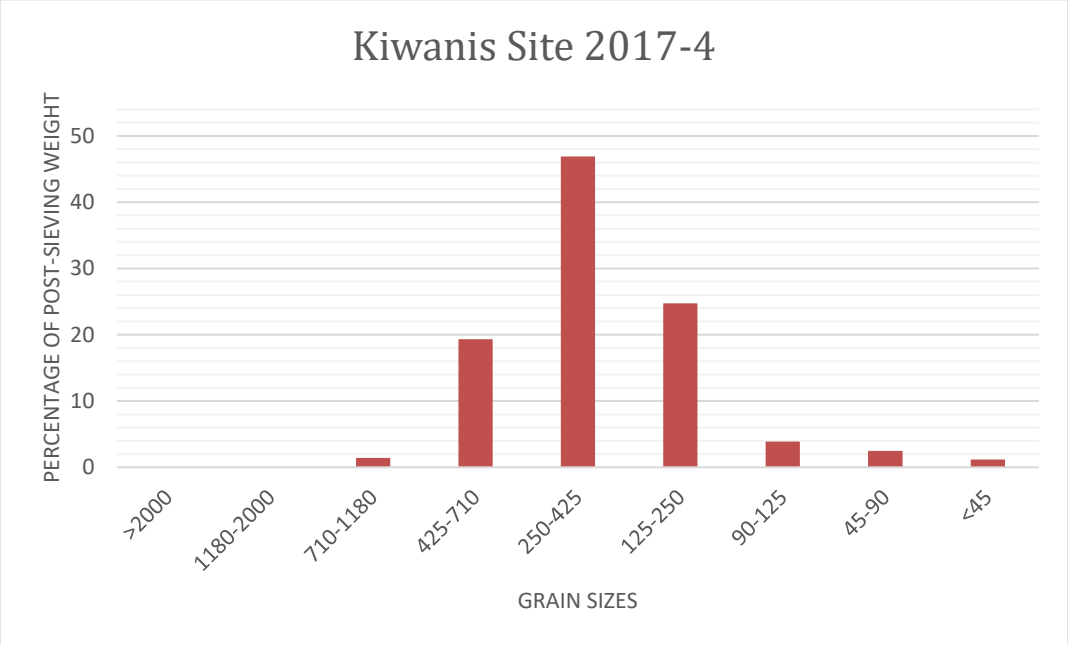

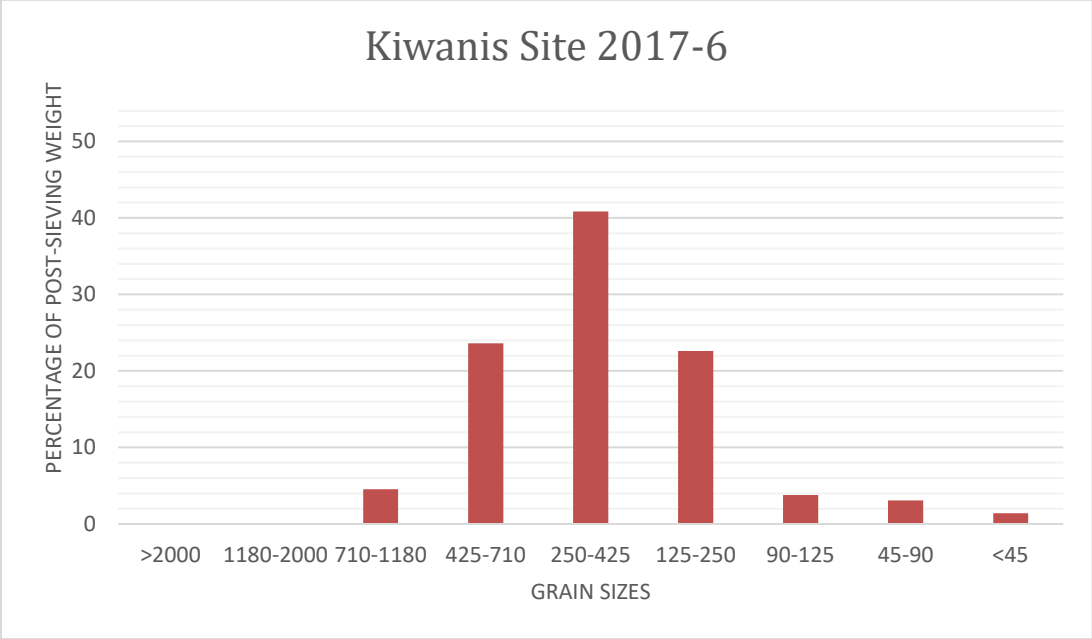
Kiwanis Site 2017-6
PERCENTAGE OF POST-SIEVING WEIGHT
0
10
20
30
40
50
>2000
1180-2000
710-1180
425-710
250-425
125-250
90-125
45-90
<45
GRAIN SIZES

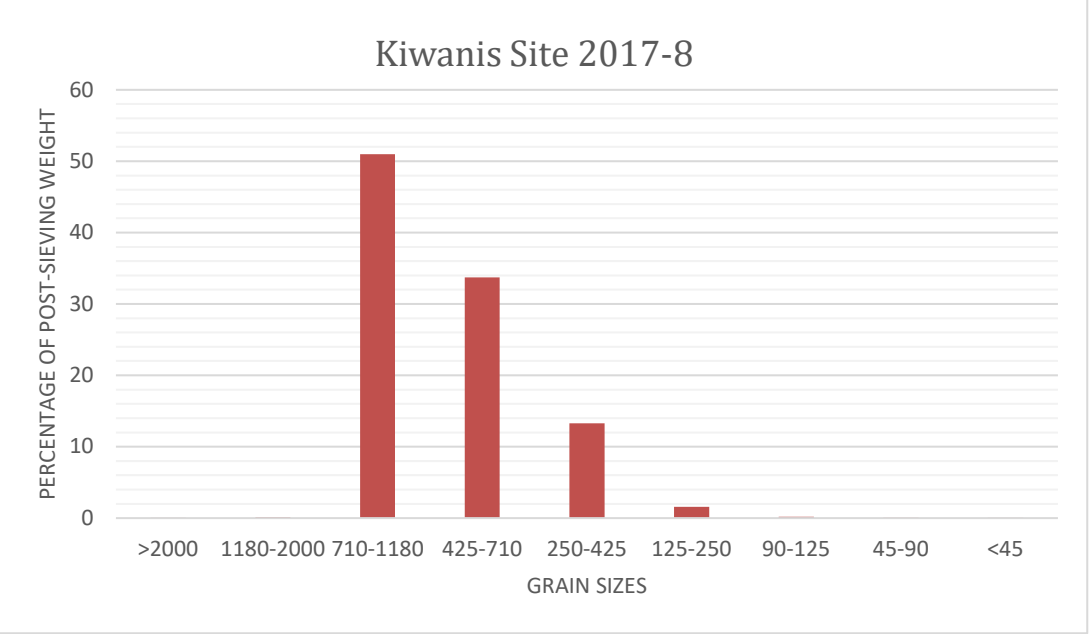
Kiwanis Site 2017-8
PERCENTAGE OF POST-SIEVING WEIGHT
0
10
20
30
40
50
60
>2000
1180-2000
710-1180
425-710
250-425
125-250
90-125
45-90
<45
GRAIN SIZES

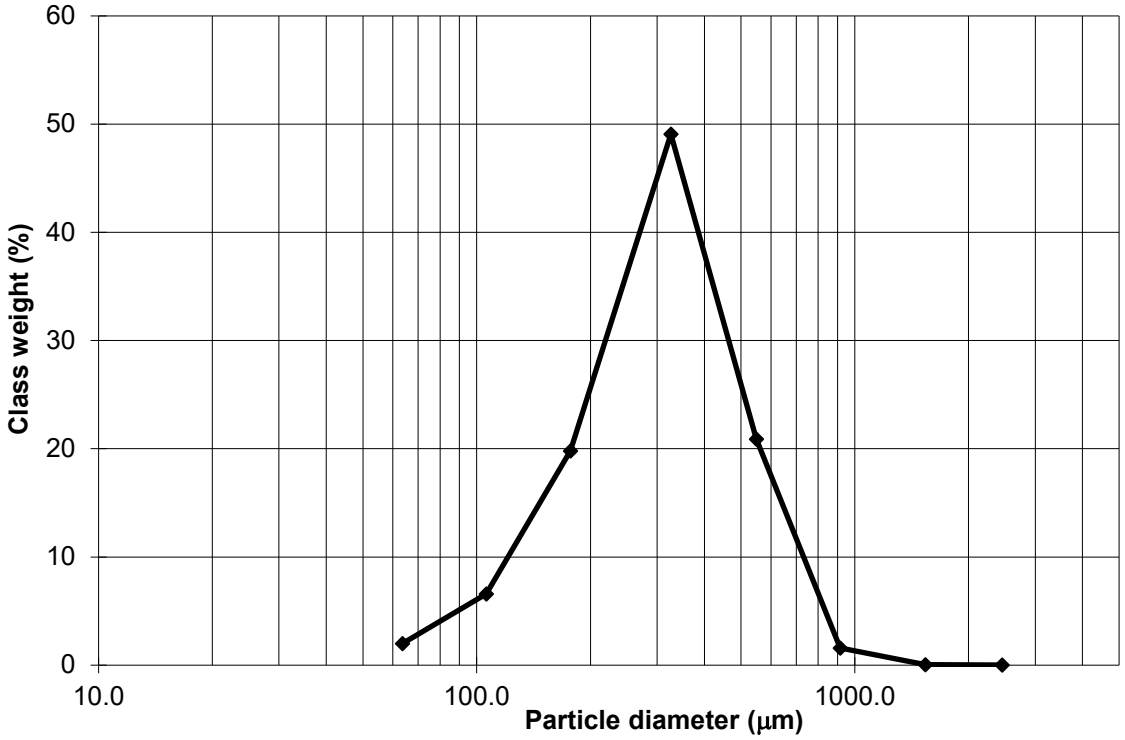
60
50
40
30
20
10
0
Class weight (%)
10.0
100.0
1000.0
Particle diameter (μm)

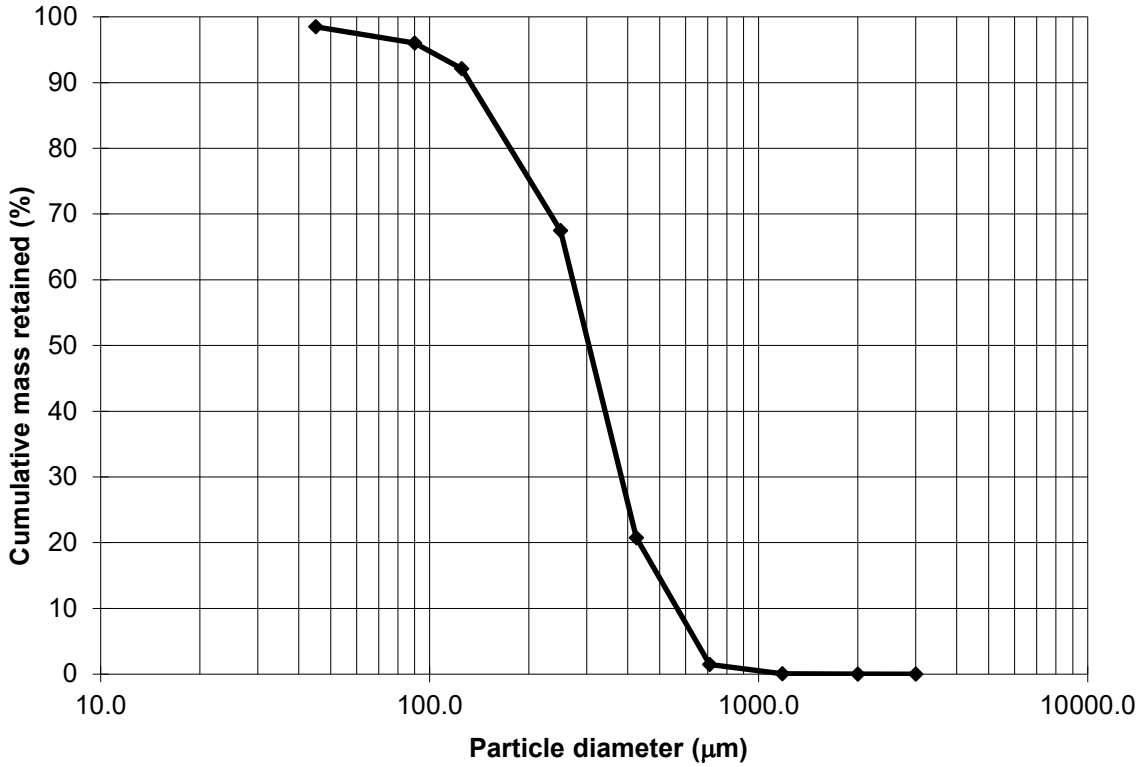
100
90
80
70
60
50
40
30
20
10
0
Cumulative mass retained (%)
10.0
100.0
1000.0
10000.0
Particle diameter (μm)

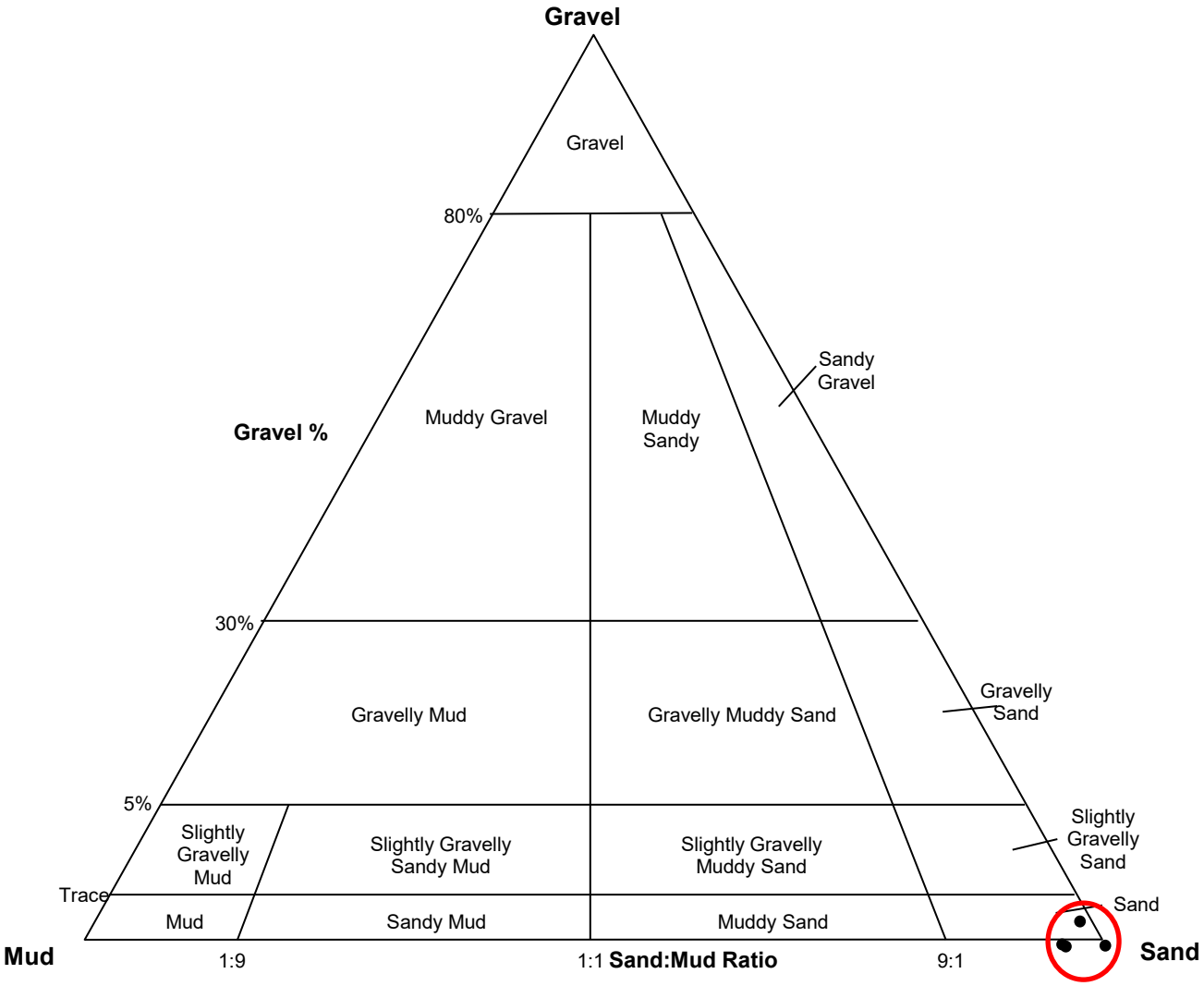

Sample locations within ternary chart located within red circle.

Appendix C

OSL Radial Plots from the Kiwanis Site

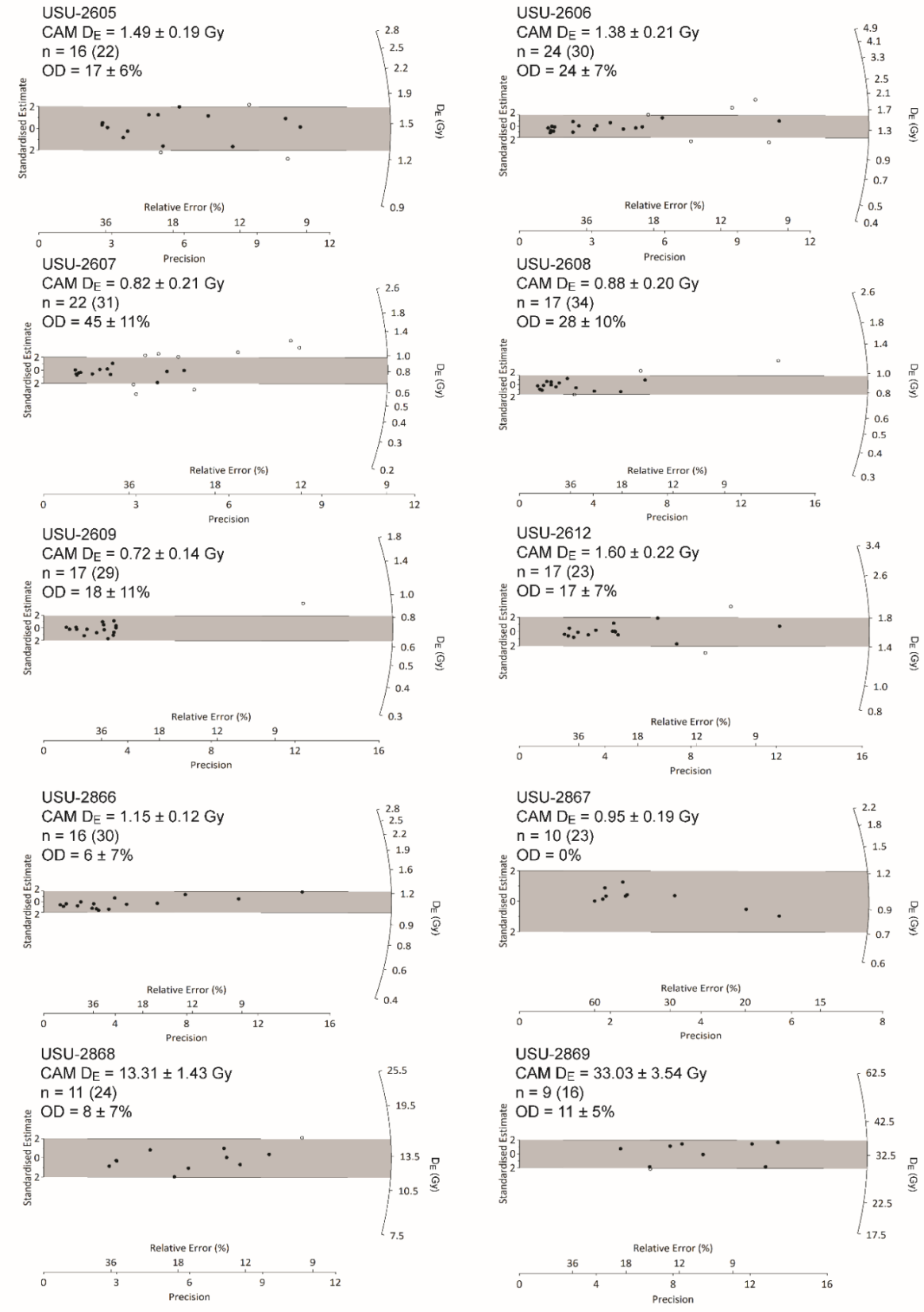

Appendix D

Grain Size Distributions from the Steffes and Zanoni and Hurlburt Sites

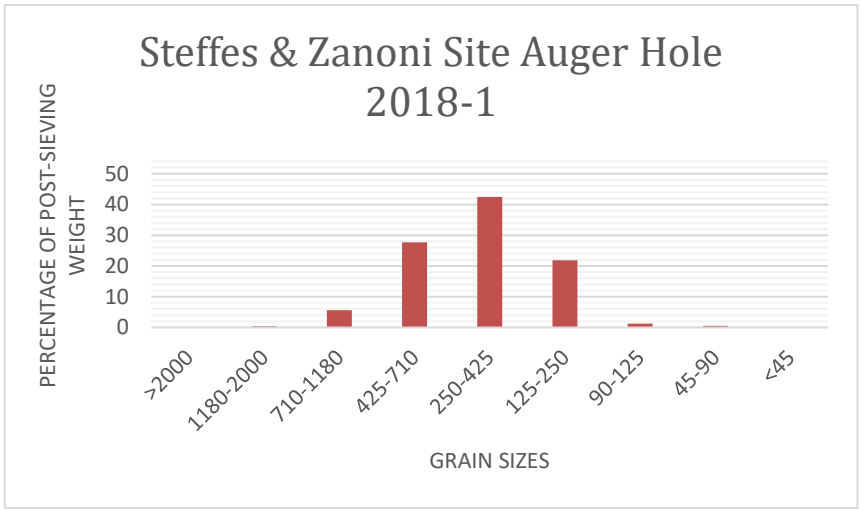

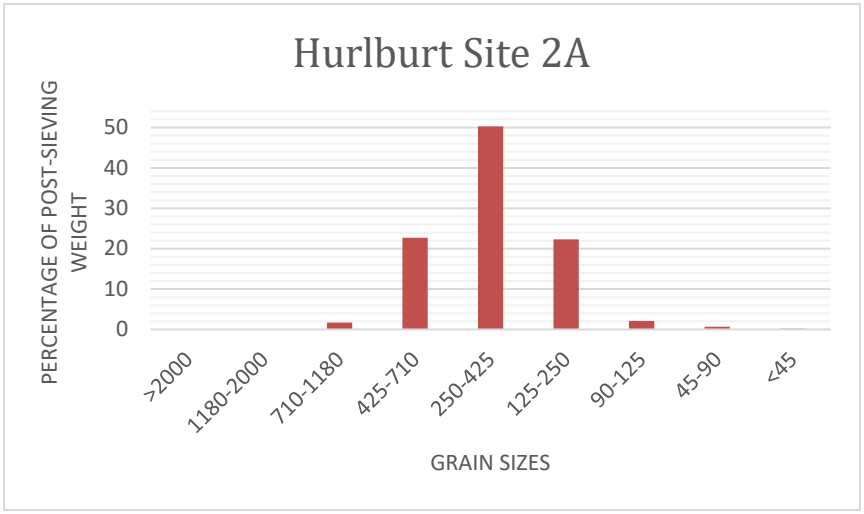

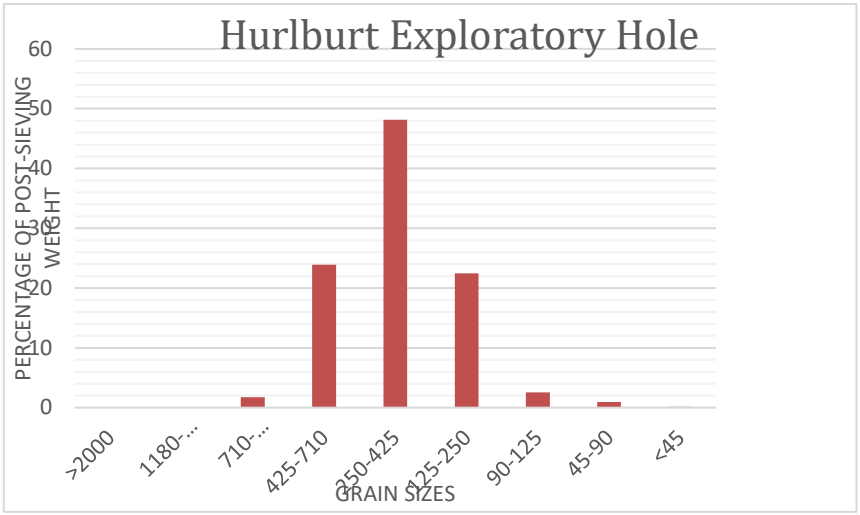

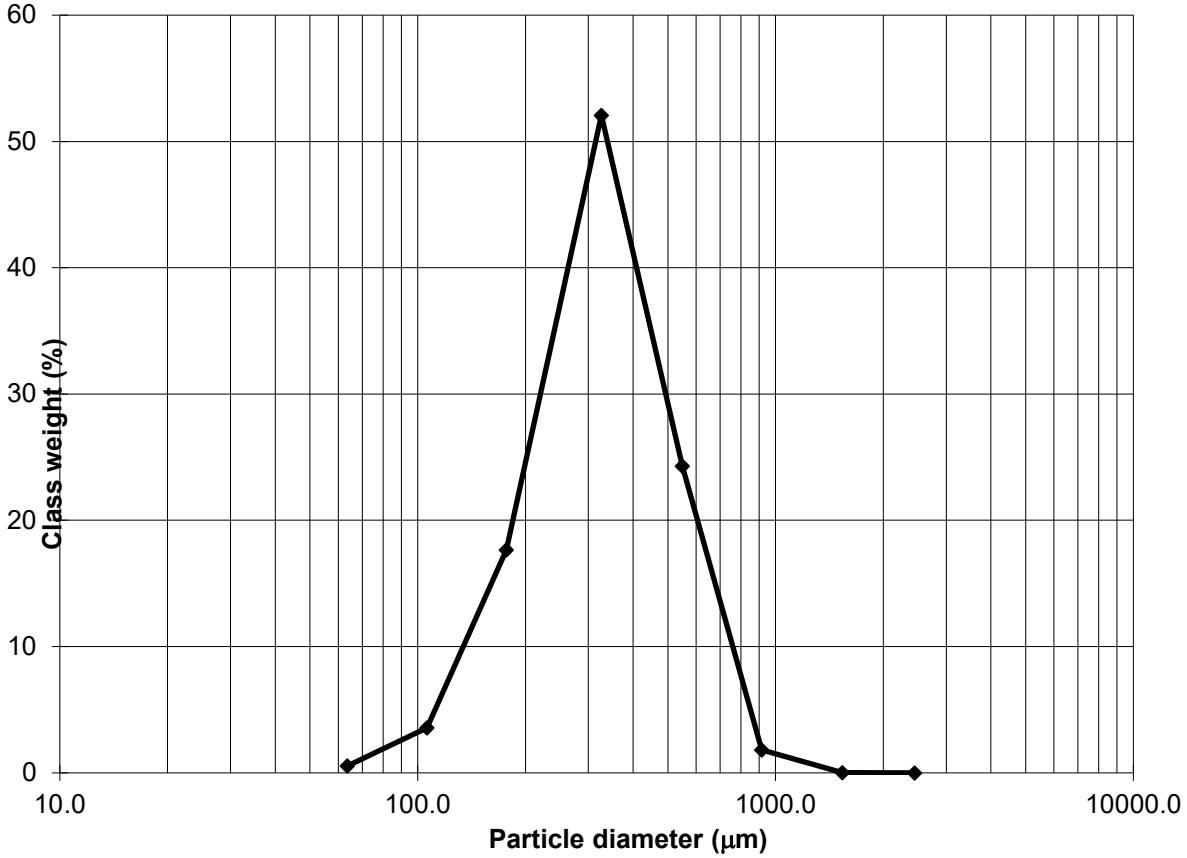

Particle size distribution for the Hurlburt site samples.

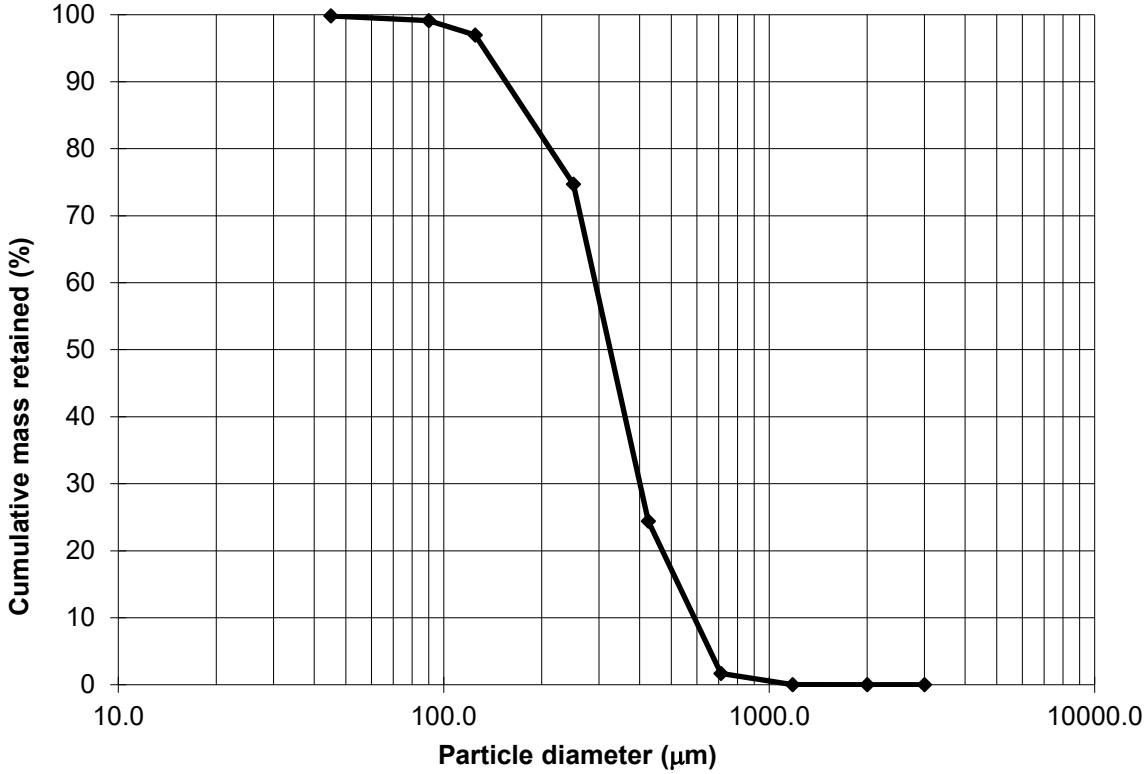

Cumulative particle size distribution for the Hulrburt site samples.

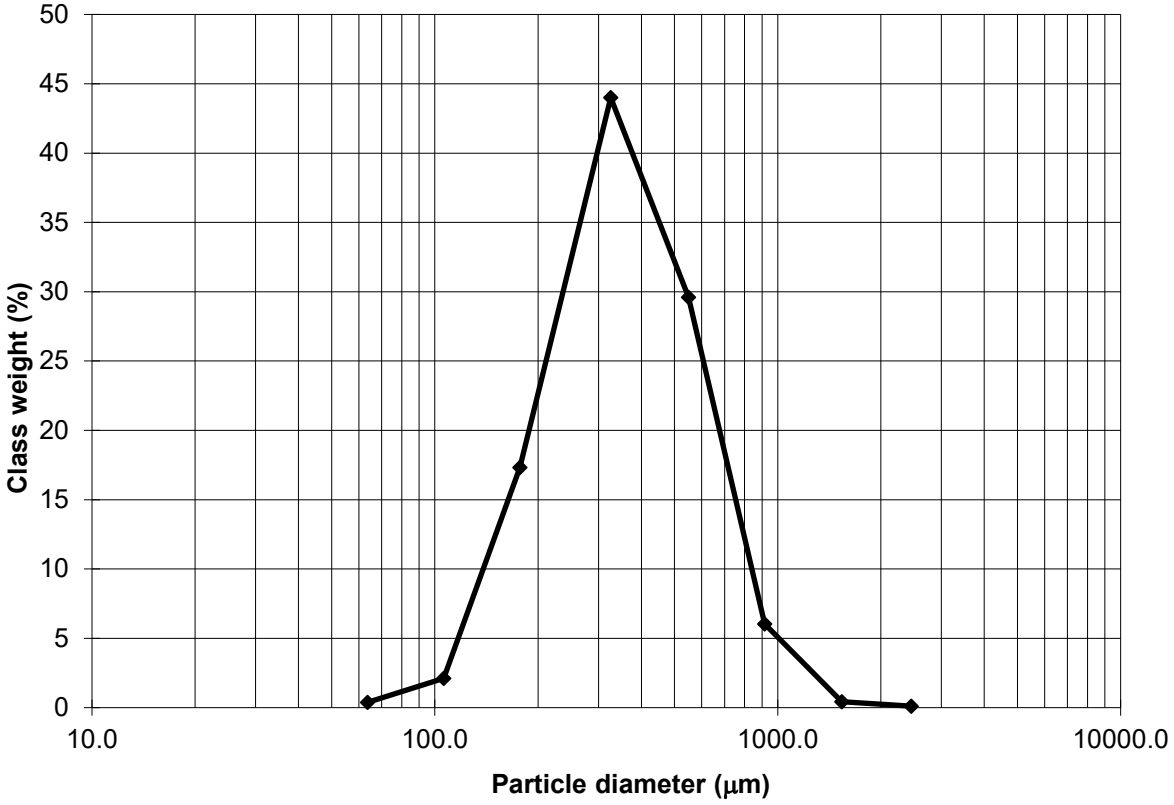

Particle size distribution for the Steffes and Zanoni site sample.

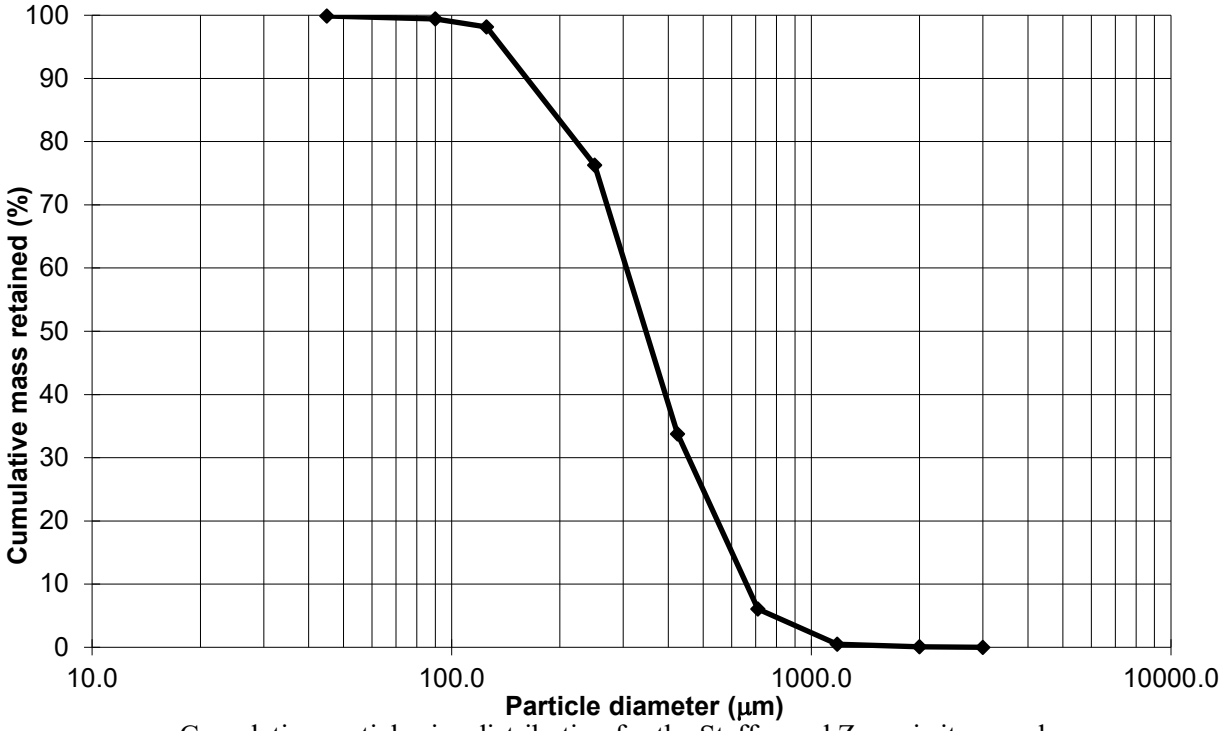

Cumulative particle size distribution for the Steffes and Zanoni site sample.

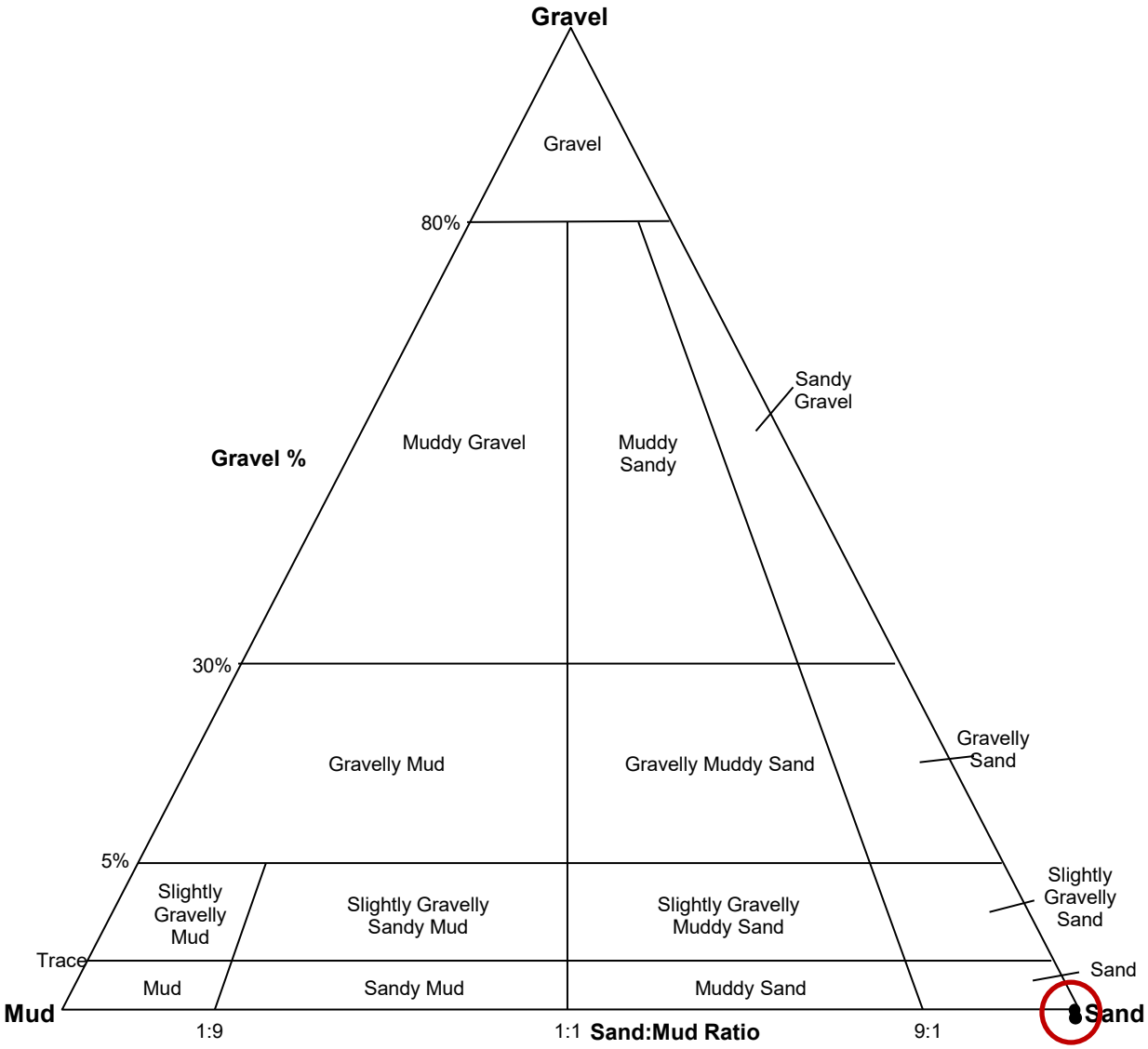

Sample locations within ternary chart located within red circle.

Appendix E

OSL Radial Plots from the Steffes and Zanoni and Hurlburt Sites